

Artificial Reservoir Engineering Study

Richard McFarlane, Justin Wiwchar, Ted Frauenfeld, Roy Coates, Karen Budwill, Xinkui Wang, Yu Feng, Hart Golbeck, Haibo Huang, and Jose Alvarez Martine

REPORT PREPARED FOR
PETROLEUM TECHNOLOGY ALLIANCE CANADA
BY ALBERTA INNOVATES – TECHNOLOGY FUTURES.

HEAVY OIL AND OIL SANDS
250 KARL CLARK ROAD
EDMONTON, ALBERTA T6N 1E4
CANADA

CONFIDENTIAL

Contract No. HOOS-007.11

December 2012

Revised April 2012

DISCLAIMER

“The information supplied by Alberta Innovates - Technology Futures for this report was prepared for general information only and is not intended to be relied upon as to its accuracy or completeness, whether from a scientific, research, technical, professional, economic, or other basis. The information is not to be treated as endorsed by PTAC, participants, or Alberta Innovates Technology Futures. The reader must seek out its own advisors to assess the value of any information contained in this report.”

ACKNOWLEDGEMENT

The authors are grateful for discussions with colleagues at AITF including Brigida Meza, Joyce Chen, Xiaohui Deng, and Doug Lillico. We also acknowledge assistance of Kelly Knorr and Norm Freitag at Saskatchewan Research Council for providing information about their reservoir models and facilities. We also acknowledge the assistance of Kate Cullen in the preparation of this report. Finally, we are grateful for patient assistance of Wendy Holgate (AITF) and Arlene Merling (PTAC) helping us to get this project underway.

EXECUTIVE SUMMARY

A review of various *in situ* recovery processes, their mechanisms, scaling of these mechanisms, and design and use of physical models was undertaken. The scope of the review was restricted to bitumen and heavy oil deposits in sandstone reservoirs that may contain shale barriers, water and gas zones, and thief zones. The recovery processes examined included SAGD, solvent-steam, *in situ* combustion, electrical heating, and biological processes. The state of the art of reservoir physical models employed for investigation of these processes was assessed through a literature review. The ability to predict field performance by upscaling results from scaled models is one of the great advantages of such models. However, this ability is significantly compromised when some process mechanisms are not accounted for or cannot be properly scaled. In such cases, field-scale or field-element models may be the best alternative.

Reservoir geomechanics is one area where physical models have not been very successful. Geomechanics may play an important role in thermal and high pressure processes such as SAGD and ES-SAGD. The role of geomechanics in these processes is inconclusive precisely because reservoir physical models cannot easily explore these effects. Mixing/dispersion is not typically scaled by physical models. This is a major problem for investigating solvent-steam processes where oil and solvent mixing is critical. Major efforts are underway at AITF to address this limitation by the use of field-scale and field-element models.

For *in situ* combustion, scaled models are not practical because the essential reactions kinetics cannot be scaled. Nevertheless, larger models do offer an advantage through minimizing heat loss that strongly affects combustion reaction kinetics. Similarly, scaling of biological processes is impractical because biochemical reaction rates cannot be scaled. However, larger models for biological process have value for investigating the effects of pressure drops, microbial transport, and mortality at remote distances from the injection point of the biological cultures in reservoir compatible fluids.

Compared to SAGD, steam-solvent, *in situ* combustion, and biological processes, electrical heating processes are challenging to represent in small or scaled models. Scaling of electrical and electromagnetic processes requires that electrical (i.e., temperature-dependent conductivity, dielectric constant, and magnetic permeability) and thermal similitudes are consistent and simultaneously incorporated in the model. Fluid transport, geomechanical, gravitational, and capillary effects provide additional complexity. Field-scaled or close to field-scale models employing reservoir media may be the most practical for reliable interpretation of data from physical models for electrical heating.

Cost data indicate that larger models than those currently in use may be prohibitively expensive as their size and pressure place them on the steepest part of the cost curve. New approaches to design are required to build and operate practical field-scale models. Knowledge gained at AITF through the construction and operation of intermediate 2D field-scale models and field-element models can provide a useful bridge to the new generation field-scale models.

TABLE OF CONTENTS

| | |
|--|------|
| ACKNOWLEDGEMENT | II |
| EXECUTIVE SUMMARY | III |
| TABLE OF CONTENTS | IV |
| LIST OF TABLES | VIII |
| LIST OF FIGURES | VIII |
| 1.0 INTRODUCTION | 1 |
| 1.1. BACKGROUND | 1 |
| 1.2. SCOPE | 2 |
| 1.3. APPROACH | 2 |
| 2.0 STEAM-ASSISTED GRAVITY DRAINAGE (SAGD) | 4 |
| 2.1. INTRODUCTION | 4 |
| 2.2. SAGD MECHANISMS | 5 |
| 2.3. PARAMETERS AFFECTING SAGD | 6 |
| 2.4. EXPERIMENTAL EVALUATION OF SAGD PROCESSES | 7 |
| 2.5. CYCLIC STEAM STIMULATION | 7 |
| 3.0 SOLVENT-STEAM | 9 |
| 3.1. INTRODUCTION | 9 |
| 3.2. EXPANDING SOLVENT-SAGD (ES-SAGD) | 9 |
| 3.2.1. <i>Initial Lab Tests</i> | 9 |
| 3.2.2. <i>Parametric Studies</i> | 10 |
| 3.2.3. <i>Numerical Simulations</i> | 10 |
| 3.2.4. <i>Mechanistic Study</i> | 11 |
| 3.2.5. <i>Field Tests</i> | 12 |
| 3.2.5.1. <i>Burnt Lake ES-SAGD Pilot</i> | 12 |
| 3.2.5.2. <i>Firebag ES-SAGD Pilot</i> | 12 |
| 3.2.5.3. <i>Senlac SAP Pilot</i> | 12 |
| 3.2.5.4. <i>Christina Lake SAP Pilot</i> | 12 |
| 3.3. SOLVENT ASSISTED PROCESS | 13 |
| 3.4. STEAM-ALTERNATING-SOLVENT | 13 |
| 3.5. STEAM-BUTANE HYBRID | 13 |
| 3.6. PURE SOLVENT PROCESSES | 13 |
| 3.6.1. <i>N-Solv</i> | 13 |
| 3.6.2. <i>VAPEX</i> | 14 |
| 3.6.3. <i>Cyclic Solvent Stimulation</i> | 15 |
| 4.0 <i>IN SITU</i> COMBUSTION | 16 |
| 4.1. INTRODUCTION | 16 |
| 4.2. ISC DESCRIPTION AND MECHANISMS | 16 |
| 4.2.1. <i>Combustion Zone</i> | 17 |

| | | |
|----------|--|----|
| 4.2.2. | <i>Fuel Deposition Zone:</i> | 17 |
| 4.2.3. | <i>Condensation and Displacement Zone:</i> | 18 |
| 4.3. | WET COMBUSTION | 18 |
| 4.4. | ISC CONFIGURATIONS AND VARIATIONS..... | 19 |
| 4.4.1. | <i>Traditional ISC</i> | 19 |
| 4.4.2. | <i>New Configurations</i> | 19 |
| 4.4.2.1. | <i>Toe-to-Heal Air Injection (THAI)</i> | 19 |
| 4.4.2.2. | <i>COSH and COGD Processes</i> | 20 |
| 4.4.2.3. | <i>Top-Down ISC Process (TD-ISC)</i> | 20 |
| 4.4.3. | <i>Alternate Operating Strategies</i> | 21 |
| 4.5. | PHYSICAL MODELING OF <i>IN SITU</i> COMBUSTION | 22 |
| 5.0 | ELECTRICAL HEATING | 24 |
| 5.1. | INTRODUCTION | 24 |
| 5.2. | OHMIC HEATING MECHANISM | 24 |
| 5.2.1. | <i>Process configuration and application</i> | 25 |
| 5.2.2. | <i>DC vs. AC</i> | 27 |
| 5.3. | ELECTROMAGNETIC HEATING..... | 28 |
| 5.3.1. | <i>Dielectric heating</i> | 28 |
| 5.3.2. | <i>Inductive heating</i> | 29 |
| 5.4. | CHALLENGES | 30 |
| 6.0 | BIOLOGICALLY ENHANCED OIL RECOVERY | 32 |
| 6.1. | INTRODUCTION | 32 |
| 6.2. | INTERFACIAL TENSION REDUCTION..... | 34 |
| 6.3. | GAS PRODUCTION | 37 |
| 6.4. | VISCOSITY REDUCTION..... | 38 |
| 6.5. | PERMEABILITY PROFILE MODIFICATION (MICROBIAL FLOW DIVERSION)..... | 39 |
| 6.6. | CONSIDERATIONS FOR LABORATORY AND FIELD TESTING..... | 41 |
| 6.7. | WATERFLOODING | 43 |
| 6.7.1. | <i>Microscopic Displacement Efficiency</i> | 44 |
| 6.7.2. | <i>Macroscopic Displacement Efficiency</i> | 45 |
| 6.7.3. | <i>Overall Waterflooding Recovery Efficiency</i> | 46 |
| 6.7.4. | <i>Factors Controlling Recovery</i> | 47 |
| 6.7.4.1. | <i>Properties of Displacing/Displaced Fluids and Reservoir Characteristics</i> | 47 |
| 6.7.4.2. | <i>Waterflood Pattern</i> | 48 |
| 6.7.5. | <i>Considerations of Waterflood Technology</i> | 48 |
| 7.0 | SCALING OF PHYSICAL MODELS..... | 49 |
| 7.1. | INTRODUCTION | 49 |
| 7.2. | DIMENSIONLESS NUMBERS | 49 |
| 7.3. | DIFFUSION AND MIXING | 50 |
| 7.4. | DIMENSIONAL ANALYSIS..... | 50 |
| 7.5. | INSPECTIONAL ANALYSIS..... | 51 |
| 7.6. | RESULTS OF SCALING..... | 52 |
| 7.6.1. | <i>Low Pressure Models</i> | 52 |
| 7.6.2. | <i>Pujol and Boberg Scale Model</i> | 52 |

| | | |
|----------|---|----|
| 7.6.3. | <i>Kimber's Scaling Study</i> | 52 |
| 7.6.4. | <i>Scaling of Dispersion</i> | 55 |
| 7.7. | SCALING OF IN SITU COMBUSTION..... | 55 |
| 7.8. | SCALING OF ELECTRICAL PROCESSES..... | 57 |
| 7.8.1. | <i>Induction Approximation</i> | 58 |
| 7.8.2. | <i>Quasi-Static Approximation</i> | 58 |
| 7.8.3. | <i>The Good Dielectric Approximation</i> | 59 |
| 7.9. | MECHANISMS AND PROPERTIES NOT COVERED BY SCALING..... | 59 |
| 7.10. | SUMMARY..... | 60 |
| 7.11. | SYMBOLS USED..... | 61 |
| 8.0 | PHYSICAL MODELS..... | 62 |
| 8.1. | INTRODUCTION..... | 62 |
| 8.2. | OVERVIEW OF MODEL TYPES..... | 62 |
| 8.2.1. | <i>Low Pressure Models</i> | 62 |
| 8.2.2. | <i>Visual Models</i> | 62 |
| 8.2.3. | <i>CT Models</i> | 63 |
| 8.2.4. | <i>High Pressure Models</i> | 63 |
| 8.2.5. | <i>Partially Scaled Models</i> | 63 |
| 8.2.6. | <i>Elemental Models</i> | 63 |
| 8.3. | SAGD..... | 64 |
| 8.4. | SOLVENT-STEAM..... | 65 |
| 8.5. | COMBUSTION..... | 67 |
| 8.6. | ELECTRICAL HEATING..... | 72 |
| 8.7. | BIOLOGICAL PROCESSES..... | 73 |
| 8.7.1. | <i>Biological Aspects</i> | 73 |
| 8.7.2. | <i>Water flood</i> | 73 |
| 8.7.3. | <i>Polymer Flood</i> | 75 |
| 8.8. | GENERAL APPLICATION MODEL..... | 75 |
| 8.8.1. | <i>LARGE Model</i> | 75 |
| 8.8.2. | <i>SRC Model</i> | 76 |
| 8.8.3. | <i>Transparent Annular Sand Pack</i> | 77 |
| 8.9. | MODELS USED AND DEVELOPED AT AITF..... | 77 |
| 8.9.1. | <i>Large Unscaled Physical Models</i> | 78 |
| 8.9.2. | <i>Low Pressure Visual Models</i> | 78 |
| 8.9.3. | <i>High Pressure Visual Models</i> | 78 |
| 8.9.4. | <i>CT Models</i> | 78 |
| 8.9.5. | <i>Scaled Physical Models</i> | 79 |
| 8.9.6. | <i>High Pressure Elemental Models</i> | 79 |
| 8.9.7. | <i>Adiabatic Experimental Models</i> | 79 |
| 9.0 | DESIGN/OPERATION CONSIDERATIONS & COSTS..... | 81 |
| 9.1. | DESIGN/OPERATION CONSIDERATIONS..... | 81 |
| 9.2. | SCALED MODEL DESIGN AND OPERATION..... | 81 |
| 9.2.1. | <i>Design and Fabrication</i> | 81 |
| 9.2.2. | <i>Packing</i> | 82 |
| 9.2.2.1. | <i>Uniform Packing</i> | 82 |
| 9.2.2.2. | <i>Shale Barriers</i> | 83 |

| | | |
|--------|---|----|
| 9.2.3. | <i>Insulation and Heat Tracing</i> | 83 |
| 9.2.4. | <i>Data Acquisition and Control</i> | 83 |
| 9.2.5. | <i>Overburden Vessel</i> | 83 |
| 9.2.6. | <i>Saturation</i> | 84 |
| | 9.2.6.1. <i>Bottom Water</i> | 84 |
| | 9.2.6.2. <i>Gas Zone</i> | 84 |
| 9.2.7. | <i>Production Systems</i> | 85 |
| 9.2.8. | <i>Post Run</i> | 85 |
| 9.3. | FACILITIES CONSIDERATIONS | 85 |
| 9.4. | CAPITAL AND OPERATING COSTS | 86 |
| | 9.4.1. <i>Capital and Operating Costs of Models</i> | 86 |
| | 9.4.2. <i>Capital Cost of Facilities</i> | 86 |
| | 9.4.3. <i>Implications of Cost Data</i> | 88 |
| 10.0 | SUMMARY AND RECOMMENDATIONS..... | 89 |
| 10.1. | OVERVIEW | 89 |
| 10.2. | MODEL SCALING | 89 |
| | 10.2.1. <i>Challenges</i> | 89 |
| | 10.2.2. <i>SAGD</i> | 90 |
| | 10.2.3. <i>Solvent-Steam</i> | 90 |
| | 10.2.4. <i>Combustion</i> | 91 |
| | 10.2.5. <i>Electrical heating</i> | 91 |
| | 10.2.6. <i>Biological Processes</i> | 92 |
| 10.3. | COST OF SCALED MODELS | 93 |
| 10.4. | NEXT STEPS | 93 |
| | 10.4.1. <i>Context of Next Steps</i> | 93 |
| | 10.4.1.1. <i>Define Value & Benefits</i> | 93 |
| | 10.4.1.2. <i>Confidence</i> | 94 |
| | 10.4.2. <i>Path Forward – Outline</i> | 94 |
| 11.0 | REFERENCES..... | 96 |

LIST OF TABLES

| | | |
|------------|--|----|
| TABLE 6-1. | MICROBIAL GENERATED PRODUCTS AND THEIR CLAIMED EFFECTS FOR EOR ⁽⁶⁴⁾ | 33 |
| TABLE 6-2. | IDEAL RESERVOIR CONDITIONS FOR MEOR APPLICATIONS ^(65; 66) | 34 |

LIST OF FIGURES

| | | |
|-------------|---|----|
| FIGURE 2-1 | SAGD CONFIGURATION AND OPERATION | 4 |
| FIGURE 2-2 | STEAM CHAMBER EXPANSION (AFTER BUTLER ⁽¹²⁾) | 6 |
| FIGURE 3-1. | SCHEMATIC OF THE ES-SAGD PROCESS | 9 |
| FIGURE 3-2. | VAPEX CONFIGURATION | 14 |
| FIGURE 4-1. | TEMPERATURE AND SATURATION PROFILES DURING ISC PROCESS | 17 |
| FIGURE 4-2. | SCHEMATIC OF THAI PROCESS | 20 |
| FIGURE 4-3. | SCHEMATIC OF COSH PROCESS | 20 |
| FIGURE 4-4. | SCHEMATIC OF TD-ISC PROCESS | 21 |
| FIGURE 4-5. | SCHEMATIC OF MS-CAGD PROCESS | 22 |
| FIGURE 5-1. | INTERCONNECTED WATER-SATURATED PORE SPACES WITHIN BITUMEN SANDS MATRIX ⁽⁴³⁾ | 24 |
| FIGURE 5-2. | ELECTRICAL CONDUCTIVITIES OF SOME ELECTROLYTES IN WATER AT 25C | 25 |
| FIGURE 5-3. | ELECTRICAL HEATING SINGLE WELLBORE CONFIGURATION (OIL PRODUCTION EQUIPMENT NOT SHOWN) ⁽⁴⁴⁾ | 26 |
| FIGURE 5-4. | COMBINATION OF VERTICAL AND HORIZONTAL WELLS FOR ELECTRICAL HEATING SYSTEM ⁽⁴³⁾ | 26 |
| FIGURE 5-5. | CONFIGURATION OF ELECTRODES AS WELL AS PRODUCTION WELL FOR ET-DSP TM PROCESS ⁽⁴³⁾ | 27 |
| FIGURE 5-6 | ILLUSTRATION OF ESEIEH PROCESS (GLOBE & MAIL, JUN 13, 2012) | 29 |
| FIGURE 5-7 | SCHEMATIC OF EM-SAGD PROCESS ⁽⁶⁰⁾ | 30 |
| FIGURE 5-8. | VARIATION IN RESISTIVITY FOR A FROG LAKE WELL ⁽⁴⁵⁾ | 31 |
| FIGURE 6-1. | THE TITAN PROCESS: INJECTION OF PROPRIETARY NUTRIENTS CAUSES BACTERIA TO SEEK OUT OIL DROPLETS AND COAT THEM, CAUSING THE OIL TO DISLodge FROM PORE SPACES AND FLOW INTO THE WATER PATH ⁽⁷²⁾ | 36 |
| FIGURE 6-2 | EMULSION FORMATION BY BACTERIA STIMULATED DURING THE TITAN PROCESS CAUSES THIEF ZONES (LEFT SIDE OF FIGURE) TO BECOME BLOCKED SWEEPING OIL MORE EFFICIENTLY (RIGHT SIDE OF FIGURE) ⁽⁶¹⁾ | 37 |
| FIGURE 6-3 | BACTERIAL PROFILE MODIFICATION (BPM) DEVELOPED BY THE POROUS MEDIA RESEARCH GROUP AT THE UNIVERSITY OF MICHIGAN. A) INJECTED WATER FLOWS THROUGH THE WATER-FLOODED HIGH PERMEABILITY ZONE AND BYPASSES THE OIL-CONTAINING LOW PERMEABILITY ZONE. B) INJECTION OF EXOPOLYMER PRODUCING BACTERIA WITH RAPID BACTERIAL GROWTH AND EXOPOLYMER FORMATION NEAR THE WELL BORE AND PREVENTION OF DEEP PENETRATION OF BACTERIAL CELLS AND NUTRIENTS LEADS TO POOR OIL RECOVERY C) DELAYING THE ONSET OF BACTERIAL EXPONENTIAL GROWTH (I.E., INCREASING THE LAG TIME FOR GROWTH) LEADS TO DEEP PENETRATION THROUGHOUT THE RESERVOIR AND IMPROVED OIL RECOVERY ⁽⁶⁴⁾ | 40 |
| FIGURE 6-4. | EXPERIMENTAL FLOW DOWN FOR OBTAINING USEFUL MICROORGANISM FOR MEOR PROCESSES FROM TARGET RESERVOIRS ⁽⁶⁶⁾ | 42 |
| FIGURE 6-5. | WATERFLOODING PROCESS | 44 |
| FIGURE 6-6. | ILLUSTRATION OF OIL/WATER INTERFACES: CONTINUOUS PHASE VS. TRAPPED DROP (AFTER ⁽⁴⁴⁾) | 45 |
| FIGURE 6-7. | WATERFLOODING DISPLACEMENT AT MICROSCOPIC PORE LEVEL | 45 |
| FIGURE 6-8. | FRONT POSITIONS FOR A CONFINED FIVE-SPOT WELL PATTERN (AFTER ⁽⁸¹⁾) | 46 |
| FIGURE 7-1. | DIMENSIONLESS REPRESENTATION ⁽⁹²⁾ OF DISPERSION AND DIFFUSION VS. FLUID FLOW VELOCITY | 55 |
| FIGURE 8-1. | SCHEMATIC OF <i>IN SITU</i> COMBUSTION MODEL WITH SIMULATED WORMHOLE FROM CHEN <i>ET AL.</i> ⁽¹²⁸⁾ | 70 |
| FIGURE 8-2. | SCHEMATIC OF 3D MODEL FOR MS-CAGD FROM LIM AND CHEN ⁽⁸⁰⁾ | 71 |
| FIGURE 8-3. | EXPLODED VIEW OF A 2D MODEL USED FOR WET ELECTRICAL HEATING TO INVESTIGATE START-UP OF A SAGD OR VAPEX WELL PAIR ⁽¹⁰⁸⁾ | 72 |
| FIGURE 8-4. | SCALED PHYSICAL MODEL FOR THERMAL OIL RECOVERY PROCESS EXPERIMENTS | 77 |
| FIGURE 8-5. | VISUAL MODEL OF THERMAL SOLVENT PROCESS | 80 |

FIGURE 9-1. COMPARISON OF THE CAPITAL COSTS OF SCALED RESERVOIR MODELS VS. $\text{LOG}_{10}(\text{VOLUME X PRESSURE})$ 87
FIGURE 9-2. COMPARISON OF THE OPERATING COSTS OF SCALED RESERVOIR MODELS VS. $\text{LOG}_{10}(\text{VOLUME X PRESSURE})$ 87
FIGURE 9-3. CAPITAL COST OF FACILITY TO HOUSE SCALED RESERVOIR MODELS VS. $\text{LOG}_{10}(\text{VOLUME X PRESSURE})$ 88

ARTIFICIAL RESERVOIR ENGINEERING STUDY

RICHARD MCFARLANE, JUSTIN WIWCHAR, TED FRAUENFELD, ROY COATES,
KAREN BUDWILL, XINKUI WANG, YU FENG, HART GOLBECK, HAIBO HUANG,
AND JOSE ALVAREZ MARTINE

1.0 INTRODUCTION

1.1. BACKGROUND

Physical models of reservoir processes have been used for initial validation of new concepts, to generate quantitative information about recovery mechanisms, and to provide comparative information about process performance. Results from physical models can also be used to tune, check, and validate predictions from numerical simulations. While physical models can provide qualitative understanding of reservoir recovery processes, the results from such models may not always provide good quantitative predictions of field performance, i.e., the results do not scale up. Model parameters and performance related to pay zone thickness, permeability, injection and production rates, pressure drop, and time tend to scale well. Factors such as mixing processes, capillary effects and heat and mass transfer can scale poorly or are unaccounted for in upscaling of model results. The effect of the model boundaries as they relate to the heat loss and geomechanics that may play critical roles in some processes are not well accounted for in physical models or in upscaling of the results.

Larger physical models can overcome some or all of the above limitations associated with existing models and serve as a reliable proxy for time consuming and costly field trials. The benefits of these larger models could include the following:

1. Better upscaling of model results or elimination of the need for upscaling
2. While capital costs of these models may be high, the basic infrastructure would be reusable for many process trials
3. No lengthy regulatory approvals would be required for evaluating processes at or near field scale.
4. Large physical models allow more space and flexibility for instrumentation
5. More thorough post-process analysis of the altered reservoir.
6. Larger quantity of produced fluids for evaluation of performance in surface facilities, oil properties and upgrading/refining characteristics
7. Incorporation of geomechanical and capillary effects are more manageable on a larger scale model
8. Validation of reservoir simulation models

Regardless of the size of the physical model, experience and understanding of the benefits and limitations of the model in question are vital for interpreting the results and projecting them to field performance. Over the past thirty years (e.g., Ivory *et al.* ⁽¹⁾, and Stone and Ivory ⁽²⁾), the use of physical reservoir models has been an integral part of Alberta Innovates - Technology Futures (AITF) R&D programs. These programs in the areas of *in situ* heavy oil and bitumen recovery have contributed to the invention (e.g., Nasr ⁽³⁾), development (e.g., Lim *et al.* ⁽⁴⁾), and

understanding (e.g., Tremblay and Oldakowski ⁽⁵⁾) of processes currently in use or under development. The models have ranged in size from 10 cm (internal diameter) and 20 cm (length) x 10 cm x 2 cm up to 1.5 m (internal diameter) x 2.7 m (length), as well as field element models 3 m tall.

1.2. SCOPE

Producers participating in the Clean Bitumen Technology Action Plan (CBTAP) wish to examine the current state of the art in reservoir models at lab-scale and how these models accommodate the mechanisms involved in various *in situ* recovery processes. The models of interest are those focused on two main geological features:

- Canadian heavy oil and bitumen sandstone reservoirs at depths between 100 and 600 meters (excluding bitumen in carbonates)
- Reservoirs with the presence of shale barriers and water, gas, and thief zones

The *in situ* recovery processes and technology options being targeted for study include the following:

- SAGD
- Solvent and steam processes
- *In situ* combustion and air injection
- Heating with devices using electricity
- Biological processes
- Number of wells and well spacing, options for single, or multiple well patterns

1.3. APPROACH

AITF has had experience designing and building intermediate size models, which address some of the shortcomings of smaller scale models. For example, a transparent annular sand pack (TASP) model (2.4 m by 1.4 m) was designed, built, and operated ⁽⁶⁾ to examine mixing and transport mechanisms in solvent-based recovery processes. A more recent intermediate size model under construction was designed to account for field scale mixing effects in steam-solvent processes. As well, various sizes of *in situ* combustion models and models representing field elements during cold production have been designed, built, and operated. These experiences at AITF have shown that the capital and operating costs increase substantially with size. Particular operational challenges include model packing, oil cleaning and saturation with gas, and uniform saturation of the model sand pack with water and live oil. For example, experience with a large 1.5 m (ID) by 2.7 m (H) model (see Stone and Ivory ⁽²⁾) showed that packing such a model with oil sands had significant limitations caused by the introduction of trapped air and voids and was costly to operate. Confinement of the model also presented design challenges reflected in higher capital and operating costs. Designing, constructing, and operating significantly larger models than those presently used will require major changes in

thinking and approach if they are to approximate field scale performance, with all of its implied benefits, while remaining cost effective.

Based on current experience at AITF as noted above, the following activities were conducted to assess the state of the art for lab-scale reservoir models. The assessment was also used to suggest an approach to bridge the gap between current models and new functional models to meet the requirements of industry. Finally, this assessment should provide the necessary informational framework for a workshop contemplated by PTAC to explore the potential for larger scale models. The activities undertaken in this project include those listed below:

1. An overview is presented on the various *in situ* recovery processes and their mechanisms. The ability to scale the details of these mechanisms is also discussed.
2. The current state of knowledge concerning the design and operation of physical models was reviewed using published information. Any reported advantages and limitations of the models, based on their design and operation are discussed in light of the process variables that may be scaled or unscaled.
3. Design and operating considerations were compiled and are briefly discussed. Sanitized comparison cost data, where available, were compiled and are discussed.

2.0 STEAM-ASSISTED GRAVITY DRAINAGE (SAGD)

2.1. INTRODUCTION

Steam-assisted Gravity drainage, or SAGD, was developed by Roger Butler ⁽⁷⁾. SAGD is based on gravity drainage, horizontal wells, and injection of high-pressure steam for heat. The configuration is described below.

A horizontal well is drilled near the bottom of the formation. A horizontal injector is drilled parallel to it and about 5 meters above it. Steam injected into the upper well will condense and heat the sand and bitumen, mobilizing the latter and enabling it to drain to the lower producing well, where it is pumped to the surface. The steam chamber thus created expands as bitumen is produced, until most of the bitumen is drained from the drainage zone adjacent to the wells. The process is illustrated in Figure 2-1.

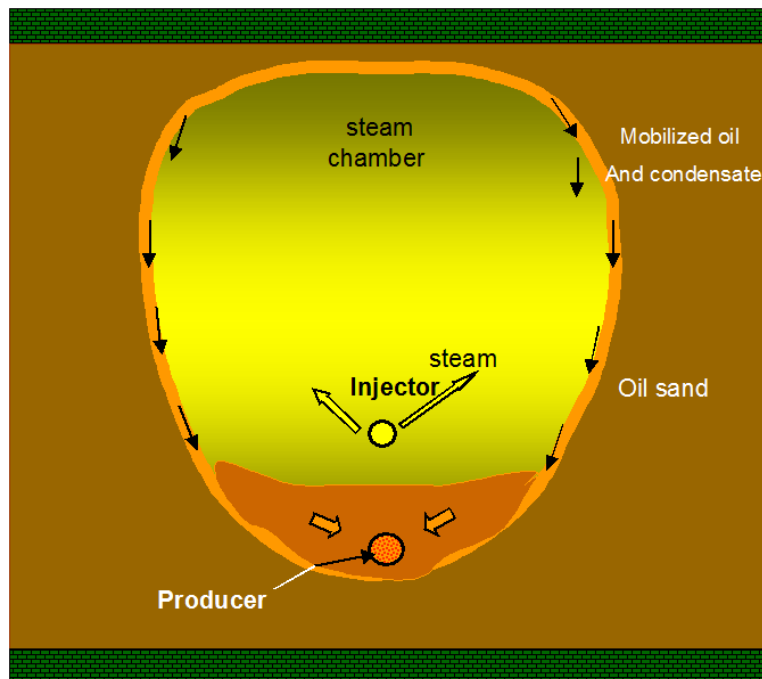


Figure 2-1 SAGD configuration and operation.

Early field trials were conducted at the Underground Test Facility (UTF) by AOSTRA ⁽⁸⁾. The process at the time relied on horizontal wells drilled from underground access tunnels. These tests demonstrated the feasibility of gravity drainage as a commercial bitumen recovery process. Development of the capability of drilling horizontal wells from the surface gave impetus to the evolution of SAGD. The technology has developed from field test to pilot plant to commercialization, and to where it is currently the major means of bitumen production from the Athabasca oil sands.

SAGD is initialized by circulating steam in both the injector and producer wells, through tubing. After several months of heating, once oil between the two wells achieves suitable mobility, circulation is stopped and the wells are switched to injection-production mode. The pressure difference between the wells is controlled so as not to cause premature steam breakthrough to the producer well during this circulation period.

In order to operate SAGD efficiently, steam trap control ⁽⁹⁾ is used. The temperature of fluids in the producer well is monitored, and the production flow rate is adjusted to maintain the temperature of the produced fluids about 5 °C to 20 °C below the steam condensation temperature at the production well pressure. The use of thermocouple or fiber optic temperature monitoring technology has enabled the detection of hot spots in the producer well where live steam is breaking through. This enables more precise control of the production well, including the use of fractional injection and production through the tubing and annulus of the injector and producer wells respectively, to maximize production while avoiding steam breakthrough. On the other hand, for some production strategies some amount of live steam production is allowed.

An area of current development is production from mature SAGD well patterns. This involves the use of non-condensable gas, injected with steam, or alone, at the conclusion of steam injection in a mature pattern. The objective is to maintain reservoir pressure, to avoid communication with neighbouring reservoirs, to permit draining of the remaining oil while injecting minimal additional heat. Experimental developments include SAGP by Butler ⁽¹⁰⁾ and various gas injection schemes including a wind-down scheme described by Aherne ⁽¹¹⁾.

SAGD is currently the preferred technology for Athabasca oil sands deposits too deep for surface mining.

2.2. SAGD MECHANISMS

Figure 2-2 shows a vertical cross section of the steam chamber. The steam chamber is expanding both upwards and sideways. Steam flows inside the chamber and condenses at the interface liberating heat to the surrounding reservoir. The liberated heat is transferred mainly by thermal conduction; the heated oil near the chamber is then mobile and drains due to gravity. Steam condensate and heated oil flow at the interface towards the lower production well. Thus, heat transfer in SAGD is a combination of convection and conduction processes. At the sides of the chamber, the interface is stable; however, at the top of the chamber the interface is unstable due to the generation of rising steam fingers created by the unfavorable mobility ratio between the steam and the cold oil. Oil heated by the steam moving inside these fingers flows around the perimeter of the fingers, down to the top of the steam chamber, and finally drains around the chamber rather than falling through it. Butler ⁽¹²⁾ indicated that, due to the low oil saturation, low oil relative permeability inside the chamber prevents oil flowing downwards into the rising steam chamber. Additionally, the steam condensate can advance upwards due to capillary imbibition, which prevents oil moving downwards due to interfacial tension effect (Figure 2-2) and, therefore, the oil flows laterally. Other mechanisms, such as changes in oil density, gas drive, and capillary pressure may contribute to the recovery factor. In particular, it is believed

that capillary pressure effect is not large in SAGD; however, water will tend to occupy the small pores, leaving only the big pores available for the steam. Therefore, the heat transfer area may be extended thus improving the SAGD performance.

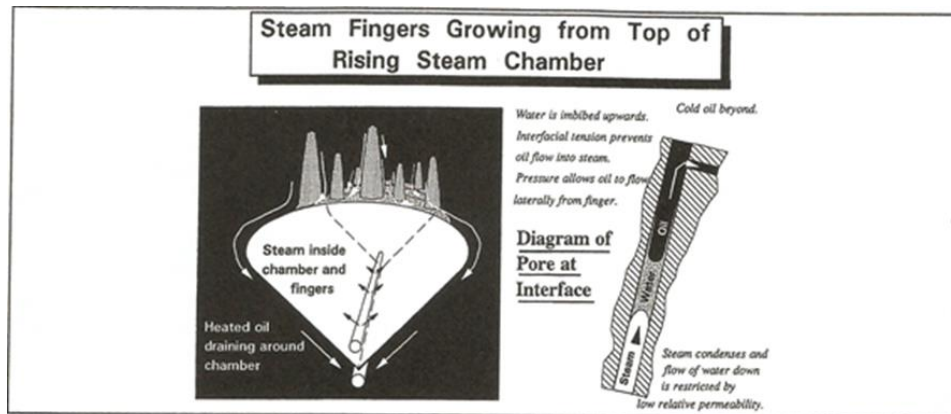


Figure 2-2 Steam chamber expansion (after Butler ⁽¹²⁾)

The steam chamber will grow upwards until it reaches the top of the formation. On the other hand, the chamber will grow laterally until it interferes with another adjacent chamber. Eventually, the drainage slope becomes too shallow and the flow path so long that the oil rate is too low for the process to be economic and this demarcates its end.

The impact of reservoir geomechanics on SAGD is not well understood and evidence of its effects is inconclusive. Additionally, because geomechanical effects are complex and not easily incorporated into physical models they have not been extensively investigated. Carlson ⁽¹³⁾ provides a comprehensive review of SAGD geomechanics. During SAGD, thermal expansion and the pressure of the steam chamber can induce stresses in the reservoir. Inclinerometers have recorded the effects (surface heave) of axial stresses at the surface of the UTF pilot. There are indications from the UTF Pilot and JOCOS Hanginstone that increases in absolute permeability, brought about by axial stresses, have affect SAGD operations and oil drainage rates.

2.3. PARAMETERS AFFECTING SAGD

McCormack ⁽¹⁴⁾ suggested that based on the generally accepted SAGD economic cutoff, a good reservoir should possess the following properties:

- pay thickness greater than 12 m
- continuous high quality pay with more than 10 wt.% of oil
- permeability higher than 3 Darcy
- no bottom water or top gas/water
- good cap rock integrity
- reservoir operating pressure greater than 1,000 kPa

Reservoirs with low thickness limit the SAGD process due to higher heat losses and lower available head pressure. The SAGD process is particularly sensitive to low vertical permeability;

therefore, any heterogeneity such as interbedded shales or inclined heterolithic stratification will negatively affect the SAGD process. Thief zones such as bottom water, top gas or top water limit the operating pressure of a SAGD process. Additionally, bottom water, top gas, or top water may act as zones of high mobility resulting in uncontrollable steam losses and, therefore, zones of wasted energy. Cap rock integrity is paramount in a SAGD process, since the cap rock provides a seal to the steam chamber. The maximum operational pressure of a SAGD process is limited by cap rock properties. Higher operational pressure implies higher steam temperature that is more favorable for reducing oil viscosity. Other parameters, such as clay content, fines movement, sand production, and steam distribution along the injector well are also important issues to consider in a SAGD process. Any parameter affecting or restricting the steam chamber expansion will have a negative impact on the overall SAGD process.

2.4. EXPERIMENTAL EVALUATION OF SAGD PROCESSES

A considerable number of experimental studies related to SAGD can be found in the open literature. Mechanistic and scaled experiments continue to improve knowledge and provide insights into the SAGD process. Some scaling criteria might result in the inadequate scaling of some mechanisms. The Pujol and Boberg ⁽¹⁵⁾ scaling criteria, for example, requires the permeability used in the laboratory to be much higher than field permeability, resulting in inadequate scaling of capillary pressure. Scaling complex reservoir conditions such as shale barriers, lean zones, bottom water, top gas, interbedded shales, inclined heterolithic stratification, cap rock conditions, etc., might be challenging, if not impossible in smaller physical models.

There is some uncertainty amongst bitumen producers regarding SAGD performance under complex conditions. Experiences from fields such as Long Lake, Tucker Lake, and Surmont provide ample demonstration of challenges. The effects of complex reservoir conditions on the performance of such demanding SAGD processes might be investigated through three-dimensional physical models. Additionally, well configurations like X-SAGD or operating strategies in complex reservoirs such as reservoirs with thief zones, might be investigated in more detail in a large three-dimensional cells rather than in a small two-dimensional models, which represent only a scaled portion of the reservoir. Scaling of the SAGD process is discussed in greater detail in later sections of this report.

2.5. CYCLIC STEAM STIMULATION

Some heavy oil or oil sand reservoirs, i.e., Cold Lake, are produced by Cyclic Steam Stimulation. Originally applied in the Orinoco Oil belt of Venezuela, CSS involves drilling a single vertical, slant, or horizontal well into the target formation. Steam is injected through the well at just above fracture pressure in order to have steam penetrate deeply into the cold, immobile oil. The injection is stopped, and the well is shut in for a brief period (typically a few days) to allow time (soak period) for transfer of thermal energy from the injected steam to the formation. The well is then placed on production. During the early stages of production, the fluids will flow freely to the surface. When the reservoir pressure has been reduced, the well is put on pumping to continue to deliver oil and water. During the final phase, oil rate (and fluid temperature) declines until the production rate is no longer economic. At this point, production is stopped and the steam injection is repeated.

CSS depends on multiple mechanisms to mobilize oil, bring it to the production well, and produce it. Some significant mechanisms include gravity drainage, reservoir compaction/dilation, solution gas drive, foamy oil flow, and thermal expansion of reservoir fluids. Beatty, Boberg, and McNabb ⁽¹⁶⁾ provide a good discussion of mechanisms. The exact portions of these mechanisms will vary from reservoir to reservoir. Some organizations have developed Type Curves ⁽¹⁷⁾ to help predict the performance of a specific reservoir site.

As the reservoir becomes more depleted, larger amounts of steam are required per barrel of oil produced due to increases in the size production zone and associated heat losses. Lower solution gas saturation in the reservoir, after successive steam injection and production cycles, also affect production rates. The well/pattern is deemed to have reached maturity when increasing steam to oil ratio (SOR) makes it uneconomic to proceed with additional steam injection cycles.

3.0 SOLVENT-STEAM

3.1. INTRODUCTION

Solvent-steam processes are still under development and are, therefore, not as advanced as SAGD or CSS. In the case of ES-SAGD, mechanistic lab-scale investigations, as well as field pilots are being pursued actively by various organizations and much remains to be learned about this process. In this section, current research into solvent-steam processes and knowledge gaps are summarized. Some of the major field pilots are briefly discussed, although available information is rather sparse. Other solvent-steam processes such as Solvent Assisted SAGD (SAP), Steam Alternating Solvent (SAS), and, Steam Butane Hybrid (SBH) are also briefly discussed. Even though they are not essential to this report, pure solvent processes are also discussed because they constitute one end of the continuum of solvent-steam process. Therefore, we also provide brief descriptions of N-Solv, Vapor Extraction (VAPEX) and Cyclic Solvent Stimulation.

3.2. EXPANDING SOLVENT-SAGD (ES-SAGD)

The Expanding Solvent-SAGD process (ES-SAGD) uses heat and solvent dilution to mobilize high viscosity oil in the reservoir. ES-SAGD uses the same well configuration as the SAGD process, but with co-injection of steam and a hydrocarbon additive at relatively low concentration. The solvent is chosen in such a way as to evaporate and condense at the same conditions as the injected water. In this way, the injected solvent will condense with the steam at the boundary of the steam chamber, and in conjunction with the heat will dilute the oil and effectively reduce the oil viscosity. A schematic of the process is shown in Figure 3-1.

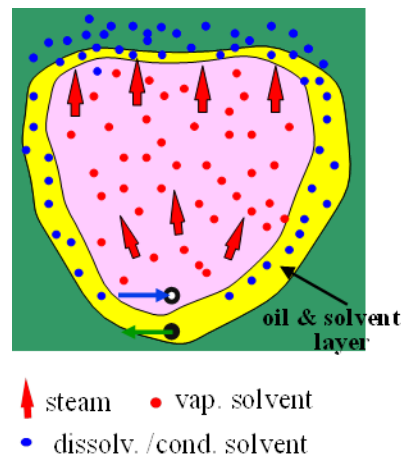


Figure 3-1. Schematic of the ES-SAGD process.

3.2.1. Initial Lab Tests

The ES-SAGD concept was initially tested in the laboratory through a series of solvent screening experiments. The experiments involved a variety of hydrocarbon solvents and a diluent of varied vaporization temperature. Models (same as those used for SAGD) were packed with

silica sand and saturated with live heavy oil, and a steam / vapor solvent mixture was injected. Using a fixed solvent-to-steam ratio, the effect of different solvents on oil drainage rate could be measured.

It was discovered that co-injection of non-condensable hydrocarbons such as C1 and C2 with steam did not improve oil production as compared to traditional SAGD. Co-injecting the more condensable C3 to C8 alkanes and the diluent with steam, resulted in better oil drainage rates with C6 and diluent improving oil drainage rates the most. Of the solvents tested, C6 has a vaporization temperature closest to the steam temperature, suggesting that the maximum oil drainage rate occurs when the solvent vaporization temperature matches the steam temperature. The results also suggest that using a solvent with a vaporization temperature ± 50 °C around the steam injection temperature would result in a significantly improved oil drainage rate.

3.2.2. Parametric Studies

Parametric studies were performed for the ES-SAGD process using lab-scale physical models. Key variables that were examined include permeability, oil viscosity, gas content in oil, steam injection rate, solvent-to-steam ratio, and injection pressure. The tests were performed in a 2D canister model inside a high temperature and pressure vessel. The model was filled with clean sand and saturated with water and oil in sequence. Steam was injected both by itself and with a solvent vapor to compare. Both produced fluids and vented gasses were measured.

These tests demonstrated that the oil production rate was increased for ES-SAGD compared to SAGD, particularly in the early stage of the test with matching injection conditions (injection temperature/pressure and steam injection rate). However, small lab scale models miss some key mechanisms related to mixing effects for heavy oil and solvents in porous media.

3.2.3. Numerical Simulations

Numerical history matching of ES-SAGD lab experiments was performed using the CMG STARS reservoir simulator to validate the numerical model and carry out a sensitivity study on significant mechanisms.

For the ES-SAGD experiments that were simulated, good or reasonably close history matching of the fluid production and temperature profile was achieved, which suggests that the numerical model is capable of capturing general characteristics of ES-SAGD at the lab-scale. Key findings from the numerical analysis of 2D ES-SAGD physical model experiments include the following:

- The co-injected solvent transports with the steam in the vapor chamber, with a portion of the solvent dissolving into the bitumen along the boundary of the vapor chamber, lowering the viscosity of the oil along the drainage front.
- Solvent components distribute differently within the reservoir. The light end of the solvent tends to spread to the chamber boundary while the heavy end tends to stay near the injector.

- Some key parameters in the numerical simulation, including solvent solubility and dispersion in the oil phase, affect oil production behaviors. High solvent loading results in a stronger solvent dilution effect.
- The effect of gas-liquid con-current and counter-current flow on oil drainage during the early stage of the process should be treated differently in the numerical model in order to adequately simulate the process in the field-scale.

The numerical model was then used to evaluate the ES-SAGD process at field-scale for an Athabasca-type reservoir with dead bitumen and a Cold Lake-type reservoir with live heavy oil. These simulations revealed the following:

- The ES-SAGD process has better oil and gas production than the SAGD process, and the cumulative oil production vs. net energy input is lower for ES-SAGD.
- High solvent loading results in increased oil production.
- The largest incremental oil production rate by the ES-SAGD process occurs shortly after solvent injection commenced, with most of the improvement occurring during the first 2-4 years.
- Better oil production from ES-SAGD results from earlier solvent injection. However, the ultimate oil recovery for the ES-SAGD process with a different solvent and co-injection starting time remains almost the same.

3.2.4. Mechanistic Study

Lab-scale physical model experiments have demonstrated increased oil production from the ES-SAGD process; however, the mechanisms involved are not fully understood. To quantify these mechanisms, studies have been initiated. Key research activities at AITF include the following:

- Fine scale numerical modeling of ES-SAGD using hexane and diluent along with measured PVT data to identify the potential impact of physics that are missing from the simulator.
- Measurement of PVT properties for Athabasca bitumen/solvent fluid mixture to support numerical analysis of an ES-SAGD lab experiment.
- Characterization of phase behaviour and properties of Athabasca bitumen / solvent fluid mixtures for different solvent candidates, and temperature/pressure conditions relevant to the ES-SAGD process.
- Modeling the Athabasca bitumen-diluent mixture fluid behaviour in reference to experimentally measured PVT data.
- CT experiments to examine fluid flow behaviour in porous medium under hybrid process conditions.
- Elemental experimentation of ES-SAGD process - semi field-scale test of steam-solvent co-injection in a large 2D visual model (1.5 m x 1.5 m)

- Field-scale evaluation of the ES-SAGD process incorporating mechanisms important to the hybrid steam / solvent co-injection process to improve the quality of numerical models.

3.2.5. *Field Tests*

3.2.5.1. *Burnt Lake ES-SAGD Pilot*

The Burnt Lake pilot was intended to validate the ES-SAGD technology by injecting a small fraction of solvent with steam into an existing three well-pair SAGD operation. The existing reservoir had been in operation for about 2.5 years, and was in the Clearwater formation. The intention was to use one of the injectors initially, and use the other injectors if performance improvements were observed. The field test was planned to run for 6 – 12 months. Pilot data had not been publicly released.

3.2.5.2. *Firebag ES-SAGD Pilot*

The Firebag pilot was intended to demonstrate the ES-SAGD technology where oil viscosity was very high. The reservoir for this pilot was in the McMurray formation. The proposed solvents for this pilot include sweet naphtha, sour naphtha, commercial condensate, and diesel, which were available at the site. The amount of solvent to be used was intended to be up to 15% v/v of the injected steam on a cold-water equivalent basis. Pilot data had not been publicly released.

3.2.5.3. *Senlac SAP Pilot*

The Senlac pilot was started in late January 2002, in the Dina/Cummings formation. The objectives of the pilot were to assess the process feasibility, as well as to evaluate the facility requirements. The solvent used was butane, and steam injection rates were relatively unchanged from the point prior to adding solvent. The pilot was terminated shortly after March 2002 when the reservoir showed the loss of containment.

3.2.5.4. *Christina Lake SAP Pilot*

Encouraged by the results of the Senlac SAP pilot, EnCana started testing SAP at its Christina Lake thermal project in the Athabasca formation with the goal of testing the applicability of steam and solvent co-injection in the Alberta oil sands. The operation was similar to that of the Senlac pilot, with the exception that the produced solvent was recovered and recycled. The pilot began in the third quarter of 2004, and initial data showed a production increase as well as a SOR decrease. Data has not been released for the period after February 2005.

3.3. SOLVENT ASSISTED PROCESS

Solvent Assisted Process (SAP) was advocated by Gupta *et al.* ⁽¹⁸⁾ as an enhancement to SAGD. In SAP, a quantity of solvent (~15 vol.%), is injected with steam in a SAGD operation. The solvent condenses at the oil boundary in the vapour chamber, dilutes and mobilizes the oil, and enhances oil drainage and production rates. It was field tested at Christina Lake by EnCana. Initial positive results were reported.

3.4. STEAM-ALTERNATING-SOLVENT

Steam-Alternating-Solvent (SAS) was advocated by Zhao ⁽¹⁹⁾. This is an enhancement of the SAGD process in which the SAGD process is started using steam only, then the steam is turned off and a volatile solvent is injected for a suitable time interval. The solvent is then stopped and steam is turned on for a similar time interval. The process is repeated until the reservoir reaches maturity (declining oil rates, most of the available oil produced). The process has not been field-tested.

3.5. STEAM-BUTANE HYBRID

Steam-Butane Hybrid (SBH) is a variation of SAGD developed at AITF by Frauenfeld *et al.* ⁽²⁰⁾. In this process, a SAGD configuration is used with injection of steam and a larger quantity of a volatile solvent (n-butane), typically at a solvent to steam ratio of 1.0 to 2.0. The steam carries the majority of the heat used to run the process. The steam and solvent mixture migrate through the vapour chamber to the vapour chamber boundary. The steam condenses first, leaving almost pure butane to condense at the vapour chamber boundary. SBH is intended to achieve the low energy consumption characteristic of VAPEX, while using a modest amount of heat in order to speed the process sufficiently to achieve SAGD-like rates. The Hayduk-Cheng correlation ⁽²¹⁾ for diffusivity of solvent in heavy oil predicts that such a speed-up is possible at operating temperatures well below those characteristic of SAGD.

The process was shown to operate at lower pressure than SAGD while providing oil rates and recovery equivalent to low pressure SAGD, but with much lower SOR, as low as 1.0. Experiments have been performed to examine the rate of gravity drainage due to solvent extraction ⁽²²⁾. The process has been tested by laboratory experiments and by numerical simulation ⁽²³⁾. Simulations predict that the process will have an advantage over SAGD in marginal reservoirs but not been field-tested.

3.6. PURE SOLVENT PROCESSES

Information about the following processes is provided for completion of the continuum of processes from pure steam to solvent plus steam.

3.6.1. N-Solv

The N-Solv process was developed by Nenniger, Hatch, and Dunn ⁽²⁴⁾. N-Solv involves a SAGD well configuration, but only solvent is injected. The solvent is typically propane in the vapour

phase, and is heated to approximately 60 °C. The solvent vapour condenses at the oil vapour chamber boundary as does steam in SAGD. The diluted oil and solvent then drain to the production well. Because the solvent has a low latent heat relative to steam, the solvent to oil ratios for N-Solv are relatively high. One consequence of this is asphaltene dropout, leaving an upgraded oil to be produced. The other consequence is that the asphaltenes (and some polars) remain in the reservoir as solids or semisolids. The residue can account for up to 1/3 of the oil in place. The process has much lower energy consumption than SAGD, and has potential for high oil rates. The process has not been field-tested.

3.6.2. VAPEX

VAPEX (Vapor Extraction) was developed by Butler *et al.* (25) as a solvent analog to SAGD. VAPEX uses a well configuration similar to that used by SAGD, namely a horizontal producer at the bottom of the reservoir, a horizontal injector several meters above it, and an expanding vapour chamber connecting the two wells. A solvent, typically propane or butane, is injected through the upper well. The solvent vapour migrates to the boundary of the vapour chamber, where, the bitumen or heavy oil is contacted by solvent vapour. The solvent vapour dissolves in the oil and mobilizes it. The mobilized oil drains to the lower well, where it is pumped to the surface. The VAPEX process has a very low energy requirement, but is much slower than SAGD, due to the low diffusion rate of solvent into cold, highly viscous oil or bitumen. A schematic is presented in Figure 3-2.

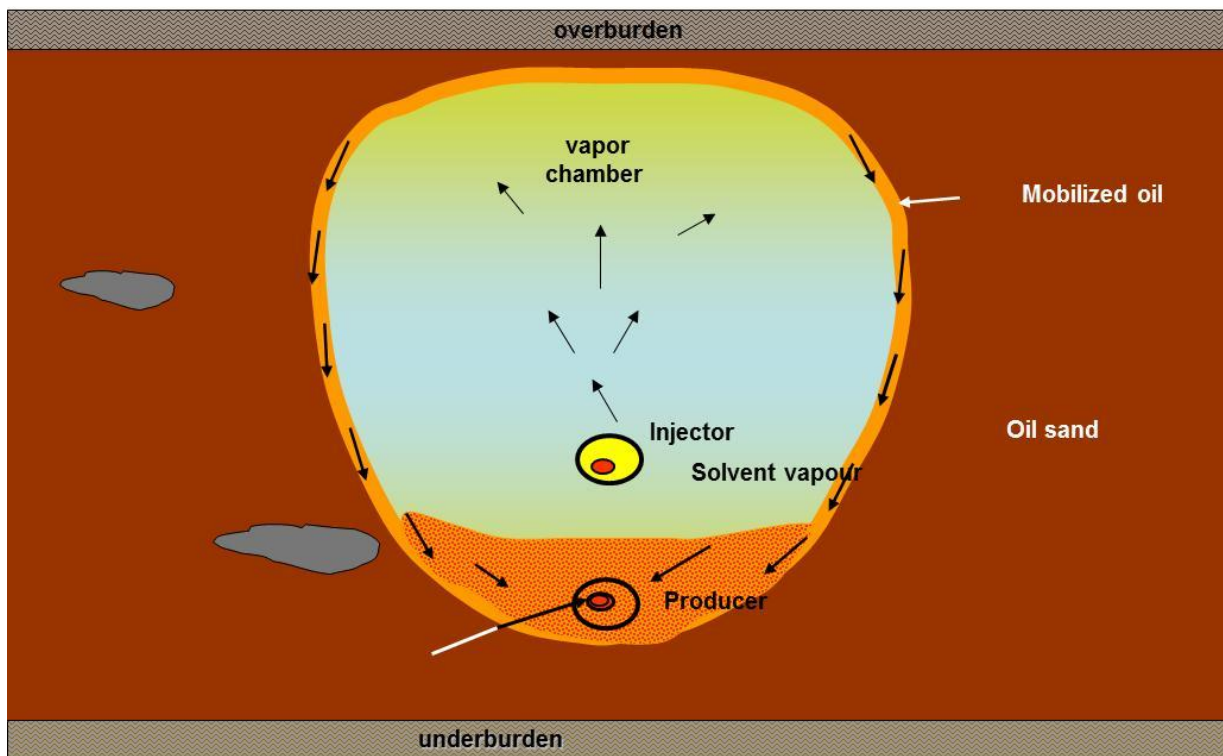


Figure 3-2. VAPEX configuration.

3.6.3. *Cyclic Solvent Stimulation*

Cyclic solvent stimulation has been advocated for heavy oil reservoirs that are thinner and lower viscosity, e.g., Lloydminster, where heat loss would preclude the application of thermal methods. In this process, a mixture of volatile solvents, e.g., CO₂ and propane, is injected into the formation through a vertical or horizontal well. After a suitable soak interval, the well is placed on production. The solvent performs two functions, namely it dilutes the oil and reduces its viscosity, and it provides a solution gas drive as reservoir pressure is reduced. Laboratory studies ⁽²⁶⁾ have indicated some potential.

4.0 IN SITU COMBUSTION

4.1. INTRODUCTION

In situ combustion (ISC) is an oil recovery process in which an oxygen-containing gas is injected into a reservoir. The oxygen reacts with a portion of the oil in place thus supplying energy to displace oil to the producing well bores. Generating heat within the reservoir gives ISC the potential to be more efficient and economical than steam injection processes; the process is not compromised by heat losses in a steam generator, transmission lines, wellbore and overburden, and the fuel comes from the residual heavier components of the reservoir oil. Other prospective advantages of ISC are that heavy equipment for steam generation is not needed, the amount of water to be handled is greatly reduced, and some degree of upgrading may be achieved. The process, however, has not gained wide spread use, largely because of past experience with failed field projects. Major causes of the failures can be attributed to the inability to achieve high temperature combustion during ignition, failure to maintain an adequate air injection to sustain high temperature combustion, and poor conformance.

There are several obstacles that need to be overcome in order to develop a successful ISC operation. The first is to maintain high temperature combustion at the combustion front. Usually high-pressure air or enriched air injection is used to ensure sufficient oxygen supply at the front. This, however, may create a second obstacle, which is fingering and air override instability. Both phenomena reduce the efficiency and eventually may cause burn out of the production well. The third obstacle is how to remove effectively the mobilized oil. The last one is particularly critical for Canadian heavy oil and bitumen where initial oil mobility is so low that the oil ahead of the combustion front is difficult to displace. Any successful *in situ* combustion process has to overcome these obstacles.

The traditional *in situ* combustion process involves patterns of vertical injection and production wells. Many field tests ^(27; 28) were conducted using the traditional vertical wells. Since this approach failed to address the second and third obstacles mentioned above, it is not surprising that these projects enjoyed limited to poor success. As horizontal drilling technology became available, new combustion processes have been proposed using the horizontal well technology. Examples of these new technologies will be discussed.

4.2. ISC DESCRIPTION AND MECHANISMS

The ISC process is initiated by injecting oxygen-containing gas into an injection well where it ignites the nearby oil, creating a combustion front. Ignition is a temperature sensitive occurrence and is usually supported in the field by a gas burner, electrical heater, or chemical additive. In reservoirs with elevated bottom-hole temperature (i.e., deep reservoirs or reservoirs heated by a preceding process), auto ignition may be achieved after a period of injection. At higher temperatures, the oxidation rate and heat produced by low-temperature oxidation (LTO) reactions may be significant enough to raise the temperature of the reservoir gradually until high temperature combustion (HTC) develops.

Oxygen-containing gas is injected while the combustion front advances away from the injection well at a rate principally governed by the type and amount of fuel available, and by the oxygen flux. Several distinct zones develop and a number of different but intimately related mechanisms become active. These zones are illustrated in Figure 4-1, which depicts a cross-section of a stable combustion front as it advances left to right between an injection and production well. The upper portion of the figure illustrates the formation temperature and the lower profile is the corresponding saturation profile.

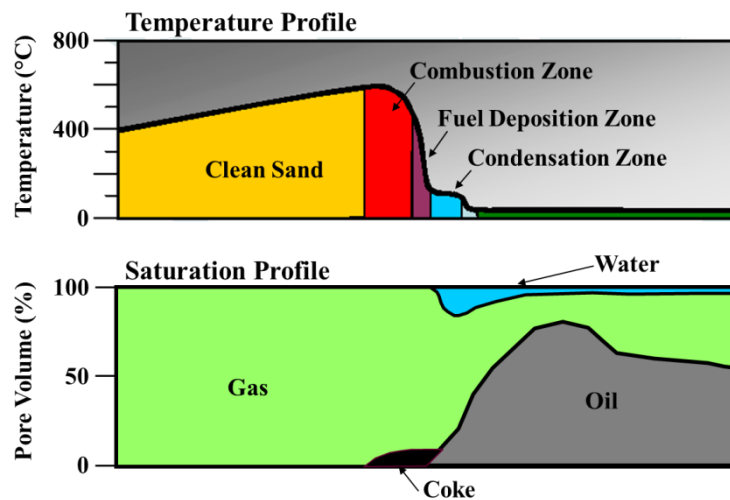


Figure 4-1. Temperature and Saturation Profiles during ISC Process.

4.2.1. Combustion Zone:

The reaction primarily taking place in this region is HTC, which is consuming a coke-like fuel being deposited at the leading edge of the advancing front. The reaction consumes oxygen and generates water (steam) and carbon oxide gases, and leaves behind clean hot sand. Temperatures in this zone can reach values of 300 to 800 °C.

4.2.2. Fuel Deposition Zone:

Ahead of the combustion zone, the temperatures are between 200 °C and 400 °C and are high enough to vaporize lighter hydrocarbons and interstitial water, which then flow ahead. Immediately ahead of the combustion, the high temperatures thermally crack remaining hydrocarbons producing a coke and gaseous hydrocarbons. In addition, unreacted oxygen flowing through the combustion zone reacts with remaining oil in low temperature oxidation (LTO) reactions. LTO is an exothermic reaction characterized by the incorporation of the oxygen into the hydrocarbon chain resulting in the generation of complex compounds with little or no production of carbon oxides. If prolonged, LTO results in the formation of a heavy solid coke-like material. The coke from thermal cracking and LTO is deposited on the sand grains and becomes the fuel consumed in the combustion zone.

4.2.3. Condensation and Displacement Zone:

Although ISC is normally thought of as a thermal process, it is also very much a displacement process. Oil downstream of the combustion zone is heated and mobilized by a number of sources:

- conduction
- latent heat released by condensing steam formed through HTC in the combustion zone and through vaporization of interstitial water
- heat imparted to the oil by the condensing hydrocarbon gases formed through distillation and cracking
- convection from the flowing combustion gasses
- mixing of the oil with the condensing hydrocarbon gases
- partial dissolution in the oil of the carbon dioxide generated in the HTC

The condensation zone is characterized by a plateau in the temperature, which is generally equivalent to the steam saturation temperature at the operating reservoir pressure. The flowing steam and gases forms a very effective gas drive to push the mobilized oil through the displacement zone.

Although the displacement mechanisms immediately ahead of the combustion front are very efficient, for the mobilized oil to be produced at the production well it must flow through the unheated region of the reservoir. This can result in the formation of a highly saturated oil bank with severely restricted gas mobility, often leading to the stalling of the combustion front and failure of the ISC operation. Most of the new ISC concepts are focused on overcoming this detrimental phenomenon, either through the application of alternative well configurations or modified operating strategies.

4.3. WET COMBUSTION

A major variation of ISC is wet combustion where water is injected with the oxygen-containing gas. The injected water scavenges heat from the burned out zone behind the combustion front, which would otherwise be lost to the recovery process. The heated water approaches the combustion front and is flashed to steam. The heat is transported through the combustion zone by the steam and transferred to the condensation zone when the steam condenses. The potential benefits of wet combustion are as follows:

- more efficient condensing steam drive
- the condensation and displacement zone is larger
- less residual oil for fuel thus lower air requirements for a given volume of reservoir

4.4. ISC CONFIGURATIONS AND VARIATIONS

4.4.1. Traditional ISC

Traditional ISC involves the use of vertical injection and production wells. Two different well configurations have been used, patterns (contiguous or isolated) and line drive. Generally, the line drive configuration has greater advantages:

- the process can make use of gravity by placing the row of producers down dip of the row of injectors
- once the first production row is intercepted by the combustion front, it is converted into injection, while behind, the former injection row is used for water injection or simply shut off
- greater control of the advancing front
- less ignition operations
- easier and more reliable tracking of the ISC front

In fact, the most successful traditional ISC commercial projects operating in recent times are all line drive configurations with a down dip combustion front advancement: Suplacu de Barcau in Romania ^(29; 30), and the Balol/Santhal ^(31; 32) projects in India.

Pattern configurations, on the other hand, are better suited to different well completions for injectors and producers. Overall oil rate can be increased by operating simultaneously as many patterns as desired and pattern configurations are more amenable to multilayer formations. Both pattern and line drive configurations of traditional ISC, however, are susceptible to gravity override of the injected gas, formation of oil banks, and poor conformance. With the development of horizontal well technology, new ISC combustion well configurations are being conceived.

4.4.2. New Configurations

4.4.2.1. Toe-to-Heel Air Injection (THAI)

In the THAI process ⁽³³⁾, combustion is obtained by injecting air into an oil-bearing formation, through an injection well located at the toe of a horizontal production well. The combustion advances horizontally as a vertical front from the “toe” to the “heel” of a production well. A sketch of the process is depicted in Figure 4-2. In this process, mobilized oil in the front of the combustion zone is drained by gravity to the production well. There is no need to push immobile oil and high temperature combustion can be maintained by sustained air injection. This process is also less subject to severe gas override instability since the production well is at the bottom of the pay zone. To date the process has been pilot tested in the Athabasca oilsands (no detailed results published) and is currently being tested in a conventional heavy oil reservoir.

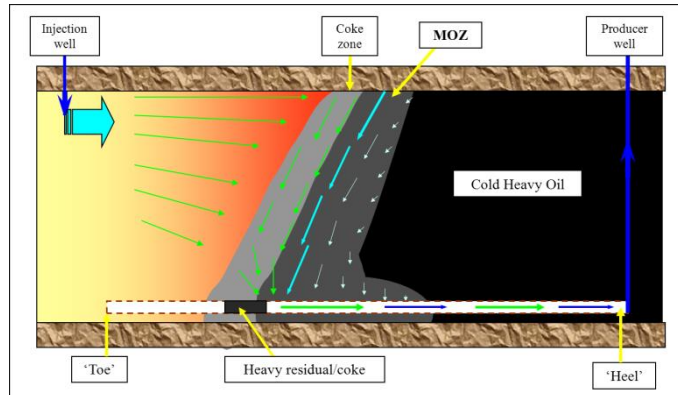


Figure 4-2. Schematic of THAI Process.

4.4.2.2. COSH and COGD Processes

A schematic of the Combustion Override Split-Production Horizontal Well (COSH) process ⁽³⁴⁾ is provided in Figure 4-3. ISC is initiated through vertical injectors perforated high in the reservoir. The combustion front then propagates downwards, towards a horizontal producer located low in the pay zone. Initially, the front is temporarily propagated laterally towards lateral gas production wells, which may produce some liquids as well. The horizontal well is designed to produce mainly liquids, while the gas producers will produce mainly gas. The Combustion Overhead Gravity Drainage (COGD) process is a variation of COSH intended for bitumen reservoirs. Neither of these concepts has been field-tested.

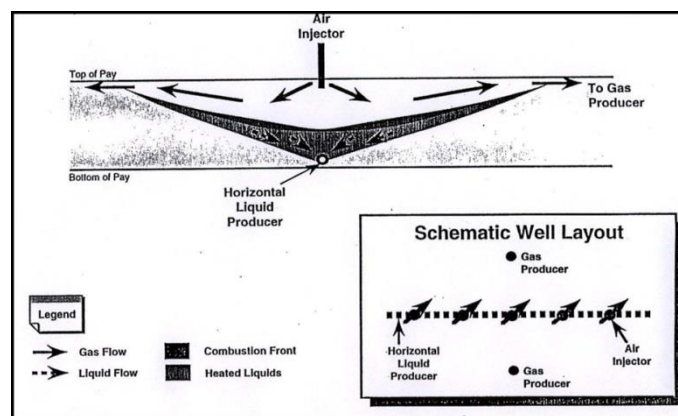


Figure 4-3. Schematic of COSH Process.

4.4.2.3. Top-Down ISC Process (TD-ISC)

The TD-ISC process ⁽³⁵⁾ is similar to the COSH process in that it utilizes an injection well completed high in the reservoir and a horizontal well located near the bottom. The TD-ISC does not utilize gas vent wells but rather it incorporates an artificial vertical high permeability path

from injector to producer to provide an initial conduit for the mobilized oil and combustion gasses to follow. Figure 4-4 shows a schematic of the concept. TD-ISC has not been field-tested.

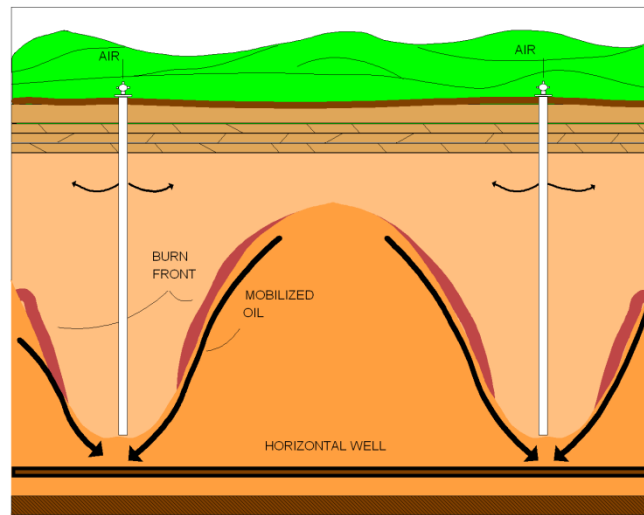


Figure 4-4. Schematic of TD-ISC Process.

4.4.3. Alternate Operating Strategies

Many of the mechanisms involved in ISC, ignition, combustion kinetics, and displacement efficiency are highly dependent on the formation temperature. Therefore, steam pre-heating is a logical method to generate sufficient mobility to allow combustion to achieve efficient operation. The concept of 'Steam Assisted *In situ* Combustion' was utilized at BP's Marguerite Lake project^(36; 37) where cyclic steam simulation was used to develop initial oil mobility in a traditional ISC configuration.

One of the most successful ISC field tests carried out in Alberta was the Morgan ISC Field Pilot⁽³⁸⁾ carried out between 1980 and 1993. The pilot project had 46 vertical wells in nine-inverted seven-spot patterns and throughout its lifetime involved successive periods of primary production, cyclic steam stimulation, steam-air stimulation, and pressure-cycling ISC (PC-ISC). In addition, operating logs report significant quantities of sand produced. The PC-ISC period was particularly productive; however, it is not apparent whether its realization is due in combination or individually to the primary sand production (formation of CHOPS like wormholes), pre-heating from previous processes, or the pressure cycling.

Recently *in situ* combustion has been considered as a follow up to SAGD⁽³⁹⁾. Conditioning the reservoir by first performing SAGD creates void space for injectivity, preheats a portion of the formation to promote rapid ignition, and establishes some oil mobility to enable advancement of the combustion front. Overall recovery from the pattern could be improved by displacing residual oil from the steam chamber, by displacing oil from trapped zones, and by recovering additional oil from the walls and ceiling of the chamber.

A second example of hybrid SAGD and ISC is MS-CAGD ⁽⁴⁰⁾. MS-CAGD involves a pair of horizontal injector/producer wells as in SAGD and horizontal offset producers, located some distance laterally from the well pair. After a period of operation in a SAGD mode, air is injected into the reservoir via the SAGD injector. The offset wells are put into production and the combustion front advances laterally from the steam chamber. Vertical vent wells are added to vent off combustion gases. For field development, the process can be extended by adding additional offset producers as necessary. Figure 4-5 shows a schematic of the MS-CAGD configuration.

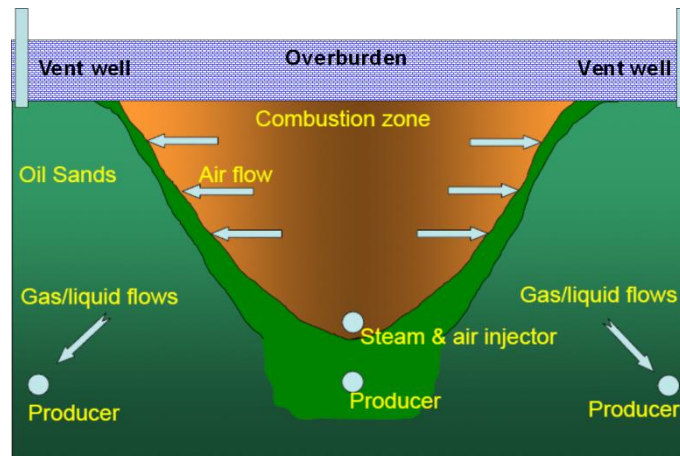


Figure 4-5. Schematic of MS-CAGD Process.

4.5. PHYSICAL MODELING OF *IN SITU* COMBUSTION

ISC depends on the occurrence of multiple chemical reactions between crude oil and the injected oxygen within the reservoir porous media. These reactions are consecutive, interdependent, and competing and occur within different temperature ranges. The extent and nature of these reactions, as well as the heating they produce, are dependent on the properties of the oil-matrix system. Generally, in physical modeling of fluid injection processes, the scaling rules involve the alteration of the oil-matrix system to conserve certain physical mechanisms. In addition, the time is also scaled. It is very difficult, if not impossible, to effectively change the kinetics of the multiple chemical reactions to account for these variations. Due to the complex mechanisms of *in situ* combustion and the difficulty in properly scaling the necessary parameters, the use of scaled physical models to provide field fluid rate and process development predictions is not practical.

Three-dimensional physical models of ISC, however, can be effectively used to provide information on the behavior of the *in situ* combustion process under specific reservoir conditions, like shale barriers for example. They can provide sweep efficiency estimates for different displacement concepts, such as well configurations or operating strategies. In these types of physical models, the field oil-matrix system is duplicated in the laboratory; rather than the model representing a scaled portion of the reservoir it can be viewed as a distinct element of the reservoir.

The degree and character of the chemical reactions involved in ISC are much more affected by heat losses than the mechanisms entailed in other recovery processes; therefore, heat loss to the surroundings is a critical consideration in designing a physical model experiment of ISC. It is virtually impossible to match perfectly the heat loss to the surroundings between a laboratory model and the field; however, if the model is sufficiently large enough, information on the behavior of *in situ* combustion is gained before heat losses from the boundary become influential.

In addition to providing information on the behavior of *in situ* combustion, results from physical model experiments provide data for developing and calibrating numerical simulation models. These numerical models can then be used to tune and predict field operations.

5.0 ELECTRICAL HEATING

5.1. INTRODUCTION

Envisioned as an alternative technology to SAGD, electrical heating of the Alberta oil sands for the recovery of bitumen has been studied since the early 1970s ^(41; 42). Electrical heating is a thermal process applied in oil sands deposits that has the same objective as other thermal technologies of accelerating the hydrocarbon recovery. Compared to the steam injection processes like SAGD, electrical heating processes are mostly free of problems related to low initial formation injectivity, poor heat transfer, shale layers between rich oil sand layers, cap rock requirement, and the difficulty of controlling the movement of injected fluids and gases ⁽⁴³⁾.

In the past decades, intensive research has been conducted on the electrical heating technology in terms of different process configurations and applications. We have arbitrarily separated the mechanisms for electrical heating into ohmic heating (i.e., with DC and low frequency AC currents) and electromagnetic heating (i.e., dielectric heating governed by Maxwell equations) to simplify this discussion.

5.2. OHMIC HEATING MECHANISM

Despite the variety of electrical heating process configurations and/or applications proposed, developed, and tested at lab scale or field scale, they are all based on raising the reservoir temperature so that the bitumen can flow. The heavy oil reservoir consists of sand, oil, water, and gas. Since the sand matrix has a very high electrical resistivity, the electrical current flow in the reservoir formation is by conduction through the water-saturated portion of the interconnected pore spaces, as shown in Figure 5-1 ⁽⁴³⁾. The conducting path for electrical current is through the continuous connate water, which envelops the non-conductive sands particles so the electrical energy is converted to heat by the “ohmic heating” (i.e., Joule heating or resistant heating) mechanism along these pathways and heat is then transferred to the oil sand particles by conduction. The large surface area between the water film and the sand particles facilitates the rapid heat transfer.

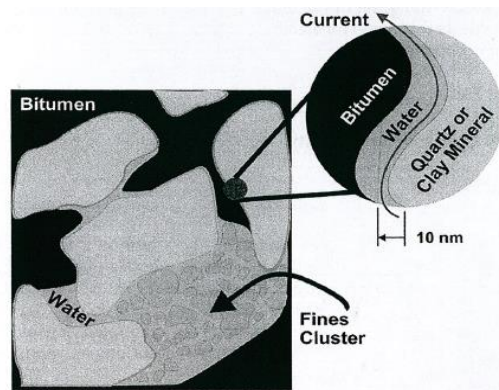


Figure 5-1. Interconnected water-saturated pore spaces within bitumen sands matrix ⁽⁴³⁾.

The water chemistry of connate water, i.e., dissolved ions and their concentrations, will significantly impact the conductivity of the reservoir formation (Figure 5-2) and thus impact the efficiency of electrical heating processes, whether alternate current (AC) or direct current (DC) is applied.

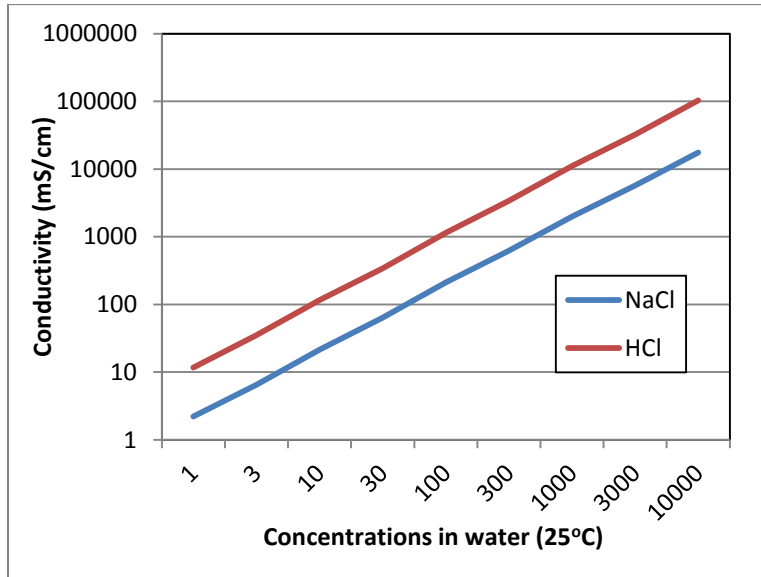


Figure 5-2. Electrical conductivities of some electrolytes in water at 25C.

5.2.1. Process configuration and application

Electrical heating processes usually have the common essential components of power supply, power delivery system, electrode assembly, and current return/ground return ⁽⁴⁴⁾. The power supply could be low frequency (e.g., 2 to 60 Hz) AC or DC. The power delivery system may consist of tubing, cables, or a combination of both, which is designed to minimize electrical losses and to be non-obstructive to the existing production well system. The electrode assembly is designed to optimize the effectiveness of heating in the oil reservoir. Electrical current leaves the power supply system and is conducted to the electrode, which is in electrical contact with the reservoir formation. From the electrode, the current is forced to flow through the reservoir and return to the power supply system.

Different configurations of electrode assembly have been proposed and investigated. Figure 5-3 shows the configuration of electrical heating electrodes in a single wellbore by Vinsome *et al.* ⁽⁴⁴⁾, where tubing and casing were used as electrodes. McGee *et al.* ⁽⁴⁵⁾ reported field test of Electrical Horizontal Well Project in the Lloydminster heavy oil area, which used a combination of vertical and horizontal wells for electrical heating system, as indicated in Figure 5-4. Figure 5-5 shows the electrode configuration as well as production well for the Electro-Thermal Dynamic Stripping Process (ET-DSP™) proposed by McGee *et al.* ⁽⁴⁵⁾. In this process, a matrix of vertical electrodes and production wells are employed, in which each electrode (anode or cathode) or

production well is in an individual wellbore. Figure 5-5 only shows the one electrode pair and its adjacent production well.

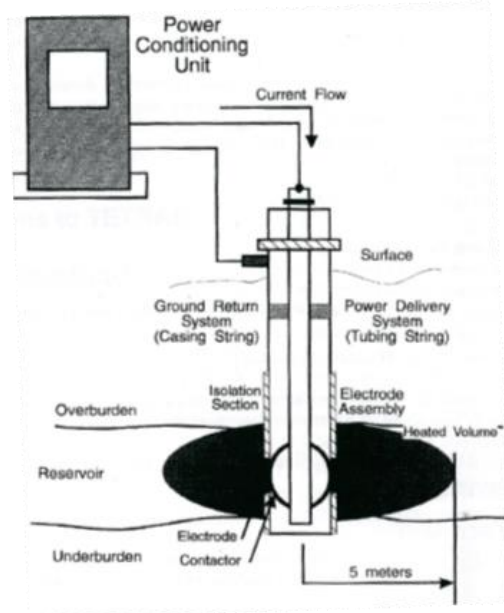


Figure 5-3. Electrical heating single wellbore configuration (oil production equipment not shown) (44).

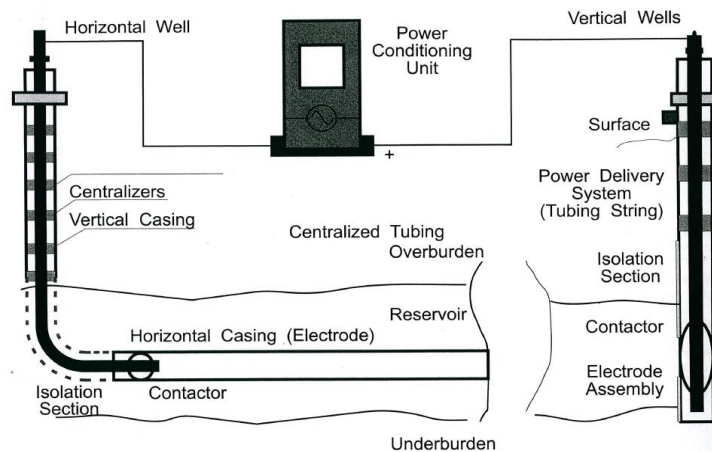


Figure 5-4. Combination of vertical and horizontal wells for electrical heating system (43).

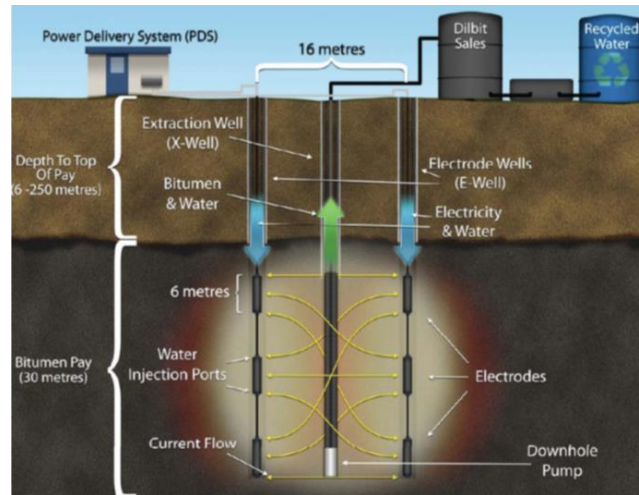


Figure 5-5. Configuration of electrodes as well as production well for ET-DSP™ process (43).

Electrical heating processes could be used as an enhanced recovery process alone (such as ET-DSP™) or combined with other methods for oil recovery. The US Patent by Hagedorn (46) in 1976 described oil recovery by combination of steam stimulation and electrical heating. The area between adjacent wells subjected to steam stimulation has high water saturation and a brine solution is injected to increase the fluid conductivity. Then the wells are completed as electrodes and current flow through the formation in order to heat the oil that was not heated to any significant amount by the steam. In 1984, Sacuta (47) patented a fluid communication channel that is developed between injection and production wells by simultaneously injecting a solvent for oil and passing electric current through the formation. Lee *et al.* at AITF studied combined application of cyclic electrical heating and cyclic gas injection process for recovering heavy oil/bitumen from a shaly lean sand reservoir (48). Electrical heating was also investigated to pre-heat a reservoir for SAGD start up. Yuan *et al.* (49) at AITF investigated wet electrical heating for SAGD start up, where the injector and producer were used as electrodes.

5.2.2. DC vs. AC

Both AC and DC have been applied to electrical heating processes, but most studies looked at AC. Compared to DC, there is the advantage of the ready availability of 60 Hz power for AC. DC is usually obtained by converter from AC to DC. However, some unique characteristics associated with DC ohmic heating were found compared to AC ohmic heating for *in situ* recovery processes due to the following mechanisms, which could facilitate enhancing oil recovery (50; 51; 52; 53):

- **Electrophoresis:** Charged particles in reservoir fluids could migrate towards the electrodes due to applied DC electric field, e.g., asphaltenes (inducing a viscosity gradient) and clay particles (unblocking pore throats).
- **Electroosmosis:** DC electric field can affect electrical double layers in the aqueous phase within pore throats and result in enhanced reservoir permeability and increased oil production.

- Electromigration: Migration of H^+ and OH^- in the aqueous phase of the reservoir will produce a local alkaline environment (low oil/water interfacial tension) around the anode and a local acidic environment (high oil/water interfacial tension) around the cathode as well as generation of gases (H_2 and O_2) at the surface of these electrodes, which will increase reservoir pressure and provide a small pressure drive.

5.3. ELECTROMAGNETIC HEATING

In electromagnetic (EM) heating processes, energy is generated in the form of waves, which can penetrate into oil-containing reservoirs to generate heat and eventually improve recovery mainly due to the reduction of oil viscosity. The frequency of the electromagnetic wave is one of the critical parameters, which dominate electromagnetic heating processes. The other dominant parameters relate to the electromagnetic properties of the reservoir, which can be frequency dependent, and includes conductivity, dielectric constant, and magnetic permeability. The energy, that electromagnetic waves carry, is dependent on frequency and higher frequencies of electromagnetics carry higher energy. However, excessively high electromagnetic frequencies may not be suitable for heating reservoirs because they have lower penetration lengths into reservoirs. A moderate range of electromagnetic frequencies (100 kHz - 100GHz) has been investigated for application in various electromagnetic heating processes ^{(54), (55), (56), (57), (58)}. Generally, the two different mechanisms for electromagnetic heating processes in reservoirs are dielectric heating and inductive heating.

5.3.1. Dielectric heating

Dielectric heating is the process in which a high frequency, alternating electric field (e.g., radio wave or microwave EM radiation) heats a dielectric material by inducing molecular rotation dipoles comprising the dielectric fluid. EM induced molecular rotation will occur in materials containing polar molecules with an electrical dipole moment, e.g., water molecules, oil components, resins, and asphaltenes. As the electromagnetic field is oscillating, rotating molecules push, pull, and collide with other molecules distributing the energy to adjacent molecules and atoms in the material, releasing the energy as heat.

An example of an electromagnetic heating process in heavy oil reservoirs, based on the dielectric heating mechanism, is the “Enhanced/Effective Solvent Exaction Incorporating Electromagnetic Heating” (ESEIEH) process (Figure 5-6) created by a consortium of companies including Harris Corporation, Laricina Energy, Nexen, and Suncor ⁽⁵⁹⁾. This process involves two horizontal wells, as in the SAGD process, with the upper well as the antenna and injector and the lower well as the producer. The electromagnetic energy is emitted from the antenna into the reservoir and heats the oil, and then a solvent is injected to dilute the bitumen and further reduce bitumen viscosity. The concept of the ESEIEH process was initially evaluated at Suncor’s Steepbank mine in 2012 and an expanded pilot field test is scheduled in 2013.

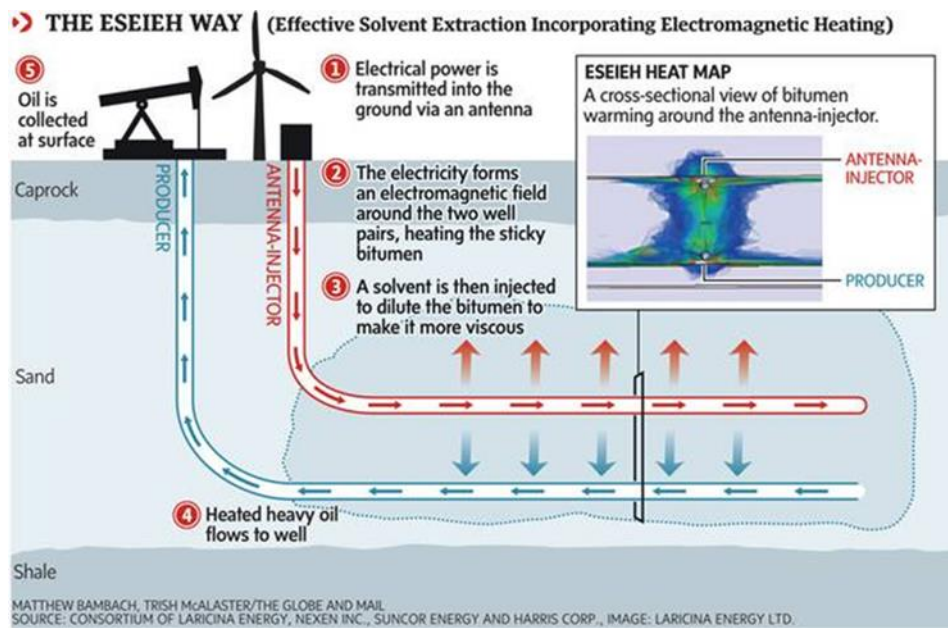


Figure 5-6 Illustration of ESEIEH process (Globe & Mail, Jun 13, 2012)

5.3.2. Inductive heating

Inductive heating is the process of heating an electrically conducting object (e.g., metal or conductive connate water phase in a reservoir) by the generation of an electrical eddy current leading to Joule heating of the object. An example of inductive heating in daily life is the induction stove used for household cooking. In this instance, eddy currents are generated in the metal cookware, which creates sufficient heat for cooking.

The EM (Electromagnetic)-SAGD process proposed by Siemens AG is based on the inductive heating mechanism for heavy oil reservoirs. Figure 5-7 shows the schematic of the EM-SAGD process⁽⁶⁰⁾, in which an electrical coil is placed around the SAGD well pair in reservoirs and an alternating current is applied through the coil to generate an electromagnetic field. The generated electromagnetic field then creates eddy currents in the conductive connate water phase. Due to the Joule heating effect, the connate water phase and subsequently the entire reservoir is heated. By combining the electromagnetic heating and SAGD processes, the EM-SAGD technology reportedly has the potential to achieve higher oil recovery compared to SAGD process alone. Alberta Oilsands Inc. is currently working with Siemens AG to apply this technology to its Clearwater project in northern Alberta.

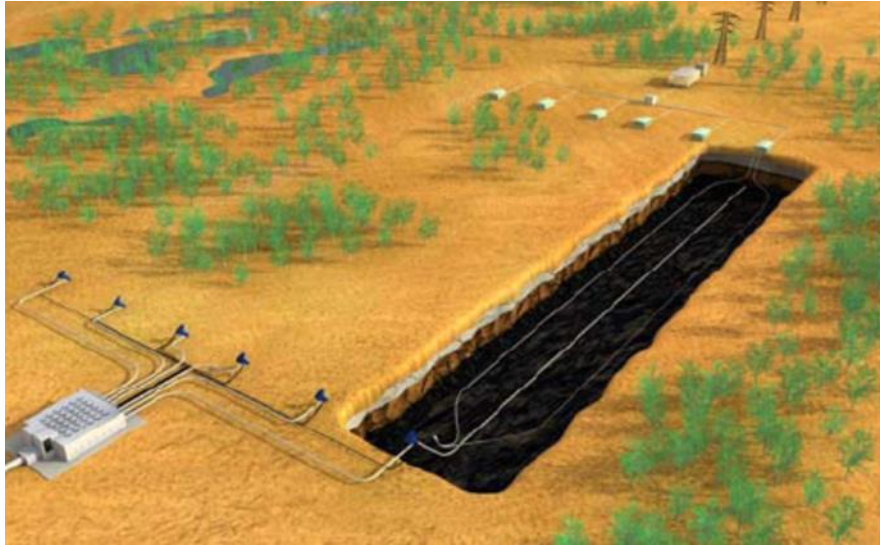


Figure 5-7 Schematic of EM-SAGD process ⁽⁶⁰⁾.

5.4. CHALLENGES

Although numerous attempts have been made in past decades to use electric heating for oil recovery, further advances into field applications have not been realized due to technical and economic challenges. The field test of the Electrical Horizontal Well Project in the Lloydminster heavy oil area experienced premature equipment failure and sand production. One major cause of equipment failure is due to the temperature of the electrodes, normally the injector/production wells, tends to spike to high values. Further away from the wells there is an insignificant increase in temperature. Additionally, the high temperatures at the electrodes can result in evaporation of the formation water, which is the medium providing the conductive path for the electric current. Once the water vaporizes, the current flow stops, and so does the heating effect.

Electrical and electromagnetic heating are complex processes during which the properties of reservoir (e.g., electrical conductivity, dielectric constant, magnetic permeability, and thermal conductivity) change as oil sands increases in temperature, and bitumen and water are produced. This results in a dynamic process whereby the heat, mass, and electrical field are strongly coupled and in a transient state throughout the entire recovery process. Therefore, adequate understanding of the electrical heating process, as well as accurate characterization of the reservoir formation (i.e., reservoir electrical conductivity, dielectric constant, and magnetic permeability), is essential. Figure 5-8 shows a variation of reservoir formation resistivity for a Frog Lake Well in the Electrical Horizontal Well Project in the Lloydminster heavy oil area ⁽⁴⁵⁾.

Water saturation of the reservoir has a significant impact on electrical properties and will likely determine success of the electrical and electromagnetic processes. Generally, electrical heating processes are not appropriate for a low water saturation reservoir as they usually have low electrical conductivity. On the other hand, very high water saturation is not necessarily

desirable for electrical heating since too much heat may be lost to the water. The heterogeneous water saturation in the reservoir would also increase the complexity of electrical heating.

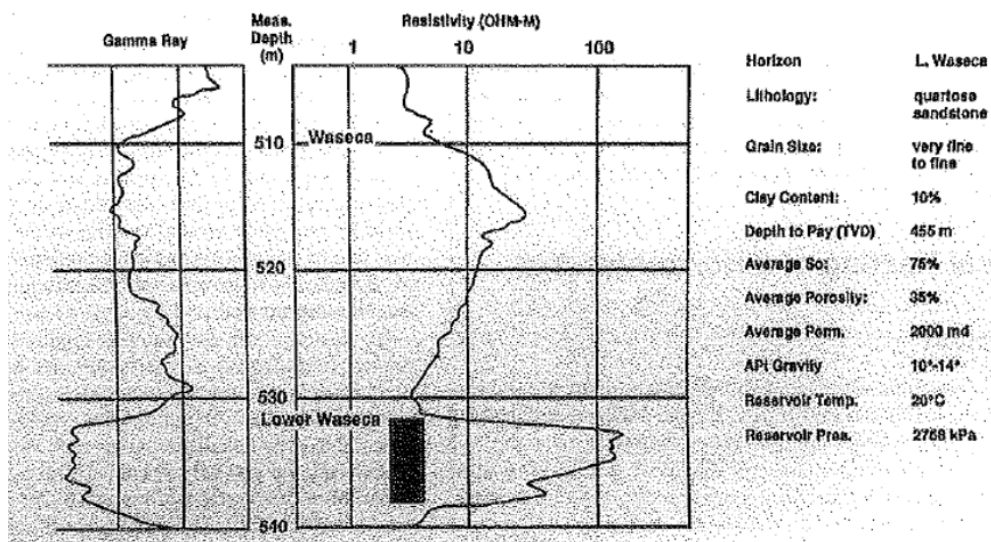


Figure 5-8. Variation in resistivity for a Frog Lake well (45).

The scaling approaches employed for SAGD and solvent-steam processes are not amenable to scaling of EM heating processes in a reservoir. Physical scaling of electrical and electromagnetic processes requires that electrical (conductivity, dielectric constant, and magnetic permeability) and thermal similitudes are consistent and simultaneously incorporated in the model. Fluid transport, geomechanical, gravitational, and capillary effects provide additional complexity. Scaling of EM heating processes is discussed in more detail in a later section of this report.

6.0 BIOLOGICALLY ENHANCED OIL RECOVERY

6.1. INTRODUCTION

Most of the proposed biological oil recovery processes utilize microbes although there also are proposed processes that utilize enzymes. The focus of this section will be on microbially enhanced oil recovery (MEOR) as many of the same issues will also apply to systems with enzymes. Compared to some of the other recovery processes, the MEOR process mechanisms are not well understood. This section summarizes current knowledge and gaps for MEOR processes and provides a brief overview of waterflooding, which is one means for introducing microbes and enzymes into a reservoir.

Primary recovery of oil using the natural pressure drive of the reservoir produces approximately 5-10% of the total reserve ⁽⁶¹⁾. Secondary production techniques increase oil recovery by waterflooding the production well. However, due to the high interfacial tension between oil and water, this can result in significant quantities of oil being bypassed by the water and recovery efficiencies vary from 10 to 40% of the oil in place ⁽⁶¹⁾. Tertiary production techniques, also called enhanced oil recovery (EOR), use additives such as chemical surfactants, thickening agents, and plug-forming polymers to: 1) lower oil/water interfacial tension, 2) make the water more viscous, and 3) form insoluble plugs ⁽⁶²⁾. The main disadvantage to using these additives is the cost. It is often not economical to use tertiary production techniques, despite the possible increase in the number of barrels of oil recovered.

Microbial enhanced oil recovery (MEOR) is similar to the tertiary production technique of chemical injection, but the chemical effect is generated *in situ* ⁽⁶³⁾. Microbes, either indigenous to the formation or introduced from external sources, feed on carbon (from the oil directly or injected as carbohydrates), and nitrates and phosphates added to the injection water to generate the chemical-like effects through biological action (Table 6-1). The advantages of using microorganisms over chemical methods are as follows:

- Microorganisms are self-replicating.
- Microorganisms are relatively inexpensive to produce.
- Nutrients for microbial growth are often economically priced.

MEOR processes should, therefore, be evaluated on the same criteria as other EOR processes and deemed advantageous to use only if the MEOR process is more efficient and cost effective than another EOR process ⁽⁶⁴⁾.

Table 6-1. Microbial generated products and their claimed effects for EOR ⁽⁶⁴⁾.

| Product | Effect |
|-------------|---|
| Acids | Increase in rock porosity and permeability Production of CO ₂ through reaction of acids with carbonate minerals |
| Biomass | Selective and nonselective plugging Emulsification through adhesion to oil Changing wettability of mineral surfaces Reduction of oil viscosity |
| Gases | Reservoir repressurization Oil swelling Viscosity reduction Increased permeability caused by solubilization of carbonate rocks |
| Solvents | Dissolution of oil |
| Surfactants | Lowering of the interfacial tension Emulsification |
| Polymers | Mobility control Selective and nonselective plugging |

The concept of using microorganisms to enhance oil recovery has been around since the 1920's ⁽⁶³⁾, and since then a number of diverse microbiological technologies have been developed to enhance oil recovery. These can be categorized into several major classes based on their mechanisms:

- Interfacial tension (IFT) reduction
 - Biosurfactants can reduce the IFT between the flowing aqueous phase and residual oil saturation, and potentially increase oil recovery
 - Bacteria and their products can alter the oil-wettability of reservoir rock minerals and increase recovery
- Viscosity reduction
 - Microbes degrade long-chain hydrocarbons reducing the viscosity and allowing easier displacement of the oil
- Gas production
 - Microbes generate CO₂ and methane during the metabolism of hydrocarbons in the reservoir. If enough gas is generated, it can get adsorbed into the oil and lower its viscosity
 - The gas can also displace oil by forcing it out of pores
- Permeability profile modification
 - Introduced microbes or stimulated indigenous bacteria plug channels (by biomass or bio-products generation)

- Subsequent waterfloods get diverted towards unswept regions thus recovering more oil

Over the past 50 years, over 400 MEOR field trials using variations of the above processes have been conducted ⁽⁶⁵⁾. Some of these were actually wellbore or formation damage repair and not MEOR tests. Ideal reservoir conditions or factors affecting the successful outcomes of an MEOR process have emerged from an evaluation of these tests ^(65; 66) and are summarized in the following table (Table 6-2).

Table 6-2. Ideal reservoir conditions for MEOR applications ^(65; 66).

| Variable | Ideal Reservoir Condition |
|---|---|
| Production mode | Secondary - fields under waterflood |
| Microbial Pathway (growth conditions) | Anaerobic, restricted electron acceptors (sulfate not ideal) |
| Permeability | >50 to 100 milliDarcy (50 to 75 is the minimum permeability that allows microbes to pass through pore openings) |
| Temperature | <60 to 80°C |
| Salinity (injected and produced waters) | Approximately 6% total dissolved solids (maximum 10% TDS). |
| pH | pH between 5-9 with 6-8 being ideal |
| Oil viscosity | <500 cP (preferred) |
| Oil saturation | 45-70% |
| Reservoir pressure | <3000 psi (preferred) |

Maudgalya *et al.* ⁽⁶⁵⁾ and Gray *et al.* ⁽⁶⁷⁾ have critically reviewed MEOR laboratory tests and field trials reported in the literature and have determined which processes have a high likelihood for successful full-scale application. The following sections provide details on these main MEOR processes.

6.2. INTERFACIAL TENSION REDUCTION

Interfacial tension (IFT) between the oil and the aqueous phases is largely responsible for trapping the oil in the porous matrix. Ultra-low values (several orders of magnitude reduction) of IFT are needed for mobilization of the oil. In order to achieve these ultra-low IFT values, very high concentrations (> g/l) of synthetic surfactants must be used, which makes chemical surfactant flooding expensive ⁽⁶⁸⁾. Surfactants increase the capillary number (the ratio of viscous to capillary forces) by reducing the interfacial tension ⁽⁶⁷⁾. The viscous force promotes oil flow and is opposed by the capillary force acting on the oil globules.

Microbially-produced biosurfactants may be an economical method to recover residual oil since they are effective at low concentrations as indicated by their low critical micelle concentrations ^(69; 70). However, the recovery of residual oil by biosurfactant from model porous systems is inconsistent and low ⁽⁶⁸⁾. In one study, residual oil was recovered when a biosurfactant-producing bacterium and the nutrients needed to support growth were introduced into

sandstone cores, but residual hydrocarbon recoveries were often low (5 to 20%) and required multiple pore volumes of recovery fluid ⁽⁶⁸⁾.

Laboratory tests have demonstrated that the efficacy of biosurfactants can be improved with the additions of a viscosifying agent such as partially hydrolyzed polyacrylamide and a low molecular weight alcohol such as 2, 3-butanediol ⁽⁶⁸⁾. Viscosifying agents are often added to chemical surfactant floods to increase the viscosity of the water phase ⁽⁶⁸⁾. Alcohols are usually added to prevent surfactant liquid crystal formation and act to increase the effective surfactant concentration ⁽⁶⁸⁾. This suggests that a combination of microorganisms and/or a variety of microbial products, such as acids, gases, solvents, polymers, emulsifiers, and/or biosurfactants collectively helps recover residual oil from low production oil reservoirs. Further research is needed to determine whether these products are effective alone or if combinations of products are needed.

One major drawback to using both chemical and biological surfactants is the adsorption of the surfactants to mineral surfaces and reservoir rocks. Large amounts of surfactants are required in order to mobilize residual crude oil. Thus, IFT reduction through biosurfactants would be inefficient to mobilize large quantities of oil, especially if the reservoirs have been extensively waterflooded and, thus, have low oil saturation levels ⁽⁶⁵⁾.

There are two methods to introduce or generate biosurfactants in the reservoir ⁽⁶⁷⁾: 1) the production of biosurfactants *in situ* from crude oil components, and 2) the injection of specific biosurfactant-producing cultures and nutrients. In the first case, mass balance calculations based on laboratory tests suggest that the microbes would be required to degrade large amounts of the crude oil to generate a significant amount of biosurfactant. Furthermore, the residual oil not metabolized by the microbes would be much heavier than the original oil and more difficult to mobilize. In the second case, competition from indigenous microbes for the injected nutrient could occur and thus sustained biosurfactant production (and subsequently sustained nutrient injection) would be required in order to flood the reservoir. Finally, other bacteria may degrade the biosurfactant.

Researchers at the University of Oklahoma have carried out extensive research and field-testing on biosurfactants and yet researchers are still uncertain whether *in situ* biosurfactant production can be induced deep in reservoirs at the scales needed for economic oil recovery ⁽⁷¹⁾. Moreover, the development of a large population of bacteria in a reservoir to produce biosurfactants may actually result in the retardation of oil mobility by creating thick biolayers at the oil-water interface, thus canceling the effects of the biosurfactants.

A process that is similar to IFT reduction is the biological altering of oil/water wettability of reservoir rock minerals. There are two main mechanisms for the biological alteration of wettability:

1. Direct attachment of bacteria to mineral surfaces
 - The contact angle of oil wetting a mineral surface can be changed due to a heterogeneous mixture of mineral and bacterial surface properties

- This mechanism is limited to pores that are large enough to be accessible to bacteria, which are in the range of 1 μm or more
2. Absorption of bacterial metabolites to mineral surfaces
- Bacterial metabolites such as bio-surfactants absorb to mineral surfaces rendering the surface more or less hydrophobic
 - This mechanism can operate at any pore diameter
 - The coating of mineral surfaces with exopolysaccharides or other biopolymers alter the contact angle of oil much in the same way as the direct attachment of bacteria to the mineral surface

Titan Oil Recovery ⁽⁷²⁾ has developed an MEOR process based on the concept of IFT reduction. Their patented process (“Titan Process”) is based on a proprietary nutrient mixture that changes the characteristics of bacterial cell membranes once injected into the reservoir. The bacteria become oleophilic, seeking out and attaching themselves to oil droplets (Figure 6-1). The oil droplets become distorted, and break apart and dislodge from the pore spaces and, thus, become recoverable. The Titan Process also claims that an emulsion forms between the oil, water, and bacteria. This emulsion can block thief zones, channeling, and fingering zones resulting in greatly improved sweep efficiencies and reduction in the water cut (Figure 6-2).

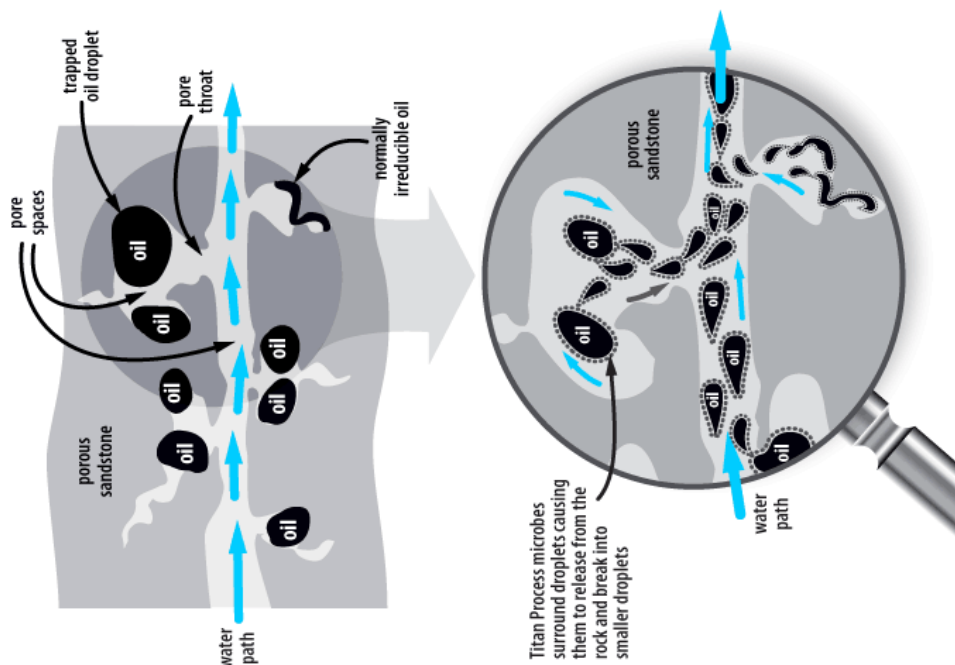


Figure 6-1. The Titan Process: injection of proprietary nutrients causes bacteria to seek out oil droplets and coat them, causing the oil to dislodge from pore spaces and flow into the water path ⁽⁷²⁾.

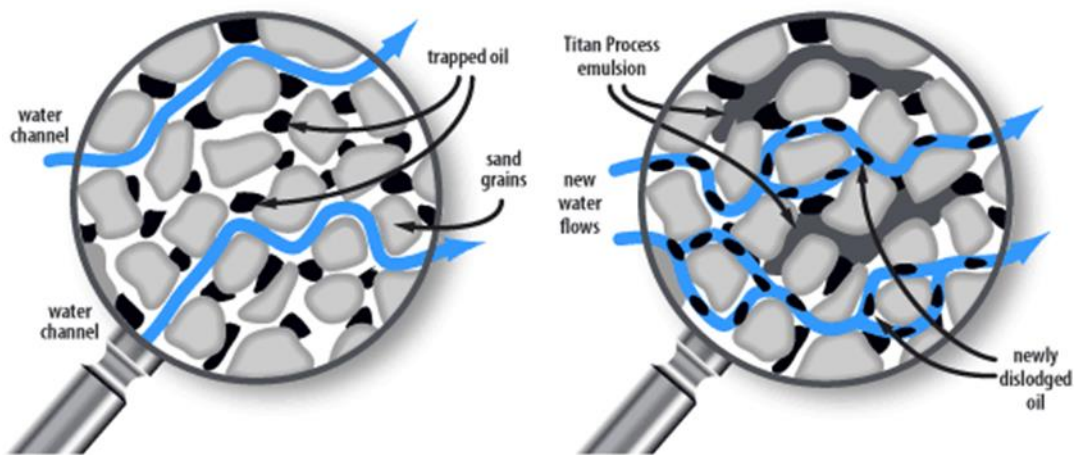


Figure 6-2 Emulsion formation by bacteria stimulated during the Titan Process causes thief zones (left side of figure) to become blocked sweeping oil more efficiently (right side of figure) ⁽⁶¹⁾.

Gray *et al.* ⁽⁶⁷⁾ identified a number of issues with using microbes to change the wettability of oil surfaces. Firstly, any roughness and heterogeneities on the solid surfaces can lead to severe hysteresis effects in contact angle measurements. Secondly, this process would not work well in sandstone formations, as residual oil saturation of sandstones does not vary significantly with wettability. In contrast, a change from oil-wet to water-wet conditions in carbonate reservoirs significantly enhances oil recovery and, thus, this MEOR process would be applicable in these reservoirs.

6.3. GAS PRODUCTION

Anaerobic bacteria and Archaea can generate CO₂ and methane from the metabolism of organic matter. There are three main mechanisms for increased oil recovery by *in situ* gas production ⁽⁶⁷⁾:

1. Reduction of the residual oil saturation
2. Reduction of oil viscosity
3. Repressurization

The residual oil after waterflooding is dispersed in the pore network as blobs that cannot connect with each other and flow. Thus, the reservoir is highly under saturated. Initial gas generated by microbes (whether through the consumption of the oil or added nutrients) will likely dissolve in the oil rather than form a distinct gas phase ⁽⁶⁷⁾. This may then result in an increase in sweep efficiency and oil rate due to a reduction in the residual saturation due to swelling of the oil.

Microbial gas can dissolve in the oil and lower its viscosity. Lower oil viscosity leads to improved mobility ratios. This is most likely to occur in undersaturated reservoirs. Sweep

efficiency could also increase with gas dissolution. Improved oil recoveries and sweep efficiencies are only likely to be significant in reservoirs with unfavorable mobility ratios ⁽⁶⁷⁾.

In undersaturated reservoirs, microbial gas can dissolve in the oil and lower its viscosity leading to improved mobility ratios. It is important to note that the residual oil saturation to water will not decrease due to a lower oil viscosity, however the oil recovery at an economically limiting water-oil ratio could increase.

In conventional CO₂ floods, the injection of enormous amounts of CO₂ results in the repressurization of the reservoir, and release, and solubilization of the oil. However, a major obstacle to this approach is the availability of inexpensive sources of CO₂ close to oil fields to make the economics of CO₂ injection cost-effective. With microbial *in situ* CO₂ production, modest amounts of CO₂ could be produced throughout the reservoir at oil/water interfaces and at the level of pore sizes and oil droplets ⁽⁷³⁾. The CO₂ effects would be the same as in conventional CO₂ floods, but would be more targeted. It was speculated that the amount of *in situ*-produced CO₂ needed to release oil would be less than what is needed for conventional CO₂ floods. In addition, the microbially generated CO₂ is captured by the oil and trapped chemically within the water/rock matrix. There would be none left to cause extra gas problems in the gas streams. A caveat to this process is the possibility of a free gas phase forming. In this case, the rate improvement in oil recovery would be offset by the loss of relative oil permeability in three-phase flow ⁽⁶⁷⁾. Another problem to this process is that the mobility of the gas is higher than that of oil or water and there is the likelihood that the generated gas would be produced before any significant pressure increases occurred.

The main issue with this technology overall is ensuring enough *in situ* CO₂ production in order to have a measurable effect on oil production ⁽⁶⁴⁾. If large amounts of nutrients (and nitrate to control souring) were required to create large-scale effects such as re-pressurization, microbial *in situ* gas generation as an MEOR process would not be economically feasible. If the microbes consume some oil to produce microbial gas, the viscosity of the remaining oil will be higher than the original oil, and the gas will be less soluble in the oil. Eventually an immobile heavy oil residue will remain and only gas will flow ⁽⁶⁷⁾.

6.4. VISCOSITY REDUCTION

Reducing the crude oil viscosity, especially for heavy oils, can improve the recoverability of the oil due to lower oil-water mobility ratios and less viscous fingering, which can lead to watered out channels in the reservoir ⁽⁶⁶⁾. Researchers at DuPont have enriched microorganisms capable of degrading aromatic molecules typically found in crude oil ⁽⁶⁶⁾. Special 'in-culture' crude oil viscosity measurement devices were developed and oil cultures monitored for viscosity reduction over a 2-month period. However, no change in viscosity or increase in viscosity due to the loss of light components was observed. Research was then focused on microbial reduction of aromatic compounds using hydrogen or carbon monoxide. The reduction of crude oil viscosity by hydrogenation was demonstrated ⁽⁶⁶⁾.

Any viscosity reduction mechanism is, however, subject to rate limitations ⁽⁶⁶⁾. A significant amount of oil has to be degraded to get a measurable amount of viscosity reduction. It has been

suggested that 5 to 10% of the oil must be degraded or transformed to achieve this. Mass transfer limitations will likely make viscosity reduction not feasible for use as an economical MEOR process.

6.5. PERMEABILITY PROFILE MODIFICATION (MICROBIAL FLOW DIVERSION)

Permeability profile modification was designed for reservoirs with high permeability channels that can negatively affect the overall waterflooding sweep efficiency ⁽⁶⁵⁾. In this MEOR process, microbes and nutrients are injected into the reservoir to plug these channels. The microbes flow into these high permeability zones or channels and grow there, partially plugging them. Subsequent waterfloods are diverted towards the unswept regions and recover more oil ⁽⁶⁵⁾.

Gray *et al.* ⁽⁶⁷⁾ identified several criteria for successful application of this process:

- The reservoir must have high permeability zones or fractures between injectors and producers that result in poor sweep efficiency
- The blockage created by the microbes in the channels and pores, whether it is by extracellular polysaccharides or biomass, needs to be resistant to biodegradation by the indigenous microbes. If the blockage is rapidly degraded, repeated applications of new microbes would be required, thus increasing the cost of the process
- Injected microbes must be able to survive at *in situ* conditions and be able to out-compete the indigenous microbes for added nutrients without altering the natural microbial composition too much
- The injected microbes must be able to utilize nutrients over a wide concentration range as the nutrients may become concentrated with repeated injections.

Reservoirs that have much less than 6% of the pore volume in high-permeable layers would be ideal for bacterial plugging ⁽⁶⁷⁾. Selective plugging of fractures gives the best possible ratio of beneficial oil recovery in proportion to the volume of reservoir that is affected by the treatment. The smaller the volume, i.e., fracture, the more favorable the economics the incremental oil recovered is much higher than the volume of nutrient injected to stimulate bacterial plugging.

One field test of permeability profile modification involved the isolation of a strain of bacteria (*Enterobacter*) from the target reservoir that produced an insoluble cellulose polymer that adhered to the reservoir rock ⁽⁷⁴⁾. This organism under normal reservoir conditions did not produce any polymer. However, when in the presence of high concentrations of molasses, the organism produced the polymer, which was also shown to be resistant to bacterial degradation. The researchers determined in a laboratory test that the plugging of a high permeable zone was only effective when the molasses was mixed with the cells of the organism instead of simply adding the molasses. This is an example of a treatment process called bioaugmentation and ensures that the key bacteria or bacterium (*Enterobacter* in this case) will be able to survive and plug fractures under actual reservoir conditions.

The University of Michigan has been developing a permeability profile modification technology that prolongs the lag phase of bacterial growth so that both bacteria and nutrients can be

injected deeper into the oil reservoir ⁽⁷⁵⁾. By lengthening the lag time and slowing the growth rate, rapid growth around the well bore is prevented and a larger area of porous zones within the reservoir can become blocked by bacterial biomass, thus increasing water floods through the oil-containing low permeability zones (Figure 6-3). The research group has used a variety of chemicals to inhibit the growth of their test bacterium, *Leuconostoc mesenteroides*, such as sodium benzoate, sodium dodecyl sulphate, sodium hydroxide (used to increase the initial pH) and sucrose. An increase in pH above neutral resulted in a significant increase in the lag phase of the organism.

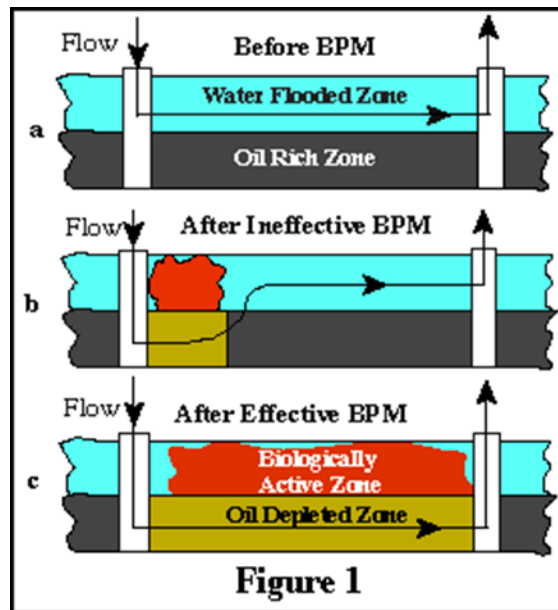


Figure 6-3 Bacterial Profile Modification (BPM) developed by the Porous Media Research Group at the University of Michigan. a) Injected water flows through the water-flooded high permeability zone and bypasses the oil-containing low permeability zone. b) Injection of exopolymer producing bacteria with rapid bacterial growth and exopolymer formation near the well bore and prevention of deep penetration of bacterial cells and nutrients leads to poor oil recovery c) Delaying the onset of bacterial exponential growth (i.e., increasing the lag time for growth) leads to deep penetration throughout the reservoir and improved oil recovery ⁽⁶⁴⁾.

Other research groups have focused on developing methods to deliver bacteria and nutrients deep into the reservoir as well. One group focused on the development of small, starved bacteria, so-called ultramicrobacteria (UMB) that would allow for the deep placement of the bacteria in the reservoirs ⁽⁷⁶⁾. A dilute nutrient media is either simultaneously or subsequently thereafter injected into the zone to substantially and uniformly resuscitate the starved bacteria. After consuming the nutrient media, the bacteria regain full cell size, proliferate, and commence production of biofilm-forming exocellular polysaccharides. The biofilm selectively seals the high permeable zones of the formation and reduces water flow through the strata. Although this process claims selectivity in concentrating in high permeability strata, skin-plugging elsewhere can still occur. There is also a lag time before plugging takes place so the well may

have to be shut in for some period before changes in permeability can occur. Further investigations into scale-up issues need to be addressed.

Of all the MEOR processes described, permeability profile modification holds the most promise for success as evidenced by lab and field tests and by the virtue of its simplicity in only depending on microbial growth for it to be effective ⁽⁶⁷⁾. However, there are still some unknowns and optimization opportunities:

- The maximum size of fracture that could be effectively blocked by bacterial action is unknown
- All biopolymers will eventually be degraded; the physical strength and stability of the bacterial plug should be optimized
- The cost of preparing and injecting batches of nutrient and bacteria into the reservoir must be calculated and incorporated into the economic analysis of the process
- The selected nutrient to induce bacterial plugging should not also stimulate sulfate reducing bacteria otherwise souring could occur
- The possibility of stimulating the organisms to degrade the oil *in situ* in order to create the biomass plugging should be developed as an alternate to injecting large quantities of nutrient

6.6. CONSIDERATIONS FOR LABORATORY AND FIELD TESTING

Although numerous laboratory tests have demonstrated that microorganisms can indeed enhance oil recovery by virtue of the products they can produce or by their activities, there is a gap in translating this to the field in an economically, practical, and scientifically valid manner ⁽⁶³⁾.

There are still many unknowns and process optimizations that need to be addressed in order for MEOR to be fully embraced as an alternate process to chemical EOR. Skepticism by the petroleum industry on the merits of MEOR have been affected by poor understanding of the mechanisms of microbial oil recovery and a lack of post-treatment analysis or calculations to validate the claims of successful field tests

Maudgalya *et al.* ⁽⁶⁵⁾ provide an excellent review of measurements, laboratory and field tests, as well as verification of results that should be undertaken to allow for robust analysis of MEOR processes. For laboratory testing of reservoir or analogous cores, the following should be considered:

- Test the mobility of the bacteria across the cores if they are being injected into the reservoir
- The microbes and nutrients must travel and saturate cores in time periods practical for field applications
- Measure microbial growth and product generation to identify nutrient limiting factors and competition with indigenous microbes

- Calculate the material balances of laboratory reactions in order to estimate the amount of products produced during field trials
- Langmuir adsorption isotherms for by-products and nutrients should be created if possible to predict adsorption losses. This will aid in the calculation of the amount of products that will be required to mobilize the oil

The development of microbial cultures for MEOR processes can be time-consuming. DuPont researchers have developed a fairly rapid method to screen and select for useful microbes from a target reservoir (Figure 6-4). They start with authentic injection water and produced fluid samples from candidate wells and using standard molecular biology methods to identify the types of microorganisms present. This, along with water chemistry, aid in the determination of the dominant metabolic activities occurring in the reservoir and, thus, enrichment protocols for selecting useful bacteria can be developed.

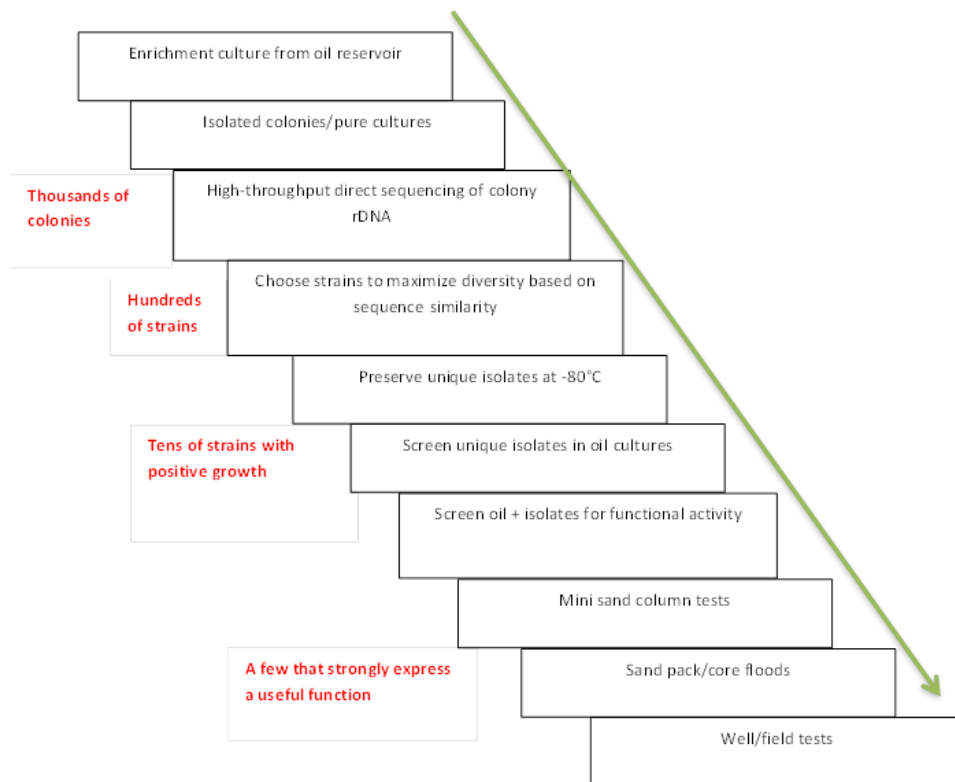


Figure 6-4. Experimental flow down for obtaining useful microorganism for MEOR processes from target reservoirs ⁽⁶⁶⁾.

For field-testing, the following should be considered ⁽⁶⁵⁾:

- Waterflooded reservoirs should be used as opposed to a single well. It is easier to verify if tertiary oil is mobilized in a waterflood than in a single well as the displacement of oil due to microbial activity flows from one well to another. Single wells are best suited for the study of microbial growth and bio-product formation under reservoir conditions

- Only one or two MEOR processes should be tested at a time. This reduces the number of reservoir constraints and simplifies the analyses
- Experimental controls, such as parts of the reservoir similar to the test area, should be established. The control area can be treated without the key nutrient, for example, and oil recovery results compared to the test area to determine whether the missing nutrient was necessary for microbial activity

A lack of systematic and standardized post-treatment analysis after most field trials has led to difficult and sometimes contradictory interpretations ⁽⁶⁵⁾. Recommended post-treatment tests include the following:

- Obtaining cores from test area to see if oil was mobilized and displaced
- Comparing pre- and post-treatment core data
- If cores are not available, conduct a tracer analysis to measure oil saturations and pressure transient tests to verify changes in the average permeability
- Analyzing the produced fluids for microbial growth and bio-product generation. Careful calibrations and measurements must be done to detect the often low concentrations of bio-products
- Analyzing decline curves to identify improved oil recoveries
- An economic analysis of the MEOR process tested should be conducted. The costs incurred for raw materials, labor, electricity, and equipment cost and earnings through extra oil produced should be calculated to determine if the MEOR process is economically viable ⁽⁶⁵⁾

Finally, a relatively accurate numerical model to simulate microbial recovery is needed that will simulate mobility control, salinity effects, and changes in product properties with reservoir temperatures. Such a model can be used to screen reservoir candidates for microbial treatments faster and help design a suitable MEOR recovery process. It is important to keep in mind that in MEOR processes, multiple mechanisms can occur simultaneously depending on a number of physical, chemical, and microbial factors. However, with robust testing (including using appropriate controls), modeling, and post-treatment verifications, MEOR can be a viable tertiary oil recovery technology.

6.7. WATERFLOODING

Waterflooding is a widely used secondary oil production method following primary recovery. It is considered one of the most economically viable EOR methods for mature fields. The waterflooding technique mainly provides extra energy to oil reservoir through injecting water from one, or more than one, injection well. The injected water maintains reservoir pressure at a relatively constant level, which is usually just above bubble-point pressure to minimize the operation cost of injection. Figure 6-5 depicts a schematic diagram of the waterflooding process, where water is injected through one or several wells while oil is replaced and produced from one or more wells. The oil bank can be mobilized and displaced efficiently towards production wells. The displacement of oil by water under immiscible conditions occurs both

microscopically and macroscopically in a reservoir ⁽⁷⁷⁾. Since water provides the necessary environment for microbes and enzymes to thrive and display activity, waterflooding techniques are both desirable and suitable for implementing MEOR processes.

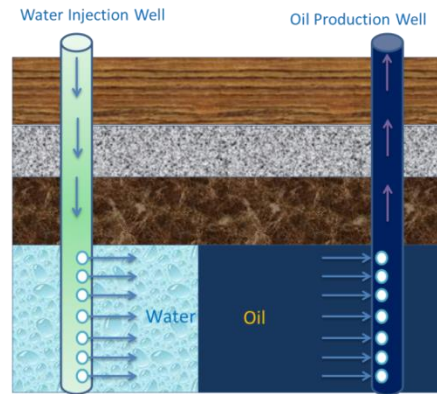


Figure 6-5. Waterflooding process.

6.7.1. Microscopic Displacement Efficiency

Under nearly all reservoir and surface conditions, water and oil are immiscible, and are always separated by a well-defined interface. The bounding surfaces between these two fluids play a crucial role in the displacement of oil banks by water in porous media. The interfacial tension (IFT) between the oil and water phases varies depending on the compositions of the phases but generally is relatively high, in the 10 to 30 dyne/cm range ⁽⁷⁸⁾.

Interaction between the surface of the reservoir rock and the fluid phases confined in the pore space influences fluid distribution in rocks as well as flow properties ⁽⁷⁸⁾. A major problem in oil recovery is overcoming the interfacial tension forces between the oil and the rock ⁽⁷⁹⁾. In a truly oil-wet rock surface, the interfacial tension forces tend to cause the oil to bind to the rock. In a water-wet rock surface, tension forces often create bubbles of oil, which block pore openings. These two types of interfacial tension forces are prime reasons why oil becomes increasingly more difficult to recover from the reservoir as water saturation increases and oil saturation decreases. Of course, this is one of the challenges that could be overcome by the use of MEOR processes.

Figure 6-6 illustrates a schematic of the interfaces between oil and water in a capillary system. The contact angle θ is used to define which fluid phase is more wetting. For low contact angles, the water phase is more wetting, whereas for high contact angles, the oil phase is more wetting. A minimum static pressure is required to force a non-wetting phase through a porous media shown in Figure 6-6, and must exceed the differential pressure between points A and B due to capillary forces ⁽⁸⁰⁾.

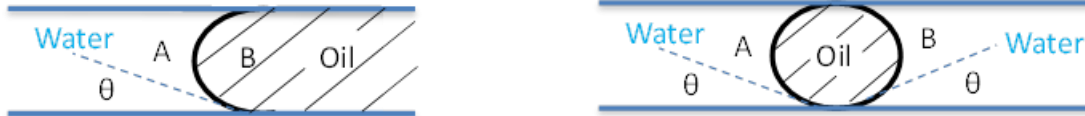


Figure 6-6. Illustration of oil/water interfaces: continuous phase vs. trapped drop (after ⁽⁴⁴⁾)

The notion of the displacement of one fluid by another can be also viewed as a “voidage displacement” ⁽⁸¹⁾ or “leakage-piston-like displacement” ⁽⁸²⁾. The leakage of the piston leave the oil behind in the sweep matrix, in the form of discontinuous droplets and residual oil saturation, which cannot be driven and displaced by the continued injection. Multiphase flow of water, oil, and gas at or well above velocities attainable in reservoirs occurs through a series of continuous but tortuous channels. Each phase flows through its own channels ⁽⁷⁸⁾.

6.7.2. Macroscopic Displacement Efficiency

On an inter-well scale, the driving force for displacement is represented by a potential gradient between an injection well and a producing well. The recovery efficiency is represented in terms of average oil saturation in the reservoir. Oil recovery in any displacement process depends on the volume of reservoir contacted by the injected fluid ⁽⁷⁸⁾. A quantitative measure of this contact is the volumetric displacement efficiency, which is a macroscopic efficiency and defined as the fraction of reservoir pore volume invaded or contacted by the injected fluid. Clearly, volumetric sweep efficiency is a function of time in a displacement process.

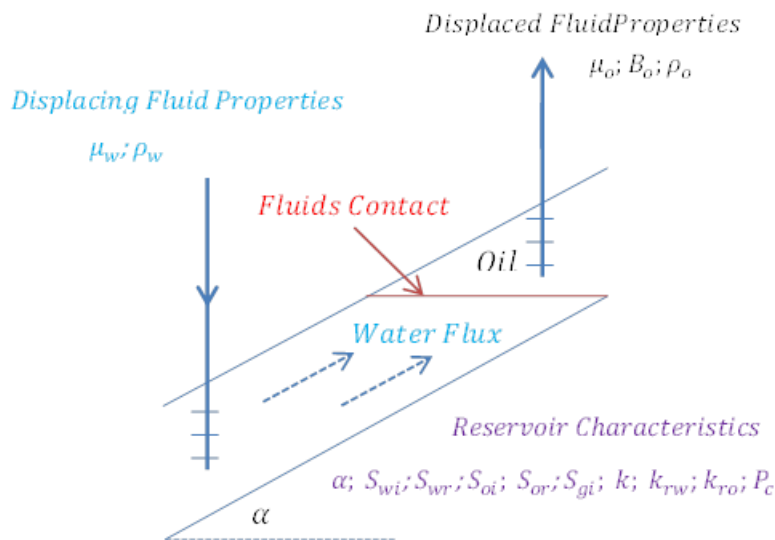


Figure 6-7. Waterflooding displacement at microscopic pore level.

Consider a linear direction with a dip angle of α , and water as a displacing fluid is injected to displace oil in the system shown in Figure 6-7. Fractional flow of water can be expressed as the following equation, with which a typical fractional-flow profile can be obtained.

$$f_w = \frac{1 + \frac{kk_{ro}A}{q\mu_o} \left(\frac{\partial P_c}{\partial x} - \Delta\rho_{ow}g\sin\alpha \right)}{1 + \frac{\mu_w k_{ro}}{\mu_o k_{rw}}}$$

Here, g is gravity constant; α is reservoir dip angle; μ_o is oil viscosity and μ_w water viscosity; k_{ro} is permeability to oil and k_{rw} permeability to water; and $\Delta\rho_{ow}$ is the density difference between water and oil. This equation includes terms for capillary pressure variation (as a function of saturation) in the system dipping at angle α .

Macroscopic displacement efficiency is the product of vertical sweep efficiency E_V and areal sweep efficiency E_A . The latter can also be expressed as the ratio of the area swept by the injected fluid and the total area of the well pattern through transient front positions⁽⁸¹⁾. The area behind each frontal position in Figure 6-8 represents the area that the injected fluid has swept up to that time. The areal sweep efficiency is then this area divided by the area of the square. The oil recovery is proportional to the areal sweep efficiency.

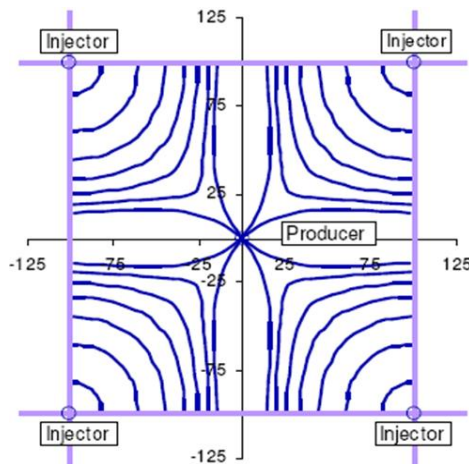


Figure 6-8. Front positions for a confined five-spot well pattern (after⁽⁸¹⁾)

6.7.3. Overall Waterflooding Recovery Efficiency

The overall waterflooding recovery efficiency might be simply stated as the product of three independent terms:

$$E_R = E_A \cdot E_D \cdot E_V$$

In this expression, areal sweep efficiency E_A is the function of mobility ratio, pattern, directional permeability, pressure distribution, cumulative injection, and operations. Microscopic displacement efficiency E_D is associated with primary depletion, viscosities μ_w and μ_o , and relative permeabilities k_{rw} and k_{ro} .

Capillary and viscous forces govern phase trapping and mobilization of fluids in porous media and, thus, microscopic displacement efficiency⁽⁸³⁾. Macroscopic displacement efficiency is the

product of vertical sweep efficiency (E_V) and areal sweep efficiency (E_A) is a measure of how effectively the displacing fluid sweeps out the volume of a reservoir, both areally and vertically. This also indicates how effectively the displacing fluid moves the displaced oil toward production wells.

The effectiveness of a waterflooding recovery process is dependent on the volume of the reservoir, which will be contacted by the injected fluid. The latter, in turn, is dependent on the horizontal and vertical sweep efficiency of the process. The following factors control the sweep efficiency: (1) pattern of injectors, (2) off-pattern wells, (3) unconfined patterns, (4) fractures, (5) reservoir heterogeneity, (6) continued injection after breakthrough, (7) mobility ratio, and (8) positions of shock front ⁽⁷⁹⁾.

The two methods that can be used to predict displacement performance ⁽⁷⁸⁾ are the Buckley-Leverett equation, or frontal advance model, and the numerical techniques for partial differential equations. The Buckley-Leverett equation states that in a linear displacement process, each water saturation moves through the porous rock at a velocity that can be computed from the derivative of the fractional flow with respect to water saturation.

6.7.4. Factors Controlling Recovery

Regarding the volumetric sweep efficiency of displacement processes, four factors generally control how much of a reservoir will be contacted by a displacement process: (1) the properties of the injected fluids, (2) the properties of the displaced fluids, (3) the properties and geological characteristics of the reservoir rock, and (4) the geometry of the injection and production well pattern ⁽⁸³⁾. Note that MEOR can affect both the properties of the injected fluids and the displaced fluids (oil, water, and gas).

6.7.4.1. Properties of Displacing/Displaced Fluids and Reservoir Characteristics

Properties of displacing and displaced fluids and reservoir characteristics are important and crucial aspects affecting waterflooding performance as they control wettability, initial and residual oil saturation to waterflooding, and the oil relative permeabilities at higher water saturations ⁽⁸⁴⁾. Capillary pressure affects waterflood performance and engineering calculations because the extent to which the water/oil flood front is vertically and horizontally “smeared out” during the waterflood is controlled by the capillary-pressure/water-saturation (P_c/S_w) imbibition curve ⁽⁸⁴⁾. The shapes of the imbibition water/oil k_r curves depend on pore geometry and wettability. The interplay between wettability and pore geometry in a reservoir rock is what is represented by the laboratory-determined capillary pressure curves and water/oil relative permeability curves.

Of the two important numbers for a reservoir rock ⁽⁸⁴⁾, initial oil saturation S_{oi} determines the initial amount of oil in place, and the residual oil saturation S_{or} represents the remaining amount of oil after waterflooding displacement. On the micro-scale, the distribution of residual oil in pores swept by displacing fluid will depend on competing viscous, capillary, and gravitational forces and is particularly influenced by pore size, pore geometry, wettability, and displacement rate. The laboratory determination of residual oil saturation in core plugs

provides an estimate of the microscopic displacement efficiency, through measurement of ultimate residual oil saturation for the pore scale recovery process ⁽⁷⁹⁾.

The mobility ratio, $M = \frac{\mu_o k_{rw}}{\mu_w k_{ro}}$, defined as the mobility of the displacing phase (for waterflooding, water) divided by the mobility of the displaced phase, determines rather “favourable displacement” (≤ 1) or “unfavourable displacement” (≥ 1). In practical terms, a favourable mobility ratio means that the displaced oil phase can move more quickly through the reservoir rock than can the displacing water phase ⁽⁸⁴⁾.

6.7.4.2. Waterflood Pattern

A variety of geometric injector/producer pattern layouts can be used for waterflooding an oil reservoir, e.g., regular four, five, seven, and nine spot; direct line drive; and peripheral flood. These geometric layouts are designed to produce an efficient waterflooding for the whole of the reservoir, assuming the rock is homogeneous. The producer/injector ratio typically is chosen based on the expected injection rates for the water injectors and the total fluid-production rates for the production wells. The goal is to have voidage replacement, with the injected volume equal to the produced volume ⁽⁸⁴⁾.

6.7.5. Considerations of Waterflood Technology

Following the primary oil recovery, waterflooding provides supplementary energy for the targeted formation, maintains the reservoir at a certain pressure level, and thus increases the volume of oil recovered from a reservoir. However, it is not always the best technology to use and it can have complicating factors. Some technical aspects should be considered during evaluating and deploying the waterflooding technology in a field project, and assessing and analyzing waterflooding performance.

Understanding the reservoir rock is the most important thing, which can start with knowing the depositional environment at the pore and reservoir levels, and several levels in between ⁽⁸⁴⁾. Then, the information on the current nature and degree of heterogeneities existing in the reservoir has to be obtained. This includes the distribution of impermeable layers such as shale, and interbedded hydrocarbon bearing layers, the variation and degree of formation continuity, interconnection, areal extent of porous and permeable layers, and the trends of fracture, fault, and directional permeability. In addition, the interconnectivities among the various parts of the reservoir, particularly the injector/producer connectivity must be well understood and determined. Moreover, a series of tests on the compatibility of the planned injection water with the reservoir’s connate water, and on the interaction of the injected water with the reservoir rock must be carried out to evaluate interactions such as clay sensitivities and rock dissolution ⁽⁸⁴⁾. Finally, the properties of the displacing/displaced fluids, e.g., water/oil and the rock characteristics need to be well understood because of the impact on wettability, residual oil saturation to waterflooding, and oil relative permeability at higher water saturations.

7.0 SCALING OF PHYSICAL MODELS

7.1. INTRODUCTION

In order to create models that have the same physical behaviour as their reservoir prototypes, it is necessary to scale the models so that the significant physical mechanisms in the field and the model have the same ratios. It is usually not possible to scale completely a physical model, so the models created are properly called partially-scaled physical models. This section discusses the scaling techniques used to create the models.

7.2. DIMENSIONLESS NUMBERS

Physical modeling to create lab models with the same behaviour as the field prototype, in general, involves using dimensionless numbers to match the ratios of significant mechanisms in the lab and the field. Dimensionless numbers have a long history of engineering application. Perhaps the best known dimensionless number is the Reynolds number, which is the ratio of inertial to viscous forces ($Re = V \cdot d \cdot \rho / \mu$). It is used to characterize fluid flow in pipes and over airfoils and other surfaces.

The Nusselt number, $N_{ul} = h \cdot L / k_f$, is used to describe the ratio of convective to conductive heat transfer from a fluid to a surface. The Prandtl Number, $Pr = \nu / \alpha = C_p \cdot \mu / k$, is used to describe the ratio of momentum transfer to thermal diffusion. Another number useful in characterizing heat transfer is the Grashof number, $G_{rD} = g \cdot \beta \cdot (T_s - T_\infty) \cdot d^3 / \nu^2$, which characterizes the ratio of buoyant forces to convective heat transfer in a convective heat transfer situation. The Rayleigh Number, $R_{ax} = G_{rD} \cdot Pr = g \cdot \beta / (\nu \cdot \alpha) \cdot (T_s - T_\infty) \cdot x^3$, is used to describe the ratio of free convective heat transfer to conductive heat transfer.

In reservoir engineering, dimensionless numbers are also used. An example is the capillary number expressed as $N_c = \mu \cdot v / \sigma$, which describes the ratio of (pore scale) capillary forces and viscous forces. A second capillary number, $N_{cg} = \Delta \rho g h / \sigma \sqrt{K}$, describes the ratio of gravitational forces to capillary forces on a macroscopic scale. When thermal processes are considered, the ratio of thermal conductivity of the reservoir to its heat capacity, thermal diffusivity, $\alpha = k_t / (\rho \cdot C_p)$, is a useful descriptive parameter. When creating scale models of a thermal process, the Fourier number, $N_F = \alpha \cdot t / L^2$, is a useful term in describing the ratio of thermal diffusivity to dimensionless time, which is a measure of the extent to which heat will penetrate into a body via conduction. Viscous fingering has also been characterized by dimensionless numbers. Chuoke⁽⁸⁵⁾ defined instability of two-phase flow in porous media, and Peters⁽⁸⁶⁾ has described a stability number useful in characterizing core floods. Other stability numbers have been developed by Peters *et al.* for miscible floods⁽⁸⁷⁾.

One application of the dimensionless number concept has led to the construction of type curves. A type curve is a curve or family of curves, which describes the relationship between two dimensionless parameters in a reservoir, typically over the productive life of the reservoir. Some examples are dimensionless pressure plots, used to forecast reservoir production history, and the many modern pressure derivative plots used in conjunction with pressure buildup tests to diagnose various aspects of a reservoir including permeability, productivity index, and

drainage radius. Reference ⁽¹⁷⁾ refers to type curves used to characterize well performance in cyclic steam stimulation.

7.3. DIFFUSION AND MIXING

Diffusivity in hydrocarbon fluids is a function of several parameters including viscosity of the solute, viscosity of the solvent, and temperature. This has been expressed by the Stokes-Einstein equation ⁽⁸⁸⁾ for low viscosity fluids. For viscous hydrocarbon fluids, the correlation by Hayduk-Cheng may be found in Reid, Prausnitz, and Sherwood ⁽⁸⁹⁾. This correlation shows that diffusivity is inversely dependent on viscosity. Since viscosity is a function of both temperature and concentration of a solvent in viscous oil and since the viscosity of the fluid in question at a given point can change with time due to change in temperature and/or solvent concentration, the transport of multiphase fluids in the reservoir is a highly non-linear problem.

The relationship between diffusion and dispersion for fluids flowing through a porous medium is illustrated in Blackwell ⁽⁹⁰⁾, Pozzi and Blackwell ⁽⁹¹⁾, and in Perkins and Johnston ⁽⁹²⁾. Blackwell ^(90; 91) reported experimental studies of low viscosity fluids in which the results were plotted as a dimensionless dispersion number, (k_d/D_0) , vs. a dimensionless velocity group $(V \cdot d_p/D_0)$. The regions in which diffusion dominated, $(V \cdot d_p/D_0 < 0.4)$, and in which convective mixing (dispersion) dominated, $(V \cdot d_p/D_0 > 4)$, were determined. They measured both longitudinal and transverse dispersion, and found that transverse dispersion was $1/24^{\text{th}}$ of longitudinal for sand packs. They also found that for sand sizes smaller than 30-mesh, the transverse dispersion increased relative to $V \cdot d_p$. Packing heterogeneities at smaller sand sizes increased dispersion. In highly viscous heavy oil reservoirs, mixing may be considerably more complex.

Natural heterogeneities in reservoir rock may transform dispersion into a scale-dependent problem. Walsh and Withjack ⁽⁹³⁾ performed CT scans of miscible core flood experiments. They observed that consolidated porous media produced dispersion results suggesting a length-dependent dispersivity, whereas unconsolidated sand packs produced results suggesting dispersivity was length-independent. When considering field-scale dispersivity, it is necessary to account for the role of natural heterogeneities in creating holdup in the pack and thus producing a scale-dependent longitudinal dispersivity.

Groundwater dispersion experiments by Sudicky ⁽⁹⁴⁾, and Farrel, Woodbury, and Sudicky ⁽⁹⁵⁾ showed this same length-dependent dispersivity, i.e., longitudinal dispersivity increased with distance the tracer front travelled. He attributed some of this dispersivity to adsorption and holdup. Heterogeneities at various scales also play a role in longitudinal dispersion. He did not observe a length dependent increase in transverse dispersion.

7.4. DIMENSIONAL ANALYSIS

In order to create a valid scaled model, it is necessary to determine systematically all of the relevant dimensionless numbers for the reservoir process/system. The techniques commonly used to do so are dimensional analysis and inspectional analysis.

Dimensional analysis, as used by Greenkorn ⁽⁹⁶⁾ and by Geertsma, Croes, and Schwartz ⁽⁹⁷⁾ has been used to develop models for a thermal reservoir process. In this method, all of the known variables describing the process are repeatedly combined until a useful set of dimensionless groups is obtained. This technique requires that the complete set of relevant variables are known. Greenkorn generalized the scaling problem using Buckingham's pi theorem. The theorem states that if we have a physically meaningful equation involving a certain number, n , of physical variables, and these variables are expressible in terms of k independent fundamental physical quantities, then the original expression is equivalent to an equation involving a set of $p = n - k$ dimensionless parameters constructed from the original variables, $\Pi_1 = f(\Pi_2, \Pi_3, \dots, \Pi_n)$ where the Π terms are the dimensionless variables of the field and the lab model ⁽⁹⁸⁾.

Greenkorn arrived at the following set of scaling:

$$K_\mu = K_\rho = K_D = 1 \text{ (same viscosity, density and diffusivity, therefore same fluids in lab and field)}$$

$$1/K_d = a \text{ (velocity scales up by } a, \text{ where } a \text{ is the geometric scaling factor)}$$

$$K_k = K_v \text{ (horizontal and vertical permeability scale up by } a)$$

$$K_t K_v = K_d \text{ (time scales down by } a^2)$$

$$K_p = 1/K_k \text{ (pressure drop scales down by } a)$$

7.5. INSPECTIONAL ANALYSIS

Inspectional Analysis is the process of determining all of the equations that describe the process and rewriting all of the equations describing heat transfer and fluid flow in dimensionless form, and examining the dimensionless terms created. This method was combined with dimensional analysis by Geertsma, Croes, and Schwartz ⁽⁹⁷⁾ to create models for several different reservoir processes, including for non-thermal water flooding, hot water flooding, and non-thermal solvent injection. They determined that for thermal processes, either gravity or capillary forces had to be neglected to produce a realizable model. Likewise, the Reynolds number must be relaxed to produce a realistic model.

Both dimensional and inspectional analysis shows that the problem of scaling thermal recovery processes and/or thermal miscible processes is that the models cannot be scaled completely. Typically, the fluid movement and heat transfer groups demand that the model flow velocity and the permeability be higher than the field values, but the dispersion scaling group demands that the (flow rate x particle diameter) group be the same for the field and the model. Likewise, capillary force scaling demands lab, field permeabilities is similar, but thermal, and gravity scaling groups demand higher permeability in the lab model.

The scaling for miscible thermal displacement is summarized by Frauenfeld ⁽⁹⁹⁾. He used both dimensional and inspectional analysis. One implication of his work is that the dispersion in lab models is typically higher than the field dispersion. Possible answers to this dilemma are to use numerical simulation, or to use unscaled elemental models, or a combination of both.

7.6. RESULTS OF SCALING

7.6.1. Low Pressure Models

Reservoir processes may be represented with models using fluids and temperatures/pressures different from the reservoir. Stegemier *et al.* ⁽¹⁰⁰⁾ described vacuum models (operating at less than atmospheric pressure) where the oil and water viscosity were modified to produce the correct viscosity ratios. These models have been used to predict performance of the Mt. Poso and Midway Sunset steam drive projects in California.

Doscher *et al.* ⁽¹⁰¹⁾ described the development of a low pressure model by using similarity groups derived by dimensional and inspectional analysis. They advocated low pressure models for steam drive and pressure cycle operations, as the low pressure models more accurately reflect the pressure relationships and enthalpy transfers due to evaporation and condensation. They cite the Mt. Poso steam flood model and the application to the Peace River tar sand steam injection and pressure cycling done by Prats ⁽¹⁰²⁾. Doscher published additional work on results obtained from low pressure models ⁽¹⁰³⁾. He concluded that low pressure models could be used to determine the optimum injection rate for a steamflood, and that the models could be used to determine parameters used to classify steamfloods. His concluding work ⁽¹⁰⁴⁾ identified some scaling parameters useful for classifying steamfloods and other thermal processes.

7.6.2. Pujol and Boberg Scale Model

For immiscible thermal displacement, there are some conflicting scaling groups, but partially scaled models have nevertheless proved useful. Pujol and Boberg ⁽¹⁵⁾ have derived the scaling groups pertinent to steam flooding. In this derivation, capillary forces are in conflict, but due to the high temperatures at which steam floods operate, capillary forces were deemed insignificant. These groups have been applied to SAGD. They also did laboratory experiments and numerical simulations for steamfloods, with scaled and unscaled capillary pressure by using surfactants. They found that the “scaled capillary pressure” case had a lower oil recovery than the “unscaled capillary pressure case” for moderately viscous oils (1,600 mPa.s). For highly viscous oils, there was little difference in recovery for scaled and unscaled capillary pressures. They concluded that capillary pressure could be neglected in lab models of steam drive in highly viscous oils.

7.6.3. Kimber's Scaling Study

A measure of heat propagation through a medium may be defined by the ratio of the heat conducted through the material to the heat stored in the material. Heat capacity is defined as the product of density and specific heat, $\rho \cdot C_p$. The thermal diffusivity is defined as follows:

$$\alpha = k_t / (\rho \cdot C_p)$$

The thermal diffusivity is, therefore, the ratio of heat conducted through the material to the heat stored per unit volume. This parameter correlates to the speed with which heat penetrates a solid.

In order to scale thermal lab models to the field, several parameters must be matched. The Fourier number for the field and lab must be matched to correlate with the degree of heat penetration by conduction at a given specific time. This generally leads to lab time being reduced as follows:

$$t_{\text{model}}/t_{\text{field}} = \alpha_{\text{model}} / \alpha_{\text{field}} (L_{\text{model}}/L_{\text{field}})^2$$

For similar field and lab thermal diffusivity, time scaling reduces to:

$$t_{\text{model}}/t_{\text{field}} = (L_{\text{model}}/L_{\text{field}})^2$$

where $(L_{\text{model}}/L_{\text{field}})$ is the scaling factor

For gravity drainage models, gravity and viscous forces must also be matched.

$$(\Delta\rho gK/(V\mu_o))_{\text{model}} = (\Delta\rho gK/(V\mu_o))_{\text{field}}$$

Velocity must be proportional to (L/t) .

If the same fluids are used in the model and the field, then the following applies:

$$(k_t/L)_{\text{model}} = (k_t/L)_{\text{field}} \text{ (thermal diffusivity is scaled), and}$$

$$(k_{t, \text{model}}/k_{t, \text{field}}) = (t_{\text{field}}/t_{\text{model}}) \cdot (L_{\text{model}}/L_{\text{field}}) = (L_{\text{field}}/L_{\text{model}}) = a$$

This scaling approach has been discussed by Pujol and Boberg ⁽¹⁵⁾. Butler ⁽¹⁰⁵⁾ summarized this approach.

There are other possibilities for creating scaled physical models. Kimber ⁽¹⁰⁶⁾ described five possible models, which may be realized. He proposed relaxing different scaling criteria in turn, to create several models. The various models would be applicable to different classes of process, depending on which mechanisms are most significant to the process under consideration. Five approaches were discussed by Kimber:

- 1. Reservoir fluids, high permeability porous media, lower pressure drop, and geometric similarity**

In order to scale geometry, viscous forces, and gravitational forces, the pressure drop in the model must be lower than in the reservoir. A higher permeability porous medium is required. This is the approach used by Pujol and Boberg, and by Butler. This approach requires that dispersion, capillary pressure, irreducible saturation, and relative permeability scaling of the porous media be relaxed. This approach accurately scales the ratio of gravitational and viscous forces, and has been used by several investigators.

- 2. Reservoir fluids, reservoir porous medium, reservoir pressure drop, and geometric similarity**

This model allows pressure changes within the model to replicate pressure changes found in the reservoir. This would allow phenomena that depend on pressure, i.e., solubility and solution gas exsolution, to be accurately scaled. Using the same porous media would allow better scaling of the irreducible saturations and relative permeabilities. Diffusion, viscous forces and heat transfer would be properly scaled. Gravitational forces would not be scaled. This scaling method would not be suitable for processes where gravity drainage is a significant factor. Dispersion would not be properly scaled by this approach. This approach would be suited to processes dominated by viscous forces.

3. Reservoir fluids, reservoir porous medium, reservoir pressure drop, and geometric scaling relaxed

In order to use scaling method #2, above, and also scale gravity, geometric scaling must be relaxed. If the vertical pressure gradient is small, the viscous and capillary forces may be scaled for horizontal reservoirs. Heat conduction in the vertical direction, capillary forces and the effects of dispersion may not be scaled. In this model the height is reduced by the scaling factor " a^2 " and injection flow rate is scaled down by " a^2 ", where a is the scaling factor. This approach is useful for steam and steam-additive processes which require gravitational scaling. It is restricted to relatively thick formations, as it creates a very thin reservoir model. Energy conduction in the vertical direction is enhanced. This may not be a problem for a steamflood, but will change the temperature gradient in the hot liquid or cold liquid zones. Heat loss to the overburden and underburden will also be enhanced.

4. Reservoir fluids, reservoir porous media, reservoir pressure drop, and gravitational scaling relaxed

The previous approaches do not scale dispersion. This approach is an attempt to scale transverse dispersion. Viscous and dispersive effects are scaled at the expense of improperly scaling gravitational and capillary effects. The vertical dimension in this model is reduced by the factor " $a^{1/2}$ " while the horizontal dimension is reduced by the scaling factor " a ". This scaling method is practically limited to thin reservoirs because of the relatively small reduction in the vertical model dimension, leading to thick experimental models.

5. Reservoir fluids, higher permeability porous medium, lower pressure drop, and geometric scaling relaxed

Approach #4 relaxes the gravitational scaling factor, which is a major shortcoming for most process modelling. Proper scaling of viscous and gravitational forces while still scaling dispersion is the objective of this approach. The approach requires a different pressure change and a different porous medium. Time is scaled down by the factor " $a^{4/5}$ " making the experiments rather lengthy. Capillary forces and thermal conduction are not scaled by this approach. L and W are reduced by the factor of " a ". Permeability is increased by " $a^{2/5}$ ", pressure drop, and flow rate are reduced by a factor " $a^{8/5}$ ". H is reduced by " $a^{8/5}$ " and time is reduced by " $a^{4/5}$ ". Both gravity and dispersion are scaled, but conduction of energy within the model is not scaled. Again, this set of scaling criteria will make for a relatively thin reservoir model, enhancing heat loss.

7.6.4. Scaling of Dispersion

Of the five models presented by Kimber, only approaches #1 and #2 will properly scale diffusion. For CSS, SAGD, and steamfloods, this is not a major limitation. When scaling solvent-based processes, however, diffusion is of overriding importance. Since virtually all real reservoir scale processes involve the action of gravity, this leaves only scaling approach #1 capable of scaling both gravity and diffusion. When dispersion is considered, this complicates matters, as dispersion is not easily scaled. Approach #1 will not scale dispersion. Models will still be useful if dispersion is smaller or of equal magnitude to diffusion. Blackwell^(90; 91) presented a dimensionless plot (Figure 7-1) to show that the total transverse dispersion was approximately equal to diffusion if the parameter $V \cdot d_p / D_0$ was < 4 . As for the field this is usually true, as for a gravity drainage case where the viscosity is on the order of 20 mPa.s, the flow velocity would be approximately 1 cm/hour. At this velocity, the dispersion will be smaller than the diffusion, and the system will be diffusion dominated. If the model is also such that dispersion is not dominant, a useful model may be created.

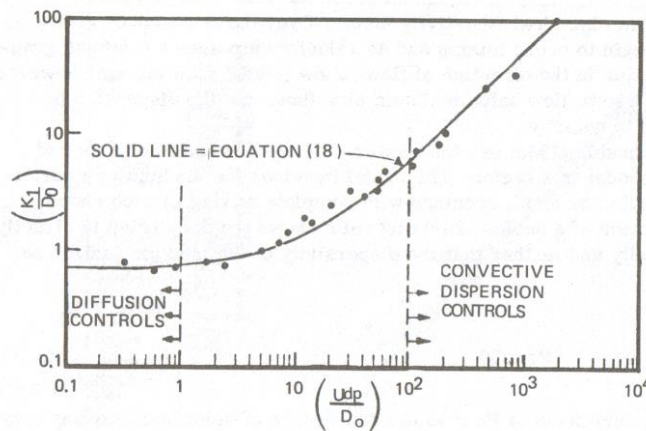


Figure 7-1. Dimensionless representation⁽⁹²⁾ of dispersion and diffusion vs. fluid flow velocity.

7.7. SCALING OF *IN SITU* COMBUSTION

Scaling of *in situ* combustion is complicated by the need to have the heat transfer around the flame front correctly scaled, so that the burning front is not extinguished by excessive heat loss. It is also necessary to scale overall heat loss and to scale gravity, especially for processes where gravity plays a significant role. The correct scaling of the active combustion zone would imply a model with field air flux, field permeability, and fire front advance velocity, combined with a guard heater system to produce an adiabatic model. The requirement of gravity scaling plus heat transfer scaling would imply a fluid velocity scaled up by the scaling factor.

Processes where pressure drive predominates could be scaled by using Kimber's Model #2. This scaling means reservoir permeability plus high velocity air flux would create a model where overall heat flux was scaled. However, it would have the same problem as the gravity scaled

model, namely that the combustion front would be exposed to a much higher air flux than in the field. One solution is the use of adiabatic combustion tubes, which act as an elemental model. This way an air flux representative of the field air flux can be maintained, thus enabling the model to represent combustion kinetics.

Binder *et al.* ⁽¹⁰⁷⁾ used a scaled *in situ* combustion model to compare *in situ* combustion results for two scaled models, one 6.87 times the dimension of the other. The models were scaled to each other by Kimber's Model #1, or Pujol and Boberg scaling. The models studied combustion in a seven-spot pattern with a thickness sufficient to permit gravity override, and with moderately viscous oil. He observed similar recovery vs. scaled time and similar air/oil ratios in both model and prototype. He concluded that scaled models were a feasible means of studying the *in situ* combustion process.

Scaling of *in situ* combustion lab models was discussed by Islam and Farouq Ali ⁽¹⁰⁸⁾. They proposed six approaches, to scale various aspects of *in situ* combustion. All six approaches consider that the porous media, fluids, and temperatures are the same in the model as in the field. The scaling groups and models identified by this study are useful when planning a combustion study, both for the experimental planning, and for numerical simulation of the experiments. The six approaches proposed are as follows:

1. Same pressure drop and geometric similarity: This set will scale viscous forces, pressure drop, capillary forces, and mass transfer. Gravitational forces and mass transfer are not scaled.
2. Same pressure drop but one-dimensional. This is the scaling method used for combustion tube experiments. Gravity was not scaled. Dispersion was not scaled. Mass transfer, viscous forces, and convection were scaled in one direction only.
3. Same pressure drop but geometric scaling relaxed to scale gravitational forces. This scaling set scaled viscous and gravitational forces. Capillary forces, vertical heat conduction, and dispersion were not scaled. This scaling criterion was also suggested by Kimber.
4. Same pressure drop but geometric scaling relaxed to scale dispersion. Dispersion was scaled but not gravity.
5. Different pressure drop to scale coke concentration. Fuel concentration is important to the dynamics of the combustion process, so this group was scaled by setting: $P_{or}/P_r = \ln a$, where a is the scaling factor.
6. Different pressure drop to scale reaction rate terms. Pressure was increased by a factor 'n' such that: $e^{n/n} = a^2$, where a is a scaling factor for reaction rates.

Gutierrez, Moore, and co-workers ⁽¹⁰⁹⁾ proposed a strategy that combines the following six elements:

- a) selecting a combustion kinetics model and combustion reaction temperature experiments to obtain combustion kinetics
- b) PVT studies to establish phase behavior of the oil
- c) combustion tube experiments to determine air and fuel requirements

- d) simulation of the combustion tube experiments to verify the combustion kinetics model
- e) upscaling of the combustion kinetics model to fit a field scale numerical simulation
- f) numerical simulation of the field case

Kumar ⁽¹¹⁰⁾ performed combustion tube experiments that showed the width of the active combustion zone was approximately one inch. The implications of the thin combustion zone are that the numerical simulation of a combustion process would have to model the active zone as blocks no wider than one inch. To model the process using field scale blocks would require upscaling the combustion kinetics to accommodate larger grid blocks. Kumar suggests that the non-scaling of the combustion front in a 3D scaled model would not affect the accuracy of the performance prediction of that model.

It appears that the scaling of combustion can be divided into gross mechanistic performance, as characterized by oil recovery, air consumption, and ultimate recovery. The performance encompasses combustion front mechanisms, such as burn temperature, burn front extinguishment, high temperature vs. low temperature combustion, and reaction kinetics, including activation energy and oil component lumping. Recovery and rate may be scaled by a Pujol and Boberg type model for gravity processes. Combustion tube experiments are used to measure details of the combustion process, i.e., burn front width and temperature, minimum air flux, and air/fuel requirements, etc. Ramped temperature oxidation experiments using a differential scanning calorimeter are useful for determining activation energy, prevalence of high temperature vs. low temperature oxidation reactions, and to verify the choice of component lumping schemes. All of these techniques may be used together to develop a comprehensive database, including history matching, to set up a numerical simulation of the field process.

7.8. SCALING OF ELECTRICAL PROCESSES

The scaling approaches described above are not typically amenable to scaling of electrical processes in a reservoir. Vermeulen *et al.* ⁽⁴²⁾ have reported scaling criteria for physical modeling of electromagnetic processes. Physical scaling of electromagnetic processes requires that electrical and thermal similitudes is consistent and simultaneously incorporated in the model. Starting with Maxwell's equations, in the case of electrical similitude, and the heat transfer equation, which incorporates conversion of electromagnetic energy into heat and for the case of thermal similitude, Vermeulen *et al.* developed a completed set of scaling parameters.

It turns out that one of the biggest challenges in scaling electrical processes relates to the electrical properties of the oil sands. If "a" represents the physical or mechanical scaling factor such that:

$$(L_{field}/L_{model}) = a,$$

$$\text{then } a = (\sigma_{model}/\sigma_{field})[(\mu_{model} * \epsilon_{field}/(\mu_{field} * \epsilon_{model}))^{1/2}]$$

where: σ : electrical conductivity

μ : magnetic permeability

ϵ : dielectric constant

The consequence of this scaling criterion is that the scale of the model can only be determined once the electrical properties of the medium to be used in the model are determined. This is not as trivial as selecting sand of a specified flow permeability to fit the scaling for conventional reservoir model. In this case, the model medium that is, primarily the oil and water composition, will likely not be the same as in the field.

Time scaling (γ) turns out to be also dependent on electrical conductivity and the dielectric constant of the field and model such that the frequency (ω) used in the field must be γ times the frequency used in the model:

$$\gamma = (time_{model}/time_{field}) = (\omega_{model}/\omega_{field}) = (\sigma_{model}*\epsilon_{field})/(\sigma_{field}*\epsilon_{model})$$

Two other scaling parameters involve the thermal properties of the systems, which relate fundamentally to the electric and magnetic field intensities in the model and the field. These scaling parameters depend on the thermal and electrical conductivities, mechanical scaling factor, and the scaling of temperature changes in the model and the field. Using all of these scaling parameters, once the size of the model and applied frequency are selected, the electrical power, input impedance, voltage, current, and current density can be determined. This fully defines the scaled model and its operation with respect to the field scale system. Vermeulen and co-workers also discuss scaling under three different conditions for Athabasca oil sands as discussed below. A fourth condition, involving the use of overburden and underburden, with different electrical properties than the oil sands, was also provided but will not be discussed here.

7.8.1. Induction Approximation

The induction approximation applies when the applied frequency in the field is below about 1 MHz. Then displacement current (in Maxwell's equations, a time varying electric field with units of current density) can be neglected. This situation applies when induced conduction currents are being created by a time-varying magnetic field such as that by a current loop placed in the reservoir. In this case, the mechanical scaling factor can be selected for convenience so it is relatively simple to create a conveniently-sized lab scale model. The same oil sands media from the field can be used in the model. However, scaling properties must still be selected so induction approximation also applies in the model.

7.8.2. Quasi-Static Approximation

In the quasi-static approximation, the time-varying electric field associated with the time varying magnetic field is negligible. The conduction current is dominant, while the displacement current is negligible and this is true for oil sands when the frequency is low, i.e., less than 1 kHz. Furthermore, the wavelength must be larger than the dimensions of the system of oil sands and electrodes. For scaling purposes, the mechanical scaling and frequency scaling can be selected for convenience. If the same oil sands as in the field are used in the scaled model, then scaling becomes even more simplified.

7.8.3. The Good Dielectric Approximation

At electromagnetic frequencies above 300 MHz in Athabasca oil sands, the ratio of the conduction current to the displacement current becomes less than 10%, i.e., displacement current dominates in Maxwell's equations. In this case, the mechanical scaling factor can be conveniently selected. If oil sands are used in the model, then the frequency-scaling factor will be the same as the mechanical scaling factor but frequencies employed in the model will likely fall in the GHz microwave region. It should be noted that at these higher frequencies (>300 MHz), the depth of penetration is less than 1 meter, so heating of the reservoir is less practical unless water is progressively evaporated as the electromagnetic radiation penetrates further and further through the now lossless medium containing no liquid water.

7.9. MECHANISMS AND PROPERTIES NOT COVERED BY SCALING

In spite of the wide application of scaling, some processes are not amenable to investigation by physical models. Geomechanics is one reservoir behavior where physical models have not been very successful in reproducing reservoir behavior. The challenge in adequately modeling geomechanical behavior is to re-create all of the physical properties of a block of reservoir sand, including cohesive strength. Scott and Proskin⁽¹¹⁾ have created a reasonable facsimile of some aspects of pore volume and pore interconnectivity of oil sands reservoir during steam stimulation, by using a small amount of gypsum as a binder with Ottawa sand. However, physical models, which include oil recovery and geomechanics simultaneously, are complex and costly.

Interbedded shale in reservoirs is another feature that is difficult to emulate in physical models. Permeability heterogeneities may be modelled to some extent by packing alternating layers of high permeability and low permeability sand. Shale may be simulated by packing pieces of non-permeable material along with the sand. However, lacking knowledge of the size and shape distribution of the shale layers in the reservoir makes it impossible to pack an accurate lab model. The advent of reservoir characterization software has made it possible to develop approximations of shale inclusions in the reservoir for numerical simulation. These shale characterizations can in principle be inserted into a physical model by inserting appropriate pieces of shale or slate into the model during packing. Significant time and effort would have to be expended to create this pack in realistic detail.

Physical behavior of shale layers in the reservoir is more difficult to model. Physical behavior may be manifested as shale weakening due to steam, shale fracturing due to thermal stresses, and shale reactivity with injected fluids. These behaviors are difficult, if not impossible, to re-create in a physical model, as not only the physical and chemical characteristics of the shale specimen would have to be matched, but also the stress environment, and the time at temperature and under the changing stress regime.

Chemical reactivity of reservoir rock is another phenomenon that is studied with core floods rather than with scaled models. A reactivity/permeability alteration experiment requires the

actual reservoir rock, fluids, pressures, and temperatures. Such experiments also require real reservoir time, perhaps hundreds of hours to observe and measure solubility and/or precipitation reactions.

Dispersion is another mechanism that is typically not scaled by physical models. This is not a problem for SAGD but processes where oil and solvent mixing occur, either in the reservoir or in the lab model, will not scale accurately. This is a significant problem when attempting to create scale models of VAPEX or of thermal-solvent processes. AITF is currently working on the development of models that will enable accurate representation of these processes.

Waterflood models for evaluation of microbial processes utilize cores from the target reservoir and reservoir fluid composition. Sand packs such as those used for combustion tube tests can also be used. Flow and pressure measurements in these models correspond to those in the field. Scaling would not be required for an MEOR waterflood and the microbial processes (e.g., gas or surfactant production) would occur over field-scale time.

7.10. SUMMARY

1. Scaling is a tool that can be applied to many reservoir processes, and has both analytical and predictive applications. The application of scaling has led to use of scaled physical models for many reservoir applications, including at AITF.
2. Dimensionless numbers are the most basic form of scaling, and are used to describe the behaviour of systems at different scales, where the commonality is the similar ratios of magnitude of the dominant phenomena. These numbers may be applied to scale reservoir processes. Type curves are an application of dimensionless numbers, where one or more phenomena are described as a dimensionless number(s), and the behavior of different systems with the same or similar dimensionless number(s) may be classified by use of a dimensionless curve or family of curves. Such classification is useful in determining reservoir parameters and in prediction of reservoir performance.
3. It is necessary to use a systematic approach to develop a set of dimensionless numbers to describe a complex reservoir process. Two scaling techniques, namely dimensional analysis and inspectional analysis, may be used to develop a set of dimensionless numbers for a specific reservoir process. Application of these dimensionless numbers may be applied to design scaled models used to study these reservoir processes.
4. Models for electrical heating require different approaches to scaling that involves the complex electrical properties of media in the field and in the model.
5. The models may be high pressure (use reservoir fluids) or low pressure (use non-reservoir fluids). There are several sub-categories of models under the above classifications. Such models in general cannot scale all phenomena significant to the reservoir process under study. It is thus necessary to relax one or more scaling constraints to make it possible to build the model. Some processes (thermal-solvent processes) may have limitations on the scaling factor, which are imposed by the difficulty of scaling mixing.
6. At AITF a wide variety of processes have been examined by using lab models, scaled and unscaled. The use of well-planned experiments is an important step, preceding numerical simulation.

7. The development of scaling for processes where mixing may be a factor is an area of current development at AITF.

7.11. SYMBOLS USED

| | |
|-------|--------------------------------------|
| c_p | constant pressure heat capacity |
| d | diameter |
| D_o | molecular diffusion coefficient |
| g | gravitational acceleration |
| h | convective heat transfer coefficient |
| H | height |
| k_t | thermal conductivity |
| k_d | dispersion coefficient |
| K | permeability in porous media |
| L | characteristic length |
| P | pressure |
| T | time |
| T | temperature |
| v | velocity |
| x | characteristic length |

| | |
|------------|---|
| α | thermal diffusivity |
| β | volumetric thermal expansion coefficient |
| ϵ | dielectric constant |
| μ | dynamic viscosity or magnetic permeability |
| ν | kinematic viscosity |
| ρ | density |
| σ | surface or interfacial tension or electrical conductivity |

8.0 PHYSICAL MODELS

8.1. INTRODUCTION

There have been many processes used and proposed for the production of heavy oil and bitumen. In order to study and develop these processes, investigations have been conducted using laboratory models, numerical simulation, and a combination of these methods. Because the mechanisms involved in thermal and non-thermal oil recovery processes may not all be thoroughly understood and quantified, or may not be represented adequately in numerical simulations, there is a preference for physical models, at least in the early stages of process development.

In this section, some of the different types of models used for SAGD, solvent-steam, combustion, electrical heating, and biological processes are briefly overviewed. This review is not intended to be an exhaustive tabulation of every physical model reported in the literature. Rather, the typical models utilized by various research groups are described. Some of the many models built and operated at AITF are also summarized.

8.2. OVERVIEW OF MODEL TYPES

8.2.1. *Low Pressure Models*

Laboratory models can be high or low pressure. The former models use reservoir fluids, pressures, and temperatures while the latter use different fluids and lower pressure and temperature. Most low pressure models are vacuum models. Vacuum models have the advantage of not requiring confining pressure hence; a large pressure vessel is not required. That means that a larger model may be housed in the same lab space. The disadvantage of vacuum models is that different fluids, pressures, temperatures, etc. may often mean that some significant area of reservoir physics is compromised in these models. The compromise may not be immediately obvious, so the safer alternative is to use high pressure models and actual reservoir fluids, pressures, and temperatures. Most of the reservoir models at AITF are high pressure models. A partial exception to this rule is some visual models and computed tomography (CT) models.

8.2.2. *Visual Models*

Visual models typically operate at lower pressure than the reservoir due to the limitations of glass or acrylic as the model walls. They may be partially scaled 2D models or elemental 2D models. Thermal visual models are possible and indeed, Nasr has used 2D visual models of the SAGD process ⁽¹¹²⁾. Thermal visual models have the limitation of high heat loss from the sidewalls of the models. This may be controlled to some extent with windows and/or heaters, but caution must be observed in not allowing the heaters to control the process.

Visual models may operate at pressures above atmospheric and as such may use butane as the solvent fluid. Cuthiell *et al.* ⁽¹¹³⁾ used a CT visual model to observe the drainage in a VAPEX

process and to analyze the effect of capillary pressure on a VAPEX process. Higher pressure visual models may be constructed by placing them inside a pressure vessel. In this case, the model may be operated using reservoir pressures and temperatures, as a partially scaled model, or as an elemental model. A model using acrylic plates was also used by Cuthiell ⁽¹¹⁴⁾ to examine viscous fingering in single-phase and two-phase systems.

8.2.3. CT Models

The classification of visual models may be extended to models where visualization is provided by a CT scanner or an x-ray machine. In the case of a CT scanner, the CT model may be 2D or 3D. The model, and confining pressure vessel, if applicable, must be constructed of materials with reasonable x-ray transparency. Such models and pressure vessels, constructed of beryllium, aluminum, titanium, or various plastics, have been built at AITF. Yuan *et al.* ⁽¹¹⁵⁾ used his model (plastic, confined in an aluminum pressure vessel) to examine the effect of gas injection on steam chamber formation in SAGD.

8.2.4. High Pressure Models

High pressure models, which use reservoir pressures and temperatures, may be further subdivided into partially scaled models and elemental models. Partially scaled models attempt to scale a subsection of the reservoir sufficiently large (a well pattern or sub-section of a pattern) so that the workings of a given process may be observed.

8.2.5. Partially Scaled Models

Partially scaled models attempt to scale the proportions of all significant mechanisms in the model to those in the field. Some compromises in scaling are always necessary to create a realizable model, hence the name “partially scaled model.” A later section will discuss the development of partially scaled models at AITF.

8.2.6. Elemental Models

Elemental models are not scaled down sections of the reservoir. They represent an element of the reservoir at a critical juncture of the process, i.e., the steam-oil boundary zone in SAGD. They use actual reservoir sand, or at least sand of the same permeability as the reservoir, actual reservoir fluids, and reservoir pressures and temperatures. The oil production and fluid interactions observed in these models may be extrapolated to the reservoir scale by using numerical simulation, by first numerically matching the model performance, then modeling the reservoir scale process using the same parameters.

Elemental models of thermal processes must deal with the heat loss that is inevitable in a physical model. If insulation is insufficient to keep heat loss at an acceptable level, additional precautions must be taken. Hence, elemental models may be further divided into isothermal models and adiabatic models. Isothermal models are heated to a single constant temperature and maintained there by electrical or steam heat. The single temperature means that there is no

temperature gradient, hence no heat flow in or out of the experiment. This is a useful approximation of the field reality, when dealing with processes where heat transfer is not the rate-limiting step. Frauenfeld *et al.* ⁽²²⁾ used an isothermal model to measure solvent front advance rate for a butane-UTF bitumen system. Nasr ⁽¹¹⁶⁾ used an isothermal model to measure steam chamber rise rate for a SAGD process.

Adiabatic models use active guard heaters and controls to reduce heat flow in or out of the model to zero, or as close to zero as possible. This will provide an accurate heat loss boundary to the elemental model (or scaled model). This type of model is needed when heat flux, heat transfer, or heat generated are critical to the process. A prime example is *in situ* combustion. For *in situ* combustion experiments, accurate control of heat loss is essential in order to prevent the combustion front from extinguishing itself, and to get an accurate picture of combustion dynamics. A model of an *in situ* combustion process was built by Coates *et al.* ⁽³⁵⁾, and Chen *et al.* ⁽¹¹⁷⁾. Adiabatic models have the disadvantage of the additional cost and complexity of the guard heater system. They also risk the process being driven or controlled by the heat flux environment set up by the guard heater system. Careful design and testing is needed to ensure neutral behavior on the part of the guard heater system.

8.3. SAGD

Nasr *et al.* ⁽¹¹⁸⁾ AITF provided an analysis of the SAGD process using numerical and experimental tools. They performed experiments using a two-dimensional scaled model that allowed for visual observations of steam chamber development. The model was rectangular, with dimensions of 0.6 m × 0.21 m × 0.03 m. Two windows made of Lexan were clamped on each side of the frame to allow for visual observations. The model was filled with glass beads having a permeability of about 2,000 Darcy and a packing porosity of about 0.35.

The model used the Pujol and Boberg ⁽¹¹⁹⁾ scaling criteria, with a geometrical scaling factor of 100. Porosity, oil properties, and thermal properties were closely preserved in the model. To preserve the ratio of gravity to viscous forces, a dimensionless scaling group was used, which resulted in the lab experiments being run at lower pressures than those in the field. Also because of the scaling criteria, the permeability in the lab was different from that in the field.

Piped steam was reduced from 4.2 MPa to 0.345 MPa, and superheated to 160 °C to avoid condensation during metering and control. Steam flow rate was measured using a 1.52 mm orifice. A research valve was installed downstream of the orifice, and was controlled by an injection pressure set-point to deliver steam at about 20 kPa. An in-line ARI resistance heater and a heat trace were used to maintain a maximum of 10 °C superheating at the injection point. Temperature sensors were located in the injection and production lines and on the model boundary. Production fluid samples were collected in glass jars at equal time intervals and analyzed in the lab.

Sasaki *et al.* ⁽¹²⁰⁾ at Akita University used several two-dimensional scaled physical models. Some of the models had a width and height of 380 mm and a thickness of 44.5 or 49.5 mm; others had a width and height of 300 mm and a thickness of 4.5 or 9.5 mm. The sidewalls of the model were 20 mm thick acrylic resin, allowing for physical and thermal visualization of the experiment.

Copper pins installed on the front plate allowed for the monitoring of temperature distribution in the model.

The model was packed with glass beads of 0.22 mm average diameter, and saturated with COSMO#1000 motor oil through two 10 mm fittings at the top and bottom of the model. The production and injection wells had a vertical separation of 100 mm, and were covered with stainless steel screen (100-mesh) to filter the glass beads.

Bagci ⁽¹²¹⁾ at Heriot-Watt University discusses experiments performed with a three-dimensional physical model. The dimensions of the model were 30 cm × 30 cm × 10 cm. The experimental set-up consisted of a steam generator, the physical model, a backpressure regulator, a water-oil separator, and a temperature scanner. Twenty-five thermocouples were installed along the center plane of the model for measuring temperature distribution. The injection and production wells were vertically separated by 5 cm, and were constructed from 8 mm diameter stainless steel tubing. The wells were perforated with several 3 mm diameter holes along their length, which were covered with 100-mesh metal screen to prevent sand production.

Fractures were simulated by placing into the pack 10 cm × 15 cm 40-mesh stainless steel screens that were attached to the steel body. The fractures were located along the length of the injection and production wells. After the wells and fractures were installed, the model was packed with a mixture of crushed limestone, oil, and water. Once the model was packed, it was placed into an insulation jacket and heated to about 50 °C. Superheated steam at 50 psi and 150 °C was injected into the model. To control the pressure of the production well, backpressure regulators were used at the fluid stream of the separator and were adjusted to 2 psi below the injection pressure. Injection temperature, model temperature distribution, injection and production pressures, and oil and water production data were all measured continuously during the experiment.

8.4. SOLVENT-STEAM

Canbolat *et al.* ⁽¹²²⁾ at Stanford University, report a scaled model for investigating SAGD with a non-condensable gas. The model consisted of a 30 cm × 30 cm × 7.5 cm stainless steel can, which had a thermal blanket for pre-heating. The injection and production wells consisted of perforated tubing wrapped with a wire screen. The injection well could be physically adjusted to 5, 10, or 15 cm above the producer. An array of twenty-five thermocouples, with 2 cm separation, was provided for monitoring temperature inside the model. Each thermocouple was inserted in the model via separate welded fittings. In this particular case, the model was packed with crushed limestone having no measureable matrix porosity. Model confinement was not discussed but given the maximum reported injection pressure of 382 kPa, it was likely that the steel walls of the can supplemented by braces provided the confinement. The scaling employed for this model was that derived and recommended by Butler ⁽¹²³⁾.

In contrast to most scaled physical models, Ardali and co-workers ⁽¹²⁴⁾ at Texas A&M University employed a 2D annular sand pack model encased in concentric aluminum pipes. The stated reasons for using an annular rather than a rectangular 2D model were pressure rating requirements and unspecified laboratory constraints. The actual pressure rating of the model

was not specified, but the steam generator associated with the fluid injection system could supply steam up to 13.8 MPa.

The aluminum annular model had an internal radius of 6.25 cm and an external radius of 16.25 cm. The height of the model was 25.4 cm. The annular space had 1.875 cm of Foamglas insulation on each surface leaving 2.5 cm of annular space for the model reservoir. The model was sealed by end caps with Viton o-rings. There was no bracing of the model or a containment vessel described. The model was equipped with 45 thermocouples arrayed in the annular space. The injection well was placed 5 cm above the production well, which was 2.5 cm from the bottom of the model. Typical fluid injection and production stations were provided. The model of an Athabasca reservoir was scaled using the Pujol and Boberg ⁽¹²⁵⁾ scaling theory. Further details on the design and operating procedure are provided by Ardali *et al.*

A relatively large 1/100th scale model, representing an Athabasca reservoir, was reported by Khaledi and co-workers ⁽¹²⁶⁾ at ExxonMobil and Imperial Oil. Model dimensions were 100 cm x 60 cm x 20 cm (LWH) and it was designed to operate at 10 MPa. The model was scaled based on the dimensional similarity method developed by Butler ⁽¹²³⁾ for SAGD.

In ExxonMobil's 3D model, the horizontal well length was 100 cm and special care was taken to ensure uniform steam distribution along the entire length of the injection well. The inter-well spacing was not specified. The model (packed glass beads) was encased by ¼-inch thick stainless steel plates to provide sufficient rigidity for a non-deformable confinement. The top and bottom of the model included concrete for overburden and underburden, which along with thermal insulation on the outside of the model was designed to scale heat losses to that in the field. The model was packed with glass beads to provide a 300 Darcy model reservoir. Care was taken to provide a high level of compression on the model packing during sealing with the lid to ensure minimal variation in porosity and model volume. Over 100 thermocouples were used to monitor temperature inside the model, wells, overburden, underburden, and sidewalls. The reservoir model was placed inside a pressure vessel, which provided external pressure on the model 700 kPa above the steam chamber pressure inside the model. The injection and production systems and their operation and control are described in some detail. Considerable attention was given to maintaining constant pressure in the steam chamber, while maximizing liquid production without bypassing live steam from the injector to producer.

Mohebati *et al.* ⁽¹²⁷⁾ at the University of Calgary, report a typical 1/100th scale rectangular, 3D reservoir model for an Athabasca reservoir, based on Pujol and Boberg ⁽¹²⁵⁾ scaling. The model can was 70.5 cm x 15.2 cm x 22.9 cm (LWH) and was constructed of 316 stainless steel. The model was packed with 250 Darcy sand sealed, water saturated and then the water was displaced by oil. There were 240 thermocouples provided to monitor the temperature of the reservoir. The production well was placed 3.5 cm from the bottom of the model and the injection well was placed 4.5 cm above that. Wall thickness of the model or bracing was not specified and no pressure rating was provided. However, the model was placed in a confinement pressure vessel and tests were conducted at pressures up to 3,500 kPa. The annulus between the walls of the confinement vessel and the model was filled with insulation.

Ayodele *et al.* ⁽¹²⁸⁾ at AITF discuss their scaled model used for testing low and high pressure ES-SAGD and SAGD processes. The model was an insulated stainless steel box, with dimensions of

24 cm × 80 cm × 10 cm. There were 21 thermocouples placed throughout the core of the model, and 8 thermocouples placed on the surface. The injector and producer wells were placed in the center of the length of the model, with the producer about 1 cm from the bottom of the model and the injector 5 cm above the producer. The model was lined with a Teflon sheet on the top and bottom of the model.

Ottawa sand was used in the model, with a scaled permeability value of 120 Darcy, which represents about 1 Darcy in the field. A porosity of approximately 32% was obtained in the experiments. The model was first saturated with water and then displaced by dead Athabasca bitumen. The initial oil saturation was between 92.6% and 95.9%. A total of five experiments were run; they included low pressure SAGD, high pressure SAGD, propane-SAGD, and ES-SAGD at low and high solvent concentration.

For the experiments, steam from a central supply was injected solely or co-injected with a solvent. The injection rate was controlled by a control valve, and a regulator controlled the injection pressure. When solvents were co-injected, a pump running at constant volumetric rate was used.

The produced fluids were collected in piston-type accumulators and passed through an intermediate condenser. Condensed fluids were collected in sample bottles for analysis. Vented gas volumes were measured by a gas flow meter and an online gas chromatograph was used to analyze produced gasses. During the tests, gas samples were passed through the gas chromatograph at 10-minute intervals to determine gas compositions. Temperature pressure and injection rates were also measured by a data acquisition system at one-minute intervals.

All the experiments were scaled using the Pujol and Boberg⁽¹¹⁹⁾ scaling approach with a scaling factor of 109.

The start-up procedure for the experiments involved steam being injected/circulated in both the injector and producer to establish communication between the well pair. After about 10 minutes, when the space between the wells was heated up, injection was stopped in the bottom well and it was converted to normal fixed pressure production mode. If a solvent was being co-injected, it also began after the 10-minute start-up time. All the experiments were run for 910 minutes (20.57 years at field-scale).

8.5. COMBUSTION

In general, there are two major types of combustion models that have been used in various laboratory studies:

- 1D combustion tube for combustion mechanistic study
- 3D physical experimental model for evaluating combustion performance

Examples of these are discussed below.

Cristofari and co-workers ⁽¹²⁹⁾ at Stanford University describe a combustion tube to investigate the effect on the propagation of the combustion front of cyclic solvent injection (CSI) employing different solvents. Since the main focus was fire front propagation, the combustion tube was designed to conduct essentially 1D experiments. These comparative experiments did not consider reservoir pressure so it was possible to use a thin-walled model to minimize heat conduction axially along the length of the tube. The model consisted of 304 stainless steel tube 100 cm long with a diameter of 7.5 cm and wall thickness of 0.41 mm. A centrally located thermowell ran the full axial length of the tube and the tube was sealed to the top and bottom end caps. An electrical band heater was placed at the top end of the tube for preheating part of the reservoir to 450°C to initiate *in situ* combustion. The tube was loaded with sand and oil while in the vertical orientation to avoid segregation due to gravity, and then inside an explosion-proof jacket. The annular space between the model and the explosion-proof jacket was filled with ceramic fiber insulation (Fiberfrax). Heat loss from this model was estimated at less than 10% of the energy output from the combustion. A rationale for the scale of the model was not provided.

Freitag and Exelby ⁽¹³⁰⁾ at Saskatchewan Research Council also employed a tubular 1D model but used high temperature corrosion and carburization resistant Incolloy 800 with 0.49 cm wall thickness rated to 4.2 MPa. No additional pressure containment vessel was used. The combustion tube had internal dimensions of 5.37 cm in diameter and 162.3 cm in length. Twenty-five thermocouples were used to measure the temperature along the center of the packed tube. Band heaters were placed upstream from each thermocouple to compensate for heat loss. A band heater was placed at the injection end of the tube for pre-heating to allow ignition and a second band heater was placed at the far end of the tube to maintain the temperature of the produced fluids. The entire tube was wrapped with a 2.5 cm thick layer of ceramic fiber insulation.

Garon and co-workers ⁽¹³¹⁾ at Gulf reported one of the earliest scaled 3D models employed for *in situ* combustion. Garon *et al.* discussed in detail the scaling methods used, which involved Pujol and Boberg ⁽¹²⁵⁾ for steamflooding and Binder and co-workers ⁽¹⁰⁷⁾ for fireflooding. The mechanisms that could not be scaled in their model included: capillary effects, relative permeability, pressure gradients (same in field and model), fluid-solids interactions (e.g., clay swelling), molecular diffusion and convective dispersion, and chemical reactions associated with combustion and pyrolysis. A scaled model was constructed for Wasbasca Grand Rapids Formation A. The model consisted of a 61 cm square top and bottom with a height of 15.2 cm. The model was constructed from 0.5 mm thick 304 stainless steel. Vertical injector and producer wells were located at diametrically opposite corners. The wells were completed over the lower one-fourth of their length using a combination of screens and gravel packs. The wells were also wrapped with flexible sheathed heater for ignition at the injector and to keep the produced fluids heated. Thirteen symmetrically arrayed thermocouples were used to monitor the temperature of the reservoir and two additional ones were used to monitor the wells. The model was packed with sand and the top plate welded on. The model was placed inside a confinement pressure vessel prior to saturating with water and oil via the two wells. The thin walls of the model allowed it to conform to the sand by positive confinement pressure, maintain model integrity, prevent fluid bypass along the internal walls, and minimized heat transfer along the walls of the model. The maximum operating temperature was 6.9 MPa.

Greaves and co-workers^{(132), (133)} at the University of Bath have constructed and operated 3D scaled model for their toe-to-heel air injection (THAI) *in situ* combustion process. The scaling used in the construction of these models was based on that proposed by Pujol and Boberg⁽¹²⁵⁾ for steamflooding and Binder and co-workers⁽¹⁰⁷⁾ for fireflooding. The model was in a box with 40 cm square top and bottom and a height of 10 cm and was constructed from 4 mm thick 316 stainless steel. A later developed cell⁽¹³⁴⁾, had a length of 60 cm reportedly to allow for longer test periods as well as higher air injection rates. The model was packed with 10 Darcy sand, which represented 0.04 Darcy in the field. Perforated 6.4 mm stainless steel tubing covered with 100 gauge wire mesh was used for injector and producer wells. For catalytic upgrading tests⁽¹³⁴⁾, the production well was placed inside either 1.25 or 2.54 cm tubing filled with catalyst pellets. The distance between the injector and producer was 40 cm in the horizontal plain, which represented a separation of 100 m in the field. Sixty sets of thermocouples, each measuring temperature near the top, middle, and bottom, were arrayed in the model to provide a 3D temperature profile. Six band heaters (40 cm long model) or nine band heaters (for 60 cm long model) were wrapped around the model to compensate for heat loss. A 6 mm thick layer of ceramic fiber was also wrapped around the entire model. These heaters were operated manually in response to peak temperature in the combustion zone and adjacent temperature nearest the wall in the model. Later modifications of the combustion model included automatic computer control. An additional heater was embedded in the top section of the model, above the air injector, to pre-heat the model to the temperature required to cause ignition.

Chen and co-workers⁽¹³⁵⁾ at AITF have created a model for *in situ* combustion as a follow-up process to cold heavy oil production with sand (CHOPS). Only 10 to 15% of the original oil in place is produced by CHOPS. Furthermore, CHOPS creates a high permeability network of wormholes, which are interconnected to adjacent wells. This network can facilitate the necessary injectivity of air to achieve high temperature combustion; connections to adjacent wells provide a production pathway. The AITF models consisted of a 20 cm diameter, 18 gauge 316 stainless steel tube with lengths of 60 cm and 100 cm. Stainless steel endcaps, 2 cm thick, and equipped with necessary ports were used to seal the tube. The injection and production wells were placed in the center of the end caps at opposite ends of the tube. Scaling for this model was not discussed.

Several ports situated along the length of the tube were used to saturate the model and functioned as ports for monitoring the pressure during the combustion process. The model was packed with actual produced sands from a Lloydminster CHOPS operation. A high permeability channel 3.5 cm in diameter was created along the central axis of the tube by packing with either high permeability (300 μm^2) frac sand or by placement of a ceramic tube (3.5 cm OD x 2.5 cm ID) with permeability of about 40 μm^2 . Ten thermocouple rods with five equally-spaced measurement points were placed along the central vertical plane of the model. Nine additional thermocouples, along with two igniters, were inserted through the injection endcap. Several band heaters were placed along the length of the tube to compensate for heat loss. The band heaters were operated to minimize the temperature difference between eighteen surface thermocouples, located under each band heater, and the adjacent thermocouple inside the model. The model was packed, saturated, and insulated before mounting in a high pressure containment vessel. Details of the operation of the model are provided by Chen *et al.*⁽¹³⁵⁾. The maximum operating pressure for the models was not specified but overburden pressure supplied by the containment vessel was up to 4 MPa.

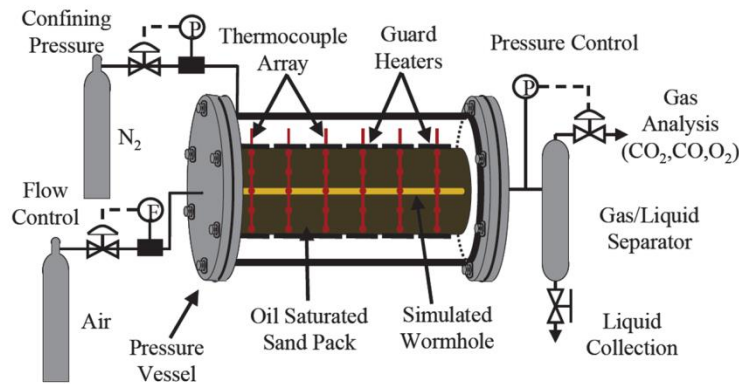


Figure 8-1. Schematic of *in situ* combustion model with simulated wormhole from Chen *et al.* (128).

Lim and Chen (136) at AITF report a 3D combustion model used to investigate their proposed multi-stage combustion assisted gravity drainage (MS-CAGD) process. The model consisted of a tube 36 cm in diameter and 60 cm long. The model was equipped at one end with an injection well placed 10 cm above a production well located 1 cm above the bottom of the model. The wells were placed 7 cm into the model from the front end. An electrical igniter was located along the injector. Both wells were located in the vertical plane passing through the center of the model.

Two offset production wells were located 30 cm and 50 cm from the front end of the model. Vent wells were also placed, at the top of the model, 20, and 40 cm from the front end of the model. Five thermocouple rods, with seven measurement points each, were placed in the central vertical plane of the model. Similarly, five thermocouple rods were placed in the central horizontal plane. Guard heaters were placed on the external surface of the model to compensate for heat loss. The temperature difference between the internal and external wall was used to control the operation of the heaters. Four heaters near the injector and producer were used for preheating the model during start-up. The model was packed and sealed by welding the lid then placed inside a pressure containment vessel where it was saturated with water and then McKay River bitumen. Further details on the operation of the model are also given. Materials of construction and scaling methods were not specified. However, it was noted that offset wells in the field were specified as being 50 m from the injector and producer well pair and 20 Darcy sand permeability was used in the model.

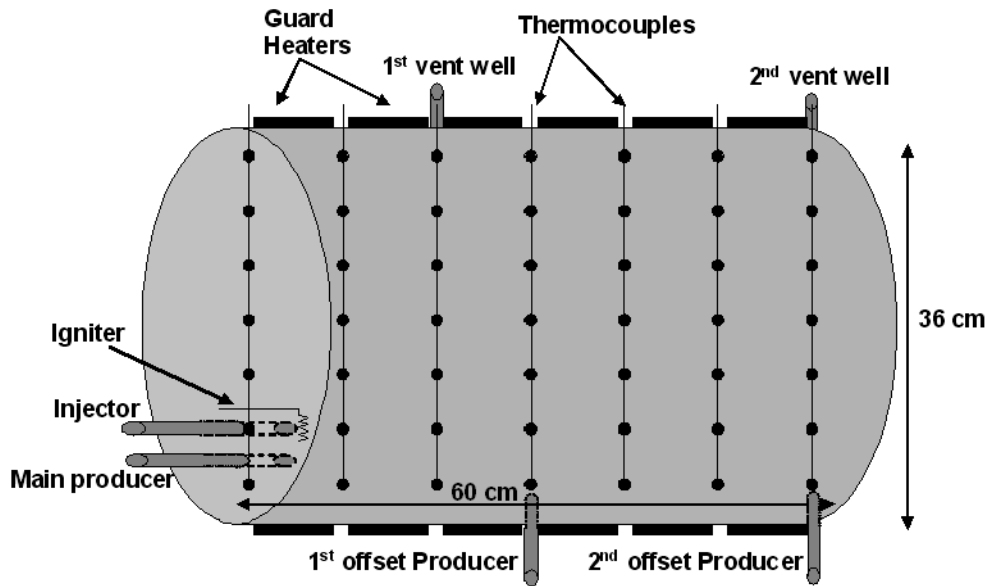


Figure 8-2. Schematic of 3D model for MS-CAGD from Lim and Chen ⁽⁸⁰⁾.

Alamatsaz and co-worker ⁽¹³⁷⁾ at the University of Calgary have designed and operated a new 1D conical combustion model that reportedly overcomes limitations of cylindrical combustion tubes for determining the minimum air flux to sustain propagation of the combustion zone. The model operated in a top-down mode, with the widest part of the cone at the bottom, to provide gravity stable operation. In this orientation, the air injection rate can remain fixed but the air flux decreases down towards the base of the cone as the combustion front advances.

The conical model was constructed from 3 mm thick Inconel 625 alloy, which possesses high strength, good corrosion resistance, and service temperatures up to 982°C. The model was composed of two pieces welded together. The topmost part was a short tube 7.8 cm in length and diameter of 5.7 cm. This tube was welded to a truncated cone with diameter of 5.7 cm at the truncated end and 31.1 cm at the base. The overall height of the model was 50.8 cm. The model was divided into 19 zones of 2.54 cm thickness and multipoint thermocouples were mounted in a spiral pattern to monitor each zone. Ten ARI metal clad heaters were wound around the model to control heat loss. Compared to other combustion tube models, these heaters were controlled by multiple thermocouples. An axial pressure profile was monitored by four pressure taps.

After packing the model with a mixture of sand, water, and bitumen (combined with a Hobart mixture to simulate a waterflooded state), thermocouples were inserted, and then the model was leak tested and insulated. The prepared model was placed inside a pressure containment vessel manufactured from 76 cm Schedule 80 steel pipe fitted with hemispherical end caps, one of which was welded while the other was flange-mounted. Operations up to 3,550 kPa were reported. Brief descriptions of the operating and control procedures were also provided by Alamatsaz *et al.*

8.6. ELECTRICAL HEATING

Yuan and coworkers ⁽¹³⁸⁾ ⁽¹³⁹⁾ at AITF devised a mechanistic 2D model for investigating ohmic electrical heating to establish inter-well communication for start-up of SAGD or VAPEX. The model represents a 2D vertical slice of the reservoir intersecting a pair of horizontal wells. The physical dimensions of the model were scaled except reservoir permeability was used.

The model was constructed from phenolic and acrylic polymer sheets, which have good thermal and electrical insulating properties (Figure 8-3). Where possible, nylon connector fittings were used and were placed along the edge of the model. Twenty-five ungrounded thermocouples, including one in each well, were used to monitor temperature. A single pressure gauge was used to monitor pressure in the model.

The external dimensions of the model were 58 cm x 43 cm x 10 cm (H x W x D). The actual dimensions of the sand pack were approximately 53 cm x 38 cm x 2.5 cm (H x W x D). Two 0.625 cm (O.D.) stainless steel tubes placed 36 cm apart were used to represent the horizontal wells. The equivalent field scale corresponding to this arrangement was a pair of 17.5 cm wells spaced 10 m apart (i.e., scaling factor of 28). The representative horizontal wells also functioned as electrodes, which were used to electrically heat the well by connection to a 300 V, 60 Hz AC power supply. For wet electrical heating, 25 wt.% NaCl solution was injected using the two wells and pressure in the model was relieved via two valves located on the vertical sides on the model. Overburden pressure was provided by an air gap between two of the polymer sheets on the face of the model opposite to that where the wells enter the model. Overburden pressure was 93 kPag. The low overburden pressure applied was probably imposed by the model construction. The model was filled with 4 Darcy sand with a porosity of 35 %, i.e., permeability was not scaled in this model. The model was saturated, using a fluid distributor built into the model, with 4 wt.% NaCl solution, which was then displaced by Hillmond heavy oil with a viscosity of 23,400 cP at 20.8 °C.

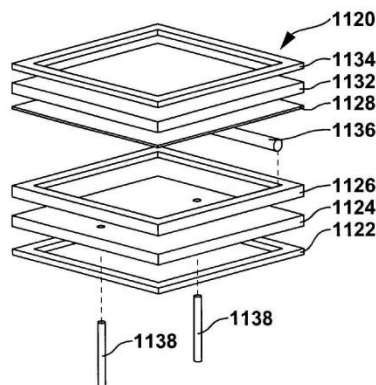


Figure 8-3. Exploded view of a 2D model used for wet electrical heating to investigate start-up of a SAGD or VAPEX well pair ⁽¹⁰⁸⁾

A physical model employing radio-frequency electromagnetic heating was developed by Kovaleva *et al.* ⁽⁵⁷⁾ at Bashkir State University. The model consisted of a sand pack prepared in a polyvinylchloride (PVC) pipe of dimensions 0.5 m in length and 2.25 cm internal diameter. The PVC pipe was packed vertically. The inner surface of the pipe was pre-treated to expose a layer of glue and dried sand, which prevented bypassing by the injected fluids. The production end of the tube was covered with a nylon micromesh, while a small diameter was used for fluid injection at the opposite end. This tubular sand pack was placed in the radio-frequency generator operating at 81.36 MHz with a maximum power output of 6 kW. The system appeared to be relatively simple and no additional information about the model was provided.

8.7. BIOLOGICAL PROCESSES

8.7.1. *Biological Aspects*

Bryant and Burchfield ⁽¹⁴⁰⁾ at NIPER (National Institute for Petroleum and Energy Research) discuss some aspects of MEOR that are important to consider when designing a physical model. Since it is crucial that the microbial formulations and reservoir fluids are compatible, it is important to use reservoir fluids at the same temperature and pressure as the field reservoir. They recommend testing the microbial formulation with the nutrient at several decreasing concentrations, since dilution will occur due to formation water and injection water. They also recommend using formation rock, preferably cores, in the models. Long-term stability testing of the microbial formulation with the reservoir fluids and rock, to ensure that the microbial formulation can survive under reservoir conditions, is also suggested. Since substances present in the reservoir fluids could be toxic or inhibitory to the microbial formulation, mixtures of microorganisms used must be cultured together in reservoir fluids at reservoir conditions.

Bryant and Burchfield ⁽¹⁴⁰⁾ recommend core flooding tests, micromodels, and other chemical tests such as phase behaviour and surface and interfacial tension measurements when microbial surfactant production is desired. They also recommend parallel or sandwiched cores be used to demonstrate fluid diversion between low-permeability and high-permeability rock.

Waterflood and polymer flood models are discussed below. These types of models are suitable proxies to investigating the fluid injection process, which is central for introducing microbes and enzymes to the reservoir.

8.7.2. *Water flood*

Todd ⁽¹⁴¹⁾ at Heriot-Watt University discusses best practices when using core flooding to investigate water injection processes. Core flooding is carried out either as a basis for formation damage modeling or for field-based injectivity predictions. As a best practice, water matching the field water should be used, as should cores from the field reservoir. If not available, cores with similar properties or synthetic cores are sometimes used. The most common core floods are linear core floods, followed by radial core floods, and finally simulated fracture core floods.

Linear core floods involve confining a cylindrical core in resin or a flexible sleeve, and either measuring the pressure drop over the core length for a fixed injection rate, or fixing the injection pressure and measuring the flow rate of the fluid exiting the core. Core diameter can vary, but is usually between 19 mm and 38 mm. Core length also varies, usually being between 2.5 cm to 10 cm. The lack of length standardization is a problem in the standard practice, especially when permeability is obtained by measuring exit flow rate at constant pressure, or measuring pressure drop at constant injection rate. Todd ⁽¹⁴¹⁾ suggests using either a standard length, or installing pressure taps at fixed intervals for longer cores. This would allow data to be compared from different experiments.

Core preparation can have a significant impact on core flood results. Some cores are cut with a core barrel and trimmed to length with a saw. Using this procedure, external material can build up on the cut face of the core, and the experiments can be impacted greatly by the characteristics of the machined face instead of the characteristics of the rock. Other cores are prepared using a broken face preparation procedure, where the core is trimmed by fracturing along a plane perpendicular to the longitudinal axis of the core. This procedure results in a relatively clean surface for the trimmed face, which has a significant impact on the depth of penetration of particles during experiments.

Core saturation is important to ensure that permeability measurements are not influenced by trapped gasses. The normal procedure is to apply a vacuum to the core and then allow water to penetrate the evacuated core. Todd ⁽¹⁴¹⁾ suggests evacuating the core and saturating it with carbon dioxide, then evacuating and saturating with deaerated water. This would allow any residual gas to dissolve in the water.

The injection fluid can be a complex issue when performing a core flood. If produced water injection is being performed, solids concentration and oil concentration are both important. In addition, many natural and added chemicals can be present. Maintaining a consistent emulsion in the lab can be difficult. In some cases, surfactants are used to help with a stable emulsion, but they can have an impact on the interaction between particles and rock pores.

Some core floods are performed in a radial configuration. Some experiments involve a central hole machined into the rock to simulate an injection well. In this case, the machined surface of the hole can have an impact on the radial flow in the experiment. Other experiments have used a geometry, which incorporates a segment of the full radius. This can make confining the segment difficult.

Crossflow configurations also exist, where the main fluid flow is parallel to the injection face of the core. This results in complex fluid dynamics and is difficult to model. Todd ⁽¹⁴¹⁾ suggests keeping the flow normal to the injection face until the simpler configuration is better understood.

Core floods can also be configured to model fractured systems. The core is cut along its length, and the fracture gap is maintained with spacers. The core is mounted in resin, and machined to create pathways normal to the fracture for fluid flow. One consideration in these types of models is the need to simulate stresses similar to reservoir conditions. Conventional biaxial loading of cylindrical cores necessitates that two out of three principal stresses are the same.

Therefore, if stress conditions are to be modeled, attempts should be made to apply stresses in ways that are more realistic.

Todd ⁽¹⁴¹⁾ suggests that using short-term core floods to provide a predictive basis for long-term injectivity predictions is somewhat unrealistic. The knowledge gap needs to be bridged from both sides by carrying out carefully controlled experiments and validatable numerical simulations for mechanistic understanding, and by collecting good field injection data from which injectivity models could be extrapolated.

8.7.3. Polymer Flood

Wassmuth *et al.* ⁽¹⁴²⁾ at AITF, details a set of polymer core flood experiments. The transport mechanisms in a polymer flood are convection, dispersion, adsorption, and capacitance. To determine the transport mechanisms, a double slug polymer injection method is used. First a polymer-in-brine slug is injected, then a pure brine slug, followed by a second polymer-in-brine slug. Injection of the two polymer slugs and the use of tracers allow the separation of the effects of inaccessible pore volume and the various retention mechanisms. The core flood effluents are analyzed for oil content, water cut, polymer, and tracer concentrations. The two distinct slugs of polymer separated by a slug of water should be observed in the effluent. The propagation of the first polymer slug is affected by adsorption and inaccessible pore volume. By the time the second polymer slug is injected, the polymer adsorption requirements of the rock have been satisfied.

Three experiments were run, with three oil viscosities and two well configurations. The first experiment used a loosely consolidated sandstone core, saturated with 280 cP oil. First, half a pore volume of water was injected into the core, followed by 6 pore volumes of polymer, chased by five pore volumes of water. A second polymer slug accounting for six pore volumes of polymer was then used. The second experiment involved higher viscosity oil, but the procedure was the same. For the third experiment, the oil viscosity was between that of experiments 1 and 2, and the well configuration was changed to a toe-to-heel flooding configuration, using two vertical injectors and one horizontal producer.

8.8. GENERAL APPLICATION MODEL

8.8.1. LARGE Model

Yale *et al.* ⁽¹⁴³⁾ at ExxonMobil, discuss a large-scale model developed for testing a range of recovery processes. The system was called "LARGE", which stands for Large-scale Apparatus for Reservoir and Geomechanical Experimentation. The goal of their system was to obtain near reservoir scale heterogeneity with more realistic fluid and rock properties. The system allowed for a physical model that was 2.1 m in diameter and 50 cm thick, and was housed in a 2,100 psi pressure vessel that was 4 m tall and 3.5 m in diameter. The footprint of the system is 10 m × 20 m, with a 15 m ceiling.

The model included an overburden spacer made of 7 cm thick polypropylene, which was used to mimic the deformation and stresses of the real overburden. The top section of the model was filled with hydraulic fluid and was pressure controlled to exert pressure on the overburden spacer and generate stress in the model reservoir. The interior of the model was lined with Hastelloy, which provided corrosion and erosion resistance.

There were a variety of sensors in the model, including pressure, stress, temperature, displacement of the overburden spacer, and flow rate. Acoustic sensors provided information about porosity, fluid saturation, elastic properties, and mechanical state. Resistivity sensors allowed the tracking of flood fronts in real time. In total, there were 150 sensors along the bottom face of the overburden spacer and 250 sensors in the bottom section of the model.

The model could be used with up to 2.5 tons of sand, and 1000L of pore fluid. The system was designed to operate at a range of -30 °C to 90 °C. Higher temperature fluids can be used as long as the reservoir temperature does not exceed 90 °C. It was deemed impractical to design the system to accept a larger temperature range.

The model was configured for a five-spot pattern of production and injection through vertical wells. It could be reconfigured for horizontal or slant wells, two-spot, quarter five-spot, or for studying radial flow into the central well. The model can support wellbore diameters up to 3 cm.

8.8.2. SRC Model

Knorr ^(144; 145) and Xu ⁽¹⁴⁶⁾ reference VAPEX and SVX experiments run at the Saskatchewan Research Council (SRC) using a large three-dimensional scaled, physical model. This model can reportedly be used as a multi-purpose model for investigating other processes. The largest models used were of dimensions 100 cm × 50 cm × 52 cm. The models used at SRC were packed with either Ottawa sand or glass beads of varying size. Permeability was determined from a modified Carman-Kozeny correlation.

The models used up to 90 uniformly spaced thermocouples in a grid formation. The injection and production wells were 100 cm long and separated laterally and vertically along the width and height of the model.

Oil was injected at temperatures between 45 °C and 55 °C. For the duration of the run, the temperature of the model was maintained at about 27 °C. After saturation, waterflooding was conducted to reduce the initial oil saturation to more field-like values.

The model was housed in an overburden pressure vessel, which was sealed and injected with warm water. The water maintained the model temperature and provided the model pressure of about 500 kPa.

8.8.3. Transparent Annular Sand Pack

AITF has developed a model, which they called a “transparent annular sand pack” (TASP), with the goal of bridging the gap between lab scale and field scale. The model is essentially a two-dimensional model that has been rolled up into a half-cylinder. It uses a transparent shell for visualization, and the sand pack fills the gap between the two half-cylinder walls. The TASP model was developed for VAPEX experiments, but can be used for other processes as well. Details of the TASP model have not been published.

8.9. MODELS USED AND DEVELOPED AT AITF

As mentioned earlier, most of the physical models used at AITF are of the high pressure variety. The use of actual oil, steam, solvents, and reservoir pressure and temperature ensures that the physics of the fluid/rock interactions is as close to that in the reservoir as possible. Because field pressures and temperatures are substantial, the models must be confined in a pressure vessel and a gas pressure applied to provide overburden pressure. The pressure vessel must be rated for the confining pressure and temperature, and must have sufficient access ports for the necessary injection, production, and saturation lines. Also needed are access ports for thermocouples and other sensor lines. The pressure vessel is, hence, an integral part of the model design. AITF has constructed several general-purpose pressure vessels suitable for partially-scaled physical model experiments. Some examples of models are given in references (147; 19; 20; 22; 112; 113; 114; 115; 35; 117) (148; 149; 150; 151; 152; 153; 154; 155; 156) (Figure 8-4). AITF has machine shop facilities capable of fabricating custom pressure vessels to suit specific experimental needs. Design, fabrication, and operation of physical models to examine thermal and non-thermal oil recovery processes are an ongoing endeavor at AITF.



Figure 8-4. Scaled physical model for thermal oil recovery process experiments.

Details on many models developed at AITF are available only in confidential reports. These include large unscaled field element models. Many proprietary techniques were developed for the design and operation of these models. Only published information on some AITF models is presented below.

8.9.1. Large Unscaled Physical Models

Early work at AITF by Redford *et al.* ⁽¹⁴⁸⁾ involved the construction of three unscaled models commonly known as the 45 cm cell ⁽¹⁴⁹⁾, the 60 cm cell and the 150 cm cell. The latter model used a pressure vessel 150 cm in diameter, packed with Athabasca oil sand, and provided with injection and production wells. High pressure steam was injected, and oil and water produced. Several experiments were run, using steam-only, and steam plus additives ⁽¹⁵⁰⁾. The results led to the later development of various steam-solvent processes, including ES-SAGD. The TASP model is another large field-scale model developed at AITF but no details have been published in the open literature.

8.9.2. Low Pressure Visual Models

Low pressure visual models at AITF have been employed to study various processes including bottom water VAPEX ⁽¹⁵¹⁾. Visual models have also been employed by Cuthiell to examine viscous fingering ⁽¹¹⁴⁾. Huang has used a large (1.4 m high) acrylic visual model (semi field-scale model) to investigate the performance of a VAPEX type process in Lloydminster heavy oil.

Nasr ⁽¹¹²⁾ used low pressure visual models to study the development of a SAGD vapour chamber from a horizontal well pair. The low pressure model used was a method of qualitative visualization of steam chamber growth parallel to and transverse to a horizontal well. Because the heat loss physics of the visual models are difficult to match to a field scenario, such models are of limited value for quantitative predictions.

8.9.3. High Pressure Visual Models

A high pressure visual model was employed by Huang at AITF to examine a high pressure VAPEX process in a heavy oil reservoir. The model had acrylic windows, and was housed in a pressure vessel along with a video camera. High pressure micro-models were developed by Fisher *et al.* ⁽¹⁵²⁾ to perform slim tube analysis of miscible and partially miscible displacement. Micromodels were also employed by Sawatzky *et al.* ⁽¹⁵³⁾ to examine the flow behaviour of foamy oil in porous media. Micromodels were also used by Bjordalen *et al.* ⁽¹⁵⁴⁾ to examine the use of microbubbles in drilling fluid.

8.9.4. CT Models

High pressure models in a CT scanner were employed by Yuan *et al.* ⁽¹¹⁵⁾ to examine growth of a steam chamber in SAGD and the SAGP process for heavy oil recovery. Low pressure CT models were also used by Cuthiell *et al.* ⁽¹¹³⁾ to study the effect of capillary pressure on gravity drainage in a VAPEX-type oil extraction process. CT models of sand production and wormhole development have been used by Tremblay *et al.* ⁽¹⁵⁵⁾ to visualize the development of wormholes

due to heavy oil production. CT models may also be used to visualize changes in oil and water saturation, and the distribution of those saturations during an oil production process.

8.9.5. Scaled Physical Models

Scaled physical model experiments have been employed by several researchers at AITF to examine different heavy oil recovery processes. Nasr ⁽¹¹²⁾ used scaled physical models to compare the effect of various additives to steam on the SAGD process. Frauenfeld *et al.* ⁽²⁰⁾ used scaled physical models to examine the effects of higher concentrations of volatile hydrocarbons with steam on the ES-SAGD process, defining a steam-butane hybrid (SBH) process as the result of high ratios of volatile solvent with steam in a SAGD-like configuration.

8.9.6. High Pressure Elemental Models

High pressure elemental models have had several applications at AITF. Nasr ⁽¹¹⁶⁾ used an elemental model to measure the rise of a steam chamber in an oil sand reservoir. Frauenfeld *et al.* ⁽²²⁾ measured the solvent front advance rate of a vapour chamber in a thermal solvent process using several isothermal experiments.

Micromodels are another category of elemental models. Javadpour and Fisher ⁽¹⁵²⁾ have developed a micromodel fabrication technique useful for creating slim tube test micromodels. Micromodels have proven to be very useful for studying a variety of oil recovery processes such as waterflooding, gels for conformance control, miscible and immiscible displacements, surfactant floods, foam injection, foamy oil flow, microbial EOR, and solution gas drive. Micromodels have also been used to study specific aspects relating to flow in porous media such as wettability, capillary pressure, interfacial tension, asphaltene deposition, heterogeneity, mass transfer, scaling, multiple contact miscibility, and gravity drainage ⁽¹⁵⁶⁾.

8.9.7. Adiabatic Experimental Models

Coates *et al.* ⁽¹¹⁷⁾ used an adiabatic model to examine the performance of *in situ* combustion in heavy oil using several adiabatic (active guard heater controlled experiments). Frauenfeld *et al.* used a very basic adiabatic model (Figure 8-5) to test the concept of a thermal solvent process using heaters in the injection and production wells to reflux volatile solvent as part of a heavy oil extraction process.

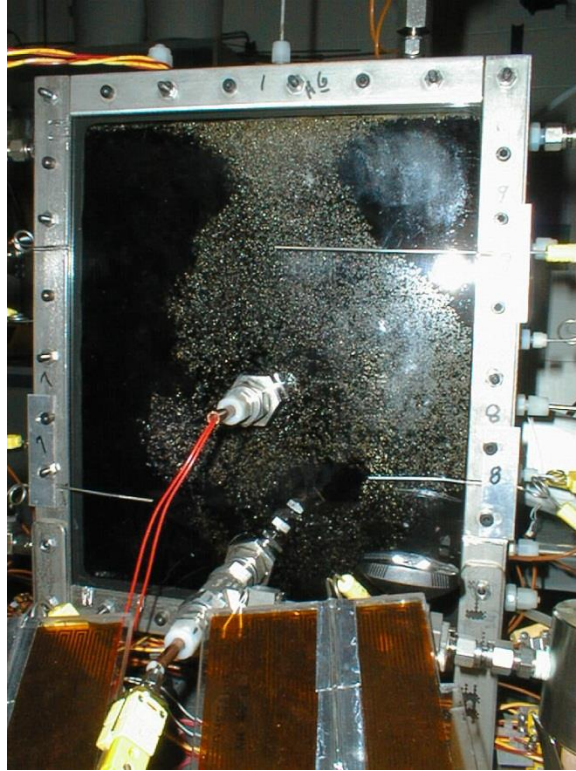


Figure 8-5. Visual model of thermal solvent process.

9.0 DESIGN/OPERATION CONSIDERATIONS & COSTS

9.1. DESIGN/OPERATION CONSIDERATIONS

There are many considerations that should be taken into account when building lab scale reservoir models and operating the associated experimental facilities. The extent to which these are considered will sometimes depend on cost and ease of operation. The models reviewed in the previous sections incorporate design features required to yield good experimental results (e.g., avoiding fluid bypass along internal walls), safety (e.g., high strength corrosion resistant alloys), and ease of operation (e.g., bolted model closure vs. welded closure). Models developed for different processes share many of the same design and operating considerations. Where these considerations differ, they are mainly due to specific conditions under which the model operates, e.g., pressure, temperature, corrosiveness, visual or opaque, etc.). Most of these process specific considerations were noted in the earlier sections dealing with these models. Here we confine the discussion to the more generic consideration necessary for most lab scale reservoir models. Some of these considerations match or map onto those used in the field.

9.2. SCALED MODEL DESIGN AND OPERATION

9.2.1. Design and Fabrication

Materials: Materials of construction are selected based on the service required. From a mechanical strength perspective, typical materials of construction include various grades of stainless steel, Inconel, and Hastelloy. Whether thick or thin metal sheets are used for the model walls will depend on the relative importance of: (a) mechanical strength of the model, (b) transferring overburden pressure to the sand pack with minimum deflection and pressure drop, and (c) reducing heat transfer along the walls. Reduced fluid bypass travel along the walls is a desirable consequence of transferring to the overburden sand pack through the thin walls of the model.

Where transparency to x-rays is necessary for visualization using a CT scanner but some mechanical strength is required, beryllium, aluminum, and titanium can be used. These choices do add significantly to material and machining/manufacturing costs.

Model size: Scaling usually determines the overall dimensions of the model and its mass. This usually dictates the location of the model, supporting structures, and possible reinforcements that may be required.

Well architecture: Size, shape, completion, and placement of the wells are typically dictated by the process being investigated and scaling. Multi-well models require that the well spacing adhere to the scaling criteria. For 2D scaled models, the model size could increase significantly as will the containment vessel required.

Saturation ports: If the model is to be saturated with water (or reservoir brine) and then oil, the number of saturation ports, their placement and saturation procedures need to be carefully

considered. The object is to achieve uniform saturation throughout the sand pack without any pockets or corners of uneven saturation. Uneven saturation can greatly influence fluid production rates and the interpretation of experimental results.

Welding procedures: This is of primary concern where model closure after packing is through welding it shut. The concern here is that the packing remains uniform during this procedure and that any special materials incorporated in the model are not damaged.

Model Integrity: By necessity, the model must be leak tight with fluids entering and exiting only through specified ports. The integrity of the model needs to be preserved so design and operations must consider the avoidance of over-pressuring the model either internally or externally. Either of these events would adversely affect the packing, permeability, and fluid saturation of the model.

A related issue is minimization of bypass fluid flow along the boundary. Various strategies can be used to minimize this unwanted type of flow. A common approach is to use a thin-walled model and apply an overburden pressure to squeeze the wall to achieve tight conformance with the sand pack. A similar result can be achieved by providing high loading, to ensure good contact between sand and walls, if using a model with a bolted closure. Caution is necessary to avoid overburden crush, which is a result of poor model design and poor packing, at corners and edges of the model. Other refinements and undisclosed strategies are employed by other research groups.

9.2.2. Packing

9.2.2.1. Uniform Packing

Models either are packed with sand from the reservoir sand or with sieved artificial sand. Generally, artificial or reservoir sands are used when permeability in the model is either scaled or unscaled, respectively. Reservoir sand is available from core material or as produced sand (e.g., Lloydminster heavy oil). Its availability could be limited or plentiful, and this may limit the size of the model. For large models, it is important to ensure availability of sufficient sand for many successful as well as failed model experiments, which may be required during the research program.

For artificial sands, cleaning and sieving of the sand is necessary to achieve the right sand size and permeability. Uniformity (angularity) of the sand grains is an important factor in achieving uniform packing and permeability. The sand also needs to be cleaned of fines that are not removed by sieving and that could accumulate and cause local restrictions and plugging during model experiments. Maintaining a desirable level of humidity reduces static charging of the sand, and ensures good grain separation during sieving, especially for the removal of fines.

Careful attention to the procedures used for packing the model with sand is required to achieve uniform permeability and avoid significant stratifications in the packing direction. Rate of sand addition to the model coupled with vibration type and frequency affect the packing. Since stratifications cannot be totally avoided, the final orientation of the model and the dominant

direction of fluid flow should be considered. If possible, the porosity of the packing and permeability should be confirmed. It is sometimes possible to examine the uniformity of packing using a CT scanner.

Some models are packed directly with oil and sand (or even oil/water/sand). In this case, achieving uniform packing and saturation could be challenging. With heavy oil and sand, the challenge in eliminating voids that could affect the path of fluid flow can be difficult to overcome completely.

9.2.2.2. Shale Barriers

Shale barriers and other low permeability barriers can also be created during packing of the model. Different permeability sands and other materials can be used. The challenge in such packing is to ensure that the zones of different permeability remain in place. For example, if low permeability sand is placed above higher permeability sand, then some means for retaining the segregation must be employed.

9.2.3. Insulation and Heat Tracing

Heating and heat losses are of particular importance for thermal processes. Heat transfer along the boundary walls of the model was discussed in term of the choice of thin versus thick metal shells. Insulation to reduce heat losses through the boundary is necessary to avoid creation of unintentional thermal gradients. Heaters may be required both for heat input as part of the process (e.g., preheat and ignition for *in situ* combustion) and for control of heat loss at the boundaries (e.g., steam and steam-solvent processes). The choice of heaters, distribution, and control of heat inputs can be important considerations. Where steam is a source of energy input, controlling the quality and quantity of steam is important. For example, for SAGD reservoir models, the aim is to ensure 100% quality steam entering into the model. Therefore, insulation, heat tracing, and temperature and pressure measurements are critical considerations.

9.2.4. Data Acquisition and Control

The number of temperature and pressure measurement points need to be considered in light of process control requirements and results interpretation (e.g., reservoir simulation history match and scale up). The control strategy for fluid production needs to be considered as in, for example, SAGD experiments where one desires to avoid production of live steam. The complexity of the injection and the production stations operating at specified temperatures and pressures require attention and are somewhat process specific.

9.2.5. Overburden Vessel

For models, where the walls of the model do not have sufficient strength to maintain model integrity, it is necessary that they be enclosed in an overburden or pressure containment vessel. The size and pressure rating of these containment vessels are amongst the main factor influencing the size and cost of the engineered facility housing these types of models.

The types of closures and model ingress/egress systems are fundamental considerations. Development of good procedures for hydraulic torquing/tensioning of the closures are seemingly trivial but necessary for successful operations. Robust instrumentation feedthroughs are essential and need to withstand many cycles of pressurization and depressurization. Sufficient supplies of compressed nitrogen to provide overburden pressure are required and need facilities for storage and handling. Finally, safety controls for catastrophic events need to be in place. This could include adequate ventilation and ambient air monitoring.

9.2.6. Saturation

Typically, after packing lab scale reservoir models with sand, they are saturated with water (or brine) followed by live or dead oil. As noted above, some models are packed directly with oil and sand and, therefore, other issues may arise. A major challenge in using models that require saturation with water and oil is the preparation of the oil itself. Importantly, oil used for lab scale reservoir model work must be free of production and treatment chemical that could alter its transport and interfacial properties.

Before the heavy oil obtained from the field (typically wellhead) is used, it generally must be cleaned to remove all solids and water. Filtration, centrifugation, and distillation (for water removal) are generally employed. These processes are typically slow and time consuming, so producing large quantities of cleaned oil can be quite costly.

Some of the best lab scale physical models will use live heavy oil for saturation of the model. Since oil from the field is usually partially or completely desaturated, it is necessary to resaturate the heavy oil with a specified gas composition (typically methane but possibly C₂ - C₄ as well) to achieve the GOR of the original reservoir fluid. Due to slow mass transfer, the preparation of the live oil is a slow and tedious process that requires a vented, temperature-controlled room.

During saturation of the model, temperature and pressure of the model and injected fluids need to be controlled. Ensuring even saturation of water and oil with no trapped gases is necessary for good model experiments.

9.2.6.1. Bottom Water

If a bottom water zone is required in a model, this can be easily achieved by judicious placement of saturation ports for water and oil. Provided the oil is of lower density than the water (typical), oil can be added through saturation ports that allow the displacement of saturation water above a specified level in the model.

9.2.6.2. Gas Zone

Creation of a top gas zone can be achieved in a similar way to that for a bottom water zone. In this case, gas can be injected into the model through suitably based gas saturation ports to displace oil at the top of the model. This creates a zone with predominantly gas saturation but

with some residual oil and water. Depending on the experiment being conducted, this residual oil and water should have little to no effect.

9.2.7. Production Systems

Monitoring of fluid production rates, sampling, and online analysis are major design and operational considerations. Smoothly operating backpressure controllers are necessary for good reservoir model performance. Production lines may need to be insulated and heat traced to maintain good flow into collection vessels. Preserving the integrity of the produced samples should be a strong consideration in the design of the production vessels. This may require adequate heat exchanger cooling of the sample to avoid losses during transfer operations. Monitoring, venting, and capture of hazardous gases are important safety controls.

9.2.8. Post Run

A well designed model will facilitate post run handling and cleanup. Ease of removal of the model from the pressure containment vessel without damage and, to excavate the sand pack for analysis of residual oil saturation, is desirable. Ease of cleaning the model, transfer lines and injection and production stations reduce turnaround time and operating cost. Solids and fluid handling and disposal must also be considered. Protection of sealing surfaces, delicate feedthroughs connections, etc. cannot be neglected.

9.3. FACILITIES CONSIDERATIONS

Engineered space is generally required for operating scaled reservoir models. Knorr and co-workers⁽¹⁵⁷⁾ at Saskatchewan Research Council provide an overview of the considerations that must be made for these types of facilities. Amongst the areas discussed in some detail were: (a) hazardous area classification, (b) control and mitigation of flammable gas releases, (c) control of ignition sources and, (d) laboratory facilities and utility services.

Hazardous area classification ultimately determines the scope of engineering controls that are required for the operation. These directly relate to the control and mitigation of flammable gases and ignition sources. Some of these issues were already discussed above in the context of model design and operations. Some additional considerations are discussed here.

Models and containment vessels will require stable support on flooring engineered to support their load. The size of the model and requirements to lift and move them necessitate high head space ideally equipped with an overhead crane with sufficient lift capacity. Forklifts may also be required for other lifts and moves not suitable for the crane.

The space requires an adequate HVAC system to maintain constant temperature during all seasons and with electronic equipment, electrical heaters, and steam generator in full operation. Additional, ventilation and make-up air for exhausting hazardous gases must be incorporated into the HVAC design. Utilities with sufficient capacity such as electrical power, steam, water, and compressed nitrogen should be widely dispersed to allow flexible access.

9.4. CAPITAL AND OPERATING COSTS

Capital and operating costs of facilities and lab scale reservoir models are generally not available from the literature. We have, therefore, accessed historical data from two research groups and normalized the costs to a typical coreflood system with a volume of 2 L and an operating pressure of 7 MPa.

9.4.1. *Capital and Operating Costs of Models*

Figure 9-1 shows the capital costs for four types of models: (a) combustion, (b) non-thermal, (c) visual, and (d) thermal. The combustion models range from 1D combustion tubes to larger 3D models. Non-thermal models included coreflood and cold heavy oil production with sand (CHOPS) models. Visual models comprised waterflood, steam-solvent, and foamy oil production models. The thermal models were essentially SAGD scaled models.

The scaled costs of the various models were plotted against $\log_{10}(V \cdot P)$, which is defined by the volume (V in litres) of the model and its operating pressure (P in kPa). The costs for all models, except the visual ones, show similar exponential behavior. The visual models show a steeper exponential increase in cost at lower values of $\log_{10}(V \cdot P)$. The cost of the visual model is mostly defined by size and the complexity of the housing and supporting structures required. The operating costs (Figure 9-2) follow a similar trend.

9.4.2. *Capital Cost of Facilities*

The facilities cost for scaled models are typically related to their overall footprint in an engineered high head facility with standard utilities as discussed above. These facility costs have also been scaled to that required for the above coreflood system with a volume of 2 L and an operating pressure of 7 MPa. The costs are plotted against $\log_{10}(V \cdot P)$ for the capital and operating costs of the scaled models (Figure 9-3). The costs show a rapid rise as the product of volume and pressure exceed about one million.

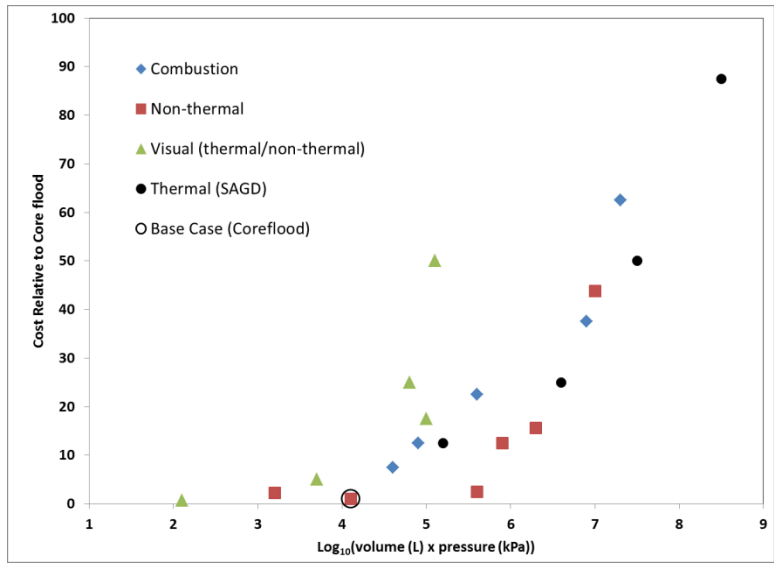


Figure 9-1. Comparison of the capital costs of scaled reservoir models vs. $\log_{10}(\text{volume} \times \text{pressure})$.

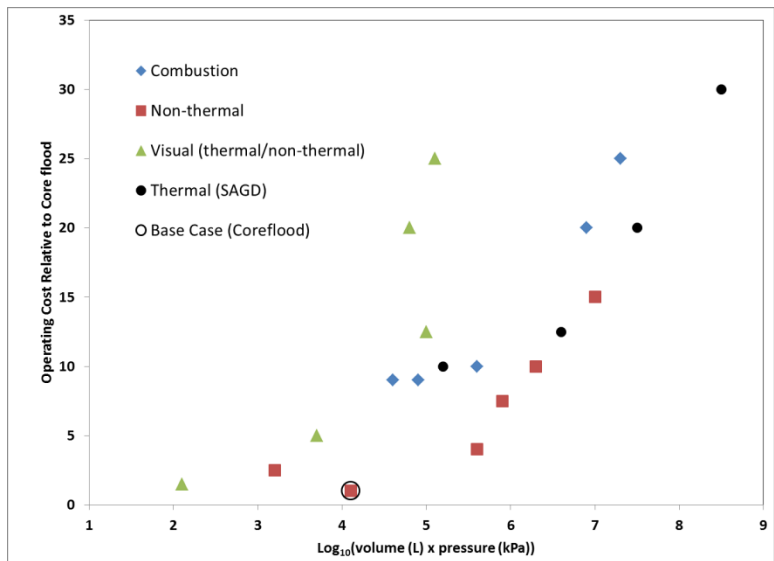


Figure 9-2. Comparison of the operating costs of scaled reservoir models vs. $\log_{10}(\text{volume} \times \text{pressure})$.

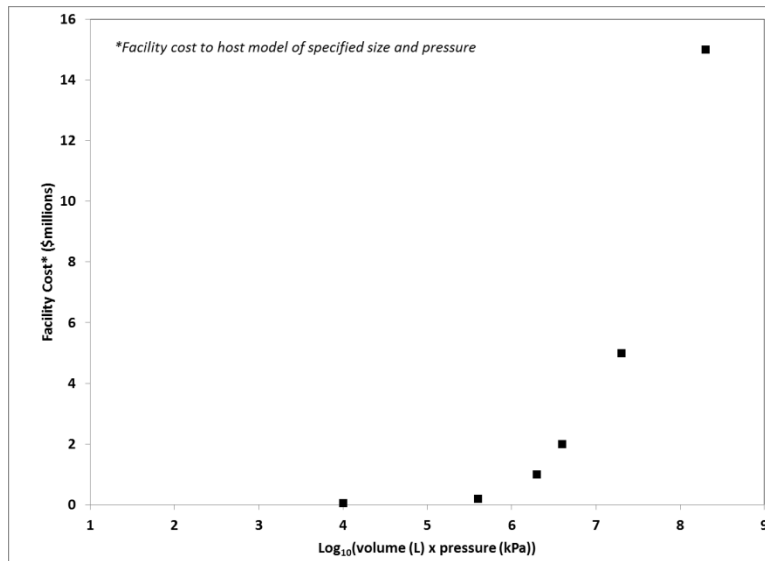


Figure 9-3. Capital cost of facility to house scaled reservoir models vs. $\log_{10}(\text{volume} \times \text{pressure})$

9.4.3. Implications of Cost Data

All of the capital and operating cost data show that the largest models currently in use are on the steep part of the cost curve. Building significantly larger models will come at substantially higher incremental costs. In order to build field scale models, new approaches to design and operation may be required.

10.0 SUMMARY AND RECOMMENDATIONS

10.1. OVERVIEW

Lab scale physical reservoir models have been used for initial validation of new *in situ* recovery processes, to understand recovery mechanisms, and to provide comparative information about process performance. Depending on the specific investigative purpose, reservoir models may be scaled or unscaled. The various models used have ranged from bench top micromodels to field-element and field-scale models. Data obtained from physical models have been used to tune and validate predictions from numerical simulations of reservoir processes.

This report provides a review of various *in situ* recovery processes, their mechanisms, scaling of these mechanisms, and design and use of physical models. The scope of this review was restricted to bitumen and heavy oil deposits in sandstone reservoirs that may contain shale barriers, water and gas zones, and thief zones. The recovery processes examined were limited to SAGD, solvent-steam, *in situ* combustion, electrical heating, and biological processes. The state of the art for reservoir physical models employed in investigation of these processes was assessed through a literature review. Not surprisingly, many of the physical models reported (e.g., SAGD, steam-solvent, and combustion) show remarkable similarities in dimensions and operation. Only examples of the main types of physical models and a few unusual ones are highlighted. Surprisingly, AITF has published reports on the widest range of model types and sizes even allowing for exclusion of new models that have not been disclosed in open literature. It is clear that physical models are still in a state of evolution as new knowledge of the existing processes increase and there is a need to investigate new processes and mechanisms.

10.2. MODEL SCALING

The ability to predict field performance by upscaling results from scaled models can be of great value. However, this ability is significantly compromised when some process mechanisms are not accounted for or cannot be properly scaled. In such cases, field-scale or field-element models may be possible; however, some mechanisms are extremely challenging to represent even in an unscaled model.

10.2.1. Challenges

Geomechanics is one reservoir behavior where physical models have not been very successful. The challenge in adequately modeling geomechanical behavior is to re-create all of the physical properties of a block of reservoir sand, including cohesive strength and initial stresses. Interbedded shale in reservoirs is another feature that is difficult to emulate in physical models. Permeability heterogeneities may be modeled to some extent by packing alternating layers of high permeability and low permeability sands. Significant time and effort is required to create a pack with realistic detail based on an actual reservoir characterization. The behavior of shale layers in the reservoir (i.e., weakening, fracturing, and reactivity) is more difficult to model. This requires that the model matches the shale specimen, stress environment, and time at temperature under the changing stress regime.

Mixing/dispersion is another mechanism that is typically not scaled by physical models. This is not a problem for SAGD, but processes where oil and solvent mixing is critical in the reservoir will be a challenge to scale properly. This is a significant problem when attempting to create scaled models of solvent-steam processes. AITF has been working on the development of, and has, demonstrated models that will enable accurate representation of reservoir processes. All of this information remains unpublished in the open literature at this time.

10.2.2. SAGD

SAGD is amongst the most widely studied *in situ* recovery processes currently employed in Alberta. Scaled physical models, field pilots, and commercial operations supported by numerical simulations, have added considerably to the body of knowledge for this process. Even though there are existing commercial SAGD operations, mechanistic and scaled experiments are still necessary to provide new insights for continuous improvement of SAGD operations in the face of many challenging reservoir conditions. Providing new insights into SAGD using physical models is challenging due to inadequate scaling of some process mechanisms.

Typical SAGD models are usually based on a thin rectangular slice of the reservoir perpendicular to the horizontal well pair according to Pujol-Boberg or Kimber scaling methods. The well pair is usually close to the bottom of the model with the top of the pay zone being the very top of the model. There is typically no overburden, underburden, or variation in permeability or saturation. Multi-well models are seldom used. When additional well pairs are incorporated, the inter-well pair separations follow the geometric scaling of the model as a whole. Models may be annular, rectangular, or vertical cylinders depending on the mechanisms being investigated.

Larger physical models can play a role in further development of SAGD and reservoir specific applications. Scaling complex reservoir conditions such as shale barriers, lean zones, bottom water, top gas, interbedded shales, inclined heterolithic stratification, cap rock conditions, and geomechanical effects are extremely challenging in scaled physical models. Unscaled field-element models focus on a critical juncture of the process (e.g., steam-oil interface in SAGD), and operate on field-scale time providing valuable insights. However, the focus on specific mechanism(s) may mean that other aspects of the process are not simultaneously modeled in these studies. Unusual well configurations, such as X-SAGD, or operating strategies for complex reservoirs, such as reservoirs with thief zones, may require larger three-dimensional models than existing models in order to incorporate adequately such features.

10.2.3. Solvent-Steam

Compared to SAGD, solvent-steam processes are more complex primarily because diffusion and mixing/dispersion are essential additional mechanisms that need to be considered. In particular, mixing processes between bitumen and solvent in porous media does not scale. Creating a useful and reliable physical model depends on whether diffusion or mixing/dispersion dominate solvent-oil mixing. Most physical models used for investigating solvent-steam processes are generally the same as those used for SAGD. These models will have

the same limitations as those listed for SAGD but also may not account for mixing effects in the porous media.

Large-scale physical models are essential to accelerating the further development of steam-solvent processes such as ES-SAGD. The main driver for larger models is the ability to incorporate mixing effects, which are fundamental to these processes. Clever designs of visual and high pressure models are required to build and operate these models at reasonable costs. Work in this direction is already underway to explore mixing effects in field-scale 2D models at AITF

10.2.4. Combustion

In situ combustion (ISC) depends on the occurrence of multiple chemical reactions between crude oil and the injected oxygen within the reservoir porous media. Generally, in physical modeling of recovery processes, the scaling rules involve the alteration of the model oil-matrix system to achieve similitude with transport phenomena and other mechanisms in the field. In addition, the time is also scaled. It is very difficult, if not impossible, to effectively change the kinetics of the multiple chemical reactions to account for these variations. Due to the complex mechanisms of *in situ* combustion and the difficulty in properly scaling the necessary parameters, the use of scaled physical models to provide field fluid rate and process predictions is extremely challenging.

Three-dimensional physical models of ISC, however, can be used to provide information on the behavior of the *in situ* combustion process under specific reservoir conditions, e.g., shale barriers, and can provide sweep efficiency estimates for different displacement concepts, e.g., well configurations or operating strategies. In these types of physical models, the field oil-matrix system is duplicated in the laboratory and the model can be viewed as a distinct element of the reservoir. In many ISC physical models, a major concern is the heat loss at the boundaries. The degree and character of the chemical reactions involved in ISC are much more affected by heat losses than the mechanisms entailed in other recovery processes. Various approaches are used to try to match the heat loss to the surroundings between a laboratory model and the field. If the model is sufficiently large, information on the *in situ* combustion process can be gained before heat losses from the boundary become influential. Larger models are also useful for incorporating complex well patterns, high permeability channels (e.g., wormholes created by cold production), shale barriers, etc.

The two main drivers for larger models for *in situ* combustion are heat loss and complexity in process configuration. Larger models minimize or eliminate the effects of heat loss during the course of the test. Larger models also allow the ability to model features that enhance and control the combustion process. These features include high permeability channels such as wormholes (following CHOPS), multiple wells, and shale barriers.

10.2.5. Electrical heating

Compared to SAGD, steam-solvent, and *in situ* combustion, few physical models for electrical heating processes are reported in the literature. This is due, in part, to electrical heating being more complex as well as the view that steam has won the war of ideas regarding the most

efficient means of providing thermal energy to the reservoir. The simplest case to model is a localized hot electrode where no current or electromagnetic energy flows through the reservoir. This is also the least interesting case. Typical electrical heating processes will involve simultaneous heating of a large portion of the reservoir by passing an electric current (ohmic heating) or by exposure to electromagnetic (EM) fields (e.g., inductive and dielectric heating). Electrical heating by passing a current can be considered a special case of electromagnetic heating. The scaling approaches employed for SAGD and solvent-steam processes are not amenable to scaling of EM heating processes in a reservoir. Physical scaling of electrical and electromagnetic processes requires that electrical (conductivity, dielectric constant, and magnetic permeability) and thermal similitudes are consistent and simultaneously incorporated in the model. Fluid transport, geomechanical, gravitational, and capillary effects provide additional complexity.

Electrical heating inherently appears to favour the use of larger unscaled models. The requirement for electrical similitude may require that a scaled model employ very different media (oil, water, and sand) than that in the field. If reservoir media from the field is used in the model then the degree of scale reduction that can be realized will depend on how the electrical properties change with EM frequency. In some cases, significant scaling may not be possible. Since these EM heating processes are not necessarily high pressure processes, the equipment required for field-scale models, except for electrical isolation, may be far simpler than that required for steam-based processes.

10.2.6. Biological Processes

Although numerous laboratory tests have demonstrated that microorganisms can indeed enhance oil recovery by virtue of the products they can produce or by their activities, there is a gap in translating this to the field in an economical and practical manner. Skepticism by the industry on the merits of biological processes for *in situ* recovery has been influenced by poor understanding of the mechanisms and a lack of post-treatment analysis to validate the claims of successful field tests. Not enough importance has been placed on reservoir physical model experiments as opposed to “beaker tests” of microbial cultures and their activity.

Reservoir physical models for microbial processes can be either cores or saturated sand packs. Microbes are grown and utilized in aqueous media so a waterflood would be a typical means for delivering microbes for biological or microbial enhanced oil recovery (MEOR). Standard protocols have been developed for lab scale corefloods and these can be adapted for lab scale MEOR waterfloods. Corefloods are not scaled experiments but rather injectivity and oil sweep tests. Similarly, MEOR waterfloods can be conducted as unscaled experiments. The timescale of the MEOR physical model experiments will be dependent on the rate of the microbial reactions (e.g., surfactant generation, gas generation, etc.) so time will also not be scaled.

The size of the model will depend on the need to assess factor such as nutrient limitations at some distance from the injection point, microbial mortality, and filtration effects due to microbial growth and distance from the injection point. Small cores used for waterflooding are not generally applicable to these situations.

10.3. COST OF SCALED MODELS

There are no published data on capital or operating costs for various physical models. Internal data, supplied by AITF, were collected and analyzed to provide cost comparisons for capital and operating costs of the models as well as capital costs for a fully equipped facility housing these models. The data were scaled relative to the cost of a coreflood facility. These data show that for all models except for low pressure visual models, the capital and operating costs increased very non-linearly with size and pressure. The capital cost of the facility for accommodating the model also increased non-linearly with size and pressure.

The cost data indicates that models, significantly larger than those currently in use, may be prohibitively expensive, as their size and pressure would place them in the steepest part of the cost curve. Therefore, cost effective larger models will require new approaches to design and operation. Knowledge gained through the construction and operation of intermediate 2D field-scale models and field-element models at AITF can provide a useful bridge to the new generation field-scale models.

10.4. NEXT STEPS

10.4.1. Context of Next Steps

Operating scenarios for *in situ* recovery can be explored cost effectively using scaled models, which incorporate, at least for the model, well-defined reservoir properties and initial reservoir conditions. Such models can provide essential knowledge, which would normally take many years at much greater cost to obtain from field pilots and commercial operations. In some instances, it may be very difficult or impossible to obtain such information from the field. However, scaling of *in situ* processes results in compromises, whereby some mechanisms are not incorporated because either they cannot be scaled (e.g., mixing effects) or they are not easily incorporated (e.g., geomechanical effects). Eliminating these compromises comes with penalties of increased model size, complexity, long operating time, and high capital and operating costs. A cost-benefit analysis is required to determine whether larger and more complex models should be pursued. It should also be considered whether these improved models will provide to the industry results with a level of subjective confidence comparable to that provided by field pilots.

10.4.1.1. Define Value & Benefits

The value and benefits being sought need to be well understood. Depending on what is sought, a combination of scaled and unscaled models may be suitable or a single unscaled model may be sufficient. These two options present different challenges and their costs will be likely quite different. As discussed in this report, field element models and unscaled 2D models have been employed for examination of specific mechanisms that do not scale well. It must be re-emphasized that processes in unscaled models and field element models occur over unscaled time, i.e., processes take just as long as in the field. Fundamental questions that must be answered include: Are unscaled reservoir models sought as a substitute for

field pilots or will they be used in combination with field pilot to, for example, reduce process uncertainty?

10.4.1.2. *Confidence*

Three obvious factors could limit the correspondence between data obtained from reservoir models and the field. First, while the constructed model may have well defined properties (e.g., permeabilities, porosity, saturations, etc.) the reservoir properties may not be as well defined. Unknown or unexpected field heterogeneities and fluid communication pathways may significantly affect field performance. Second, fluid properties in the lab may not match exactly those in the field, e.g., gradients in fluid viscosity are known to exist in some reservoirs. Third, in the absence of perfect correspondence between the model and the field, numerical field-scale simulations, based on history-matching results from the model, will be required to predict field performance. In this situation, limitations of reservoir simulations then become important in comparing results from a physical reservoir model with field observations. Given all of the above, will data from larger, more complex and costly models be accepted with a greater degree of confidence compared to that from the current scaled models? Will they reduce the necessity and/or number of field pilots and speed the application of new processes in the field?

10.4.2. *Path Forward – Outline*

The following high-level outline lists the activities leading towards the construction and operation of the next-gen reservoir models. It is expected that these activities would unfold over a period of about five years.

Step 1: Value, benefits, and confidence

The values and benefits that are expected by industry to accrue from the next-gen models need to be identified and clearly articulated. This is essential to achieve clarity on the scope of the problems to be solved. This could be done through workshops with a focus on industry experience, challenges, and limitations with field pilots. In addition to the workshops, one-on-one meetings with industry representatives will be essential to incorporate the unique perspectives needed to justify the development of new reservoir models.

Step 2: Challenges of larger-scale models

Some of the challenges associated with current and larger scale models were identified in this report. It would be useful to critically assess these challenges and potential approaches to their solution through broad consultations with experts through a workshop. Participants would include industry experts and R&D providers with expertise in building and operating physical models. R&D providers who have worked with some of the models discussed in this report are potential invitees. Industry experts involved in Step 1 (above) would be key participants. One deliverable from such a workshop would be to identify key research topics that must be addressed for larger models to be practical. Although workshops in Steps 1 and 2 could be combined into a single two-day workshop, it may be difficult to obtain a full two-day commitment for industry participation. Without the full participation of industry, the outcomes from the workshop and follow-on activities will be

sub-optimal. Follow-up one-on-one meetings with industry will again be required in conjunction with these workshops.

Step 3: Preliminary design and costing

Based on the input expectations from Step 1 and potential solutions to challenges from Step 2, a preliminary design and estimation of capital and operating cost can be completed. These data will provide a foundation for a re-assessment of the value and benefits of next-gen reservoir models.

Step 4: Program to address challenges

The critical challenges, identified in Step 2, will be used to develop and conduct a coordinated R&D program to evaluate potential solutions. Some of these solutions could be evaluated using the field-scale and field-element models currently employed at AITF.

Step 5: Detailed design and costing

Detailed design and capital and operating costs will be developed. These will consider the various solutions developed in Step 4 for comparison of costs versus benchmarks established for performance of the models. This should allow the sponsors to re-assess the value of the proposed reservoir physical model and agree on a final design.

Step 6: Development of consortium

A consortium of industry and government would need to be created to fund the initial capital investment and the ongoing costs for the facility. Ongoing costs would be separated from test costs to ensure that the facility, including trained operators, is maintained. Following creation of the consortium, requests-for-proposal can then be issued to construct, commission, and operate the model(s) and supporting facilities. A location could be specified or made contingent on the selection of an operator.

Step 7: Construction and commissioning

The successful bidder constructs and commissions the facility and the model(s). Commissioning tests could be based on either previously completed field pilots, upcoming field pilots, or a combination of these. The results would be critically evaluated to ensure that the expected value of the facility has been realized.

Step 8: Operate and innovate

The fully commissioned facility is made available for model field pilot tests. The facility becomes a centre not only for industry-led field pilots in a model reservoir but also the centre of innovation for *in situ* recovery. Consortia of companies, e.g., AACI consortium operated by AITF, could utilize the facility to carry out early field-scale evaluations of new recovery processes.

11.0 REFERENCES

1. *Effectiveness of carbon dioxide and naphtha in steam recovery processes as applied to oil sands.* **Ivory, J., Ridley, R., Nyugen, D.M., and Prowse, D.R.** Calgary, Alberta, : s.n., October 6 - 9, 1985. Proceedings of the 35th Canadian Chemical Engineering Conference.
2. *An examination of steam-CO2 processes.* **Stone, T. and Ivory, J.** May - June 1987, Journal of Canadian Petroleum Technology, pp. 54-61.
3. **Nasr, T.N.** *Hydrocarbon production process with decreasing steam and/or water/solvent ratio.* US Patent 6,591,908
4. **Lim, G., Ivory, J. and Coates, R.** *System and method for recovery of hydrocarbons by in-situ combustion.* US Patent 7,740,062
5. *Modelling of wormhole growth in cold production.* **Tremblay, B. and Oldakowski, K.** 2003, Transport in Porous Media, Vol. 53, pp. 197 - 214.
6. AACI Research Program. Confidential Report. Alberta Innovates - Technology Futures.
7. *Theoretical studies on the gravity drainage of heavy oil during steam heating.* **Butler, R.M., McNam, G.S., and Lo, H.Y.** s.l. : Canadian Journal of Chemical Engineering, 1981, Vol. 59, pp. 455-460.
8. *Review of phase A steam-assisted gravity-drainage test.* **Edmunds, N.R., Kovalsky, J.A., Gittins, S.D., and Pennacchioli, E.D.** s.l. : SPE Reservoir Engineering, May 1994, pp. 119-124.
9. *Impact of Steam Trap Control on Performance of Steam-Assisted Gravity Drainage.* **Gates, I.D. and Leskiw, C.** Calgary : Canadian International Petroleum Conference / SPE Gas Technology Symposium 2008 Joint Conference, June 17-19, 2008.
10. *The Steam and Gas Push (SAGP) - 2: Mechanism Analysis and Physical Model Testing.* **Jiang, Q., Butler, R., and Yee, C.T.** Calgary : Proceedings of the Petroleum Society 49th Annual Technical Meeting, June 8-10, 1998. Paper 98-43.
11. *Fluid Movement in the SAGD Process - A Review of the Dover Project.* **Aherne, A.L. and Maini, B.** Calgary : Petroleum Society's 7th Canadian International Petroleum Conference (57th Annual Technical Meeting), June 13-15, 2006.
12. **Butler, R.M.** *Horizontal wells for the recovery of oil, gas and bitumen.* s.l. : Petroleum Society, 1994. Monogram Number 2.
13. *SAGD and Geomechanics.* **Carlson, M.** 6, 2003 : s.n., Journal of Canadian Petroleum Technology, Vol. 42.
14. *Mapping of the McMurray Formation for SAGD.* **McCormack, M.** 8, August 2001, Journal of Canadian Petroleum Technology, Vol. 40.
15. *Scaling Accuracy of Laboratory Steam Flooding Models.* **Pujol, L., and Boberg, T.C.** Bakersfield, California : California Regional Meeting of SPE, Nov. 8-10, 1972. SPE Paper 4191.
16. *Reservoir Simulation of Cyclic Steam Stimulation in the Cold Lake Oil Sands.* **Beattie, C.I., Boberg, T.C., and McNab, G.S.** s.l. : SPE Reservoir Engineering, May 1991, pp. 200-206.
17. *Subsurface Issues Related to Resource Evaluation and Recovery.* s.l. : 2010 Primrose, Wolf Lake, and Burnt Lake Annual Presentation to the ERCB, Jan 26, 2011.
18. *Christina Lake Solvent Aided Process Pilot.* **Gupta, S.C., and Gittins, S.D.** Calgary : 56th Annual Technical Meeting, 6th Canadian International Petroleum Conference, June 7-9, 2005. Paper 2005-190.

19. *Steam Alternating Solvent Process*. **Zhao, L.** 2, s.l. : SPE Reservoir Evaluation & Engineering, 2007, Vol. 10, pp. 185-190.
20. *Experimental and Economic Analysis of the Thermal Solvent and Hybrid Solvent Processes*. **Frauenfeld, T.W., Jossy, C., Bleile, J., Krispin, D., and Ivory, J.** Calgary : CIPC / SPE GTS 2008 Joint Conference (the Petroleum Society's 59th Annual Technical Meeting, June 17-19, 2008).
21. *Review of Relation Between Diffusivity and Solvent Viscosity in Dilute Liquid Solutions*. **Hayduk, W., and Cheng, S.C.** 5, s.l. : Chemical Engineering Science, 1971, Vol. 26, pp. 635-646.
22. *Experimental Evaluation of Dispersion and Diffusion in UTF Bitumen / n-Butane System*. **Frauenfeld, T., Jossy, C., Wasylyk, B., Meza Diaz, B.** Calgary : SPE Heavy Oil Conference, June 2012. Paper 157904.
23. *Numerical Simulation and Economic Evaluation of Hybrid Solvent Processes*. **Frauenfeld, T., Jossy, C., and Ivory, J.** Calgary : Canadian International Petroleum Conference, June 16-18, 2009. Paper 2009-108.
24. *How Fast is Solvent-Based Gravity Drainage?* **Nenniger, J., and Dunn, S.** Calgary : Canadian International Petroleum Conference / SPE Gas Technology Symposium, April 17-19, 2008. Paper 2008-139.
25. *A new process (Vapex) for recovery heavy oils using hot water and hydrocarbon vapour*. **Butler, R.M., and Mokrys, I.J.** 1, s.l. : Journal of Canadian Petroleum Technology, 1991, Vol. 30.
26. *Cyclic Steam Solvent Stimulation Using Horizontal Wells*. **Chang, J., Ivory, J., Rajan, R.S.V.** Calgary : Canadian International Petroleum Conference, June 16-18, 2009. Paper 2009-175.
27. *In-situ combustion in Canadian heavy-oil reservoirs*. **Moore, R.G., Laureshen, C.J., Belgrave, J.D.M., Ursenbach, M.G., and Mehta, S.A.** 1995, Fuel, Vol. 74, pp. 1169-1175.
28. *In-situ combustion in heavy-oil reservoirs: Problems and perspectives*. **Moore, R.G., Laureshen, C.J., Belgrave, J.D.M., Ursenbach, M.G., and Mehta, S.A.** 1997, In Situ, Vol. 21, pp. 1-26.
29. *Application of Cyclic In Situ Combustion in Romania*. **Turta, T.A., et al.** July 1985, Romanian Magazine Mine Petrol si Gaze.
30. *Current Status of the Commercial In Situ Combustion (ISC) Projects and New Approaches to Apply ISC*. **Turta, T.A., Chattopadhyay, S.K., Bhattacharya, R.N., Condrachi, A., and Hanson, W.** Calgary : s.n., June 7-9, 2005, Canadian International Petroleum Conference.
31. *In-Situ Combustion Technique to Enhance Heavy-Oil Recovery at Mehsana, ONGC - A Success Story*. **Doraiah, A., Ray, S., and Gupta, P.** Bahrain : s.n., Mar. 11-14, 2007, SPE105248, presented at 15th SPE Middle East Oil & Gas Show and Conference.
32. *Enhanced oil recovery by in-situ combustion process in Balol and Santhal field in Cambay Basin, Gujarat, India: A case study*. **Chattopadhyay, S.K.,** New Delhi : s.n., Jan. 15-19, 2005, presented at Petrotech 2005.
33. *In situ combustion (ISC) process using horizontal wells and gravity drainage*. **Greaves, M. and Al-Shamali, O.** 1996, JCPT, Vol. 35, pp. 49-55.
34. *A new combustion process utilizing horizontal wells and gravity drainage*. **Kisman, K.E. and Lau, E.C.** 1994, JCPT, Vol. 33, pp. 39-45.
35. *Experimental and numerical simulation of a novel top down in-situ combustion process*. **Coates, R., Lorimer, S., and Ivory, J.** Calgary : s.n., June 19-21, 1995, SPE 30295, International Heavy Oil Symposium.
36. *Pressure-Up Blow-Down Combustion: A Channelled Reservoir Recovery Process*. **Hallam, R. J., and Donnelly, J.K.** Houston : s.n., Oct. 2-5, 1988, SPE 18071, presented at 63rd Annual Technical Conference of SPE.

37. *Performance Analysis of In-Situ Combustion Pilot Project.* **Mehra, R.K.** Bakersfield, CA. : s.n., Feb. 7-8, 1991, SPE 21537, presented at the International Thermal Operations Symposium of SPE.
38. *Performance of Morgan Pressure Cycling In-situ Combustion.* **Marjerrison, D.M. and Fassihi, M.R.** 1994, SPE/DOE 27793.
39. *Post SAGD In-Situ Combustion: Potentials and Challenges.* **Oskouei, S.J.P., Moore, R.G., Maini, B., Mehta, S.A.** Calgary, Alberta, Canada : s.n., June 12-14, 2012, SPE-157959-MS-P, SPE Heavy Oil Conference Canada.
40. *Garvity Stable Combustion Processes for Athabasca Oil Sand Reservoirs.* **Lim, G.** Edmonton, Alberta : s.n., Mar. 10-12, 2009, presented to the World Heavy Oil Congress.
41. *Physical modeling of the electrical heating the oil sand deposits.* **Chute, F.S., Vermeulen, F.E. and Cervenán, M.R.** 1978, Technical report, AOSTRA Agreement #31.
42. *Physical modeling the electromagnetic heating of oil sand and other earth-type and biological materials.* **Vermeulen, F.E., Chute, F.S. and Cervenán, M.R.** 1979, Canadian Electrical Engineering Journal, Vol. 4, pp. 19-28.
43. *The mechanisms of electrical heating for the recovery of bitumen from oil sands.* **McGee, B.C.W. and Vermeulen, F.E.** 2007, Journal of Canadian Petroleum Technology, Vol. 46, pp. 28-34.
44. *Electrical heating.* **Vinsome, K., McGee, B.C.W., Vermeulen, F.E. and Chute, F.S.** 1994, Journal of Canadian Petroleum Technology, Vol. 33, pp. 29-36.
45. *Field test of electrical heating with horizontal and vertical wells.* **McGee, B.C.W., Vermeulen, F.E. and Yu, L.** 1999, Journal of Canadian Petroleum Technology, Vol. 38, pp. 46-53.
46. **Hagedorn, A.R.** *Oil recovery by combination of steam stimulation and electrical heating.* 3946809 US, Dec. 19, 1974.
47. **Sacuta, A.** *Combination solvent injection electric current application method for establishing fluid communication through heavy oil formation.* 4450909 US, May 29, 1984.
48. *Cyclic electrical heating-gas injection process for recovering heavy oil/bitumen from shaly lean sand reservoirs.* **Lee, K. and Gumrah, F.** May 2010, AACI Report.
49. *Wet electric heating for starting up SAGD/VAPEX.* **Yuan, J.Y., Huang, H., Mintz, R., Wang, X., Jossy, C. and Tunney, C.** 2004, Canadian International Petroleum Conference, Vols. Paper 2004-13.
50. *Direct current stimulation - new approach to enhancing heavy oil production.* **Wittle, J.K. and Hill, D.G.** 2006, World Heavy Oil Conference, Vols. Paper 2006-409.
51. *Direct current electrical enhanced oil recovery in heavy oil reservoirs to improve recovery, reduce water cut, and reduce H₂S production while increasing API gravity.* **Wittle, J.K., Hill, D.G. and Chilingar, G.V.** 2008, SPE 114012.
52. *Direct current stimulatoin for heavy oil production.* **Wittle, J.K., Hill, D.G., and Chilingar, G.V.** March 2008, World Heavy Oil Congress, Edmonton, Vols. Paper 2008-374.
53. *Direct electric current oil recovery (EEOR) - a new approach to enhancing oil production.* **Wittle, J.K., Hill, D.G. and Chilingar, G.V.** 2011, Energy Sources, Part A, Vol. 33, pp. 805-822.
54. *Mathematical modeling and field applocation of heavy oil recovery by radio-frequency electromagnetic stimulation.* **Davletbaev, A., Kavaleva, L. and Babadagli, T.** 2011, Journal of Petroleum Science and Engineerin, Vol. 78, pp. 646 - 653.
55. *Electromagnetic techniques in the in-situ recovery of heavy oils.* **Vermeulen, F.E. and Chute, F.S.** 1, 1983, Journal of Microwave Power, Vol. 18, pp. 15 - 29.
56. *In situ electromagnetic heating for hydrocarbon recovery and environmental remediation.* **Vermeulen, F.E. and McGee, B.** 2000, Journal of Canadian Petroleum Technology, Vol. 39, pp. 25 - 29.

57. *Effects of electrical and radiofrequency electromagnetic heating on the mass-transfer process during miscible injection for heavy-oil recovery.* **Kovaleva, L., Davletbaev, A., Babadagli, T., and Stepanova, Z.** s.l. : Energy Fuels, 2011, Vol. 25, pp. 482 - 486.
58. *Evaluation of electromagnetic heating for heavy oil recovery from Alaskan reservoirs.* **Peraser, V., et al., et al.** Bakersfield, California : s.n., March 21-23, 2012. SPE Western Regional Meeting. SPE 154123-MS.
59. *Seeking more oil, fewer emissions.* **Rassenfoss, S.** 2012, Journal of Petroleum Technology, pp. 34 - 38.
60. *Electromagnetic heating for in-situ production of heavy oil and bitumen reservoirs.* **Wacker, B., et al., et al.** Alberta, Canada : s.n., November 15-17, 2011. Canadian Unconventional Resources Conference, 15-17 November 2011, Alberta, Canada. SPE 148932-MS.
61. *Biotechnology in petroleum recovery: the microbial EOR.* **Sen, R.** 2008, Progress in Energy and Combustion Science, Vol. 34, pp. 714-724.
62. *Enhanced oil recovery - an overview.* **Thomas, S.** 1, 2008, Oil & Gas Science and Technology - Rev. IFP., Vol. 63, pp. 9-19.
63. *Microbial enhanced oil recovery (MEOR).* **Brown, L. R.** 2010, Current Opinion in Microbiology, Vol. 13, pp. 316-320.
64. *Reservoir engineering analysis of microbial enhanced oil recovery.* **Byrant, S.L. and Lockhart, T.P.** 2002, SPE Reservoir Evaluation & Engineering (SPE 79719).
65. *Microbial enhanced-oil-recovery technologies: a review of the past, present, and future.* **Maudgalya, S., Knapp, R.M., and McInerney, M.J.** 2007, SPE 106978.
66. *Microbial EOR - Critical aspects learned from the lab.* **Jackson, S.C., Alsop, A., Choban, E., D'Achille, B., Fallon, R., Fisher, J., Hendrickson, E., Hnatow, L., Keeler, S., Luckring, A., Nopper, R., Norvell, J., Perry, M., Rees, B., Suchanec, D., Wolstenholme, S.M., Thrasher, D., and Pospisil, G.** 2010, SPE 129657.
67. *Potential microbial enhanced oil recovery processes: a critical analysis.* **Gray, M.R., Yeung, A., Foght, J.M., and Yarranton, H.W.** 2008, SPE 114676.
68. *Significant mobilization of entrapped hydrocarbons using biosurfactants with viscosity control and a low molecular weight alcohol.* **Maudgalya, S., Folmsbee, M.M., Knapp, R.M., Nagle, D.P., and McInerney, M.J.** Mexico City : s.n., Nov. 5-7, 2003. 2nd International Conference on Petroleum Biotechnology. The Development and Perspectives of Biotechnology Applied to the Oil Industry.
69. *A Commercial Microbial Enhanced Oil Recovery Technology: Evaluation of 322 Projects.* **Portwood, J.T.** 1995, Society of Petroleum Engineers.
70. *Biotechnology and Cleaner Production in Canada.* **Ah-You, K., Suleiman, M., and Jawaorski, J.,** 2000, Canadian Biotechnology.
71. *Biosurfactants and their Role in Oil Recovery.* **McInerney, M.** Calgary, AB : s.n., 2011. International Symposium on Applied Microbiology and Molecular Biology in Oil Systems.
72. **Titan Oil Recovery.** Titan Oil Recovery. [Online] [Cited: August 4, 2011.] <http://www.titanoilrecovery.com>.
73. **SPE .** SPE.org Online Communities. June 15, 2003.
74. **Fujiwara, K., Sugai, Y., Yazawa, N., Ohno, K., Hong, C.X., and Enomoto, H.** Biotechnological approach for development of microbial enhanced oil recovery technique. [book auth.] R. Vazquez-Duhalt and R. Quintero-Ramirez. *Studies in Surface Science and Catalysis.* Amsterdam : Elsevier, 2004, pp. 405-445.
75. **University of Michigan.** Porous Media Research Group. [Online] http://sitemaker.umich.edu/sfogler/bacterial_profile_modification.

76. **Costerton, J.W.F., Cusack, F. and Macleod, F.A.** 4800959 United States of America, 1989.
77. **Archer, J.S., and Wall, C.G.** *Petroleum Engineering Principles and Practice*. s.l. : Graham and Trotman Ltd., 1986. ISBN 0- 86010-665-9.
78. **Willhite, G.P.** *Waterflooding*. 1986. pp. 49-55. Vol. 35. ISBN 1-55563-005-7.
79. **Donaldson, E., Chlfnagian, G. Y., and Yen, T. F.** *Enhanced Oil Recovery, I, Fundamentals and Analysis*. . s.l. : Elsevier Science Publishers B.V.,, 1985. ISBN 0-444-4 2206.4 (Vol. 17 A)..
80. **Green, D.W., and Willhite, G.P.** *Enhanced Oil Recovery*. s.l. : Henry L. Doherty Memorial Fund of AIME, SPE., 1998.
81. **Pope, Gary A.** Multiphase and Multicomponent Unsteady State Flow in Permeable Media, (Chapter3, course notes). Austin : The University of Texas at Austin, 2003.
82. *Waterflooding Heavy Oils*. **Smith, G.E.** Casper, Wyoming : SPE Rocky Mountain Regional Meeting, 1992. SPE 24367.
83. *Three-dimensional Studies of In Situ Combustion-Horizontal Wells Process With Reservoir Heterogeneities*. **Greaves, M. and Al-Honi, M.** Calgary : Annual Technical Meeting, Petroleum Society of Canada, June 8-10, 1998.
84. **H.R. Warner Jr., Larry W. Lake (Editor-in-Chief), Edward D. Holstein (Editor of Vol. V)** , *Reservoir Engineering and Petrophysics - Petroleum Engineering Handbook*. s.l. : Society of Petroleum Engineers, 2007. Vol. V.
85. *The Instability of Slow, Immiscible Viscous Liquid-Liquid Displacements in Permeable Media*. **Chuoque, R.L., van Meurs, P., and van der Poel, C.** s.l. : Petroleum Transactions, AIME, 1959, Vol. 216, pp. 188-194.
86. *The Onset of Instability during Two-Phase Immiscible Displacement in Porous Media*. **Peters, E.J., and Flock, D.L.** s.l. : Society of Petroleum Engineering Journal, April 1981. SPE 8371.
87. *A Comparison of Unstable Miscible and Immiscible Displacements*. **Peters, E.J., and Hardham, W.D.** San Antonio, Texas : SPE Annual Technical Conference and Exhibition, October 8-11, 1989. Paper 19640-MS.
88. **Reid, R., Prausnitz, J. and Sherwood, T.** *The Properties Of Liquids And Gasses*. Third Edition. s.l. : McGraw Hill, 1977. pp. 566-567.
89. **Reid, R., Prausnitz, J., and Sherwood, T.** *The Properties Of Liquids And Gasses*. Third Edition. s.l. : McGraw Hill, 1977. pp. 573-574.
90. *Laboratory Studies of Microscopic Dispersion Phenomena*. **Blackwell, R.J.** s.l. : Society of Petroleum Engineering Journal, March 1962, p. 1.
91. *Design of Laboratory Models for the Study of Miscible Displacement*. **Pozzi, A., and Blackwell, R.J.** s.l. : Society of Petroleum Engineering Journal, March 1963, p. 28.
92. *A Review of Dispersion and Diffusion in Porous Media*. **Perkins, T.K, and Johnston, O.C.** March : Society of Petroleum Engineering Journal, 1963, p. 70.
93. *On Some Remarkable Observations of Laboratory Dispersion Using Computed Tomography (CT)*. **Walsh, M.P., and Withjack, E.M.** 9, s.l. : Journal of Canadian Petroleum Technology, September 1994, Vol. 33.
94. *A Natural Gradient Experiment on Solute Transport in a Sand Aquifer: Spatial Variability of Hydraulic Conductivity and Its Role in the Dispersion Process*. **Sudicky, E.A.** Baltimore : Symposium on Field Approaches and Measurement Techniques for Quantifying Spatial Variability in Porous Media, AGU Spring Meeting, May 1987.
95. *Stochastic and Deterministic Analysis of Dispersion in Unsteady Flow at the Borden Tracer Test Site, Ontario, Canada*. **Farrel, D., Woodbury, A.D., Sudicky, E.A., and Rivett, M.** s.l. : Journal of Contaminant Hydrology, 1994, Vol. 15, pp. 159-185.

96. *Flow Models and Scaling Laws for Flow through Porous Media*. **Greenkorn, R.A.** 3, s.l. : Industrial and Engineering Chemistry, March 1964, Vol. 56, p. 32.
97. *Theory of Dimensionally Scaled Models of Petroleum Reservoirs*. **Geeertsma, J., Croes, G., and Schwartz, N.** s.l. : AIME Trans., 1956, Vol. 207, p. 178.
98. *On Physically similar systems; illustrations of the use of dimensional equations*. **Buckingham, E.** 4, s.l. : Physical Review, 1914, Vol. 4, pp. 345-376.
99. *Non-Isothermal Miscible Displacement*. **Frauenfeld, T.** s.l. : M.Sc. Thesis, University of Alberta, Department of Petroleum and Mineral Engineering, Oct. 1981.
100. *Representing Steam Models with Vacuum Models*. **Stegemier, G.L., Laumbach, D.D., and Volek, C.W.** s.l. : Society of Petroleum Engineering Journal, June 1980, pp. 151-174.
101. *Scaled Physical Model Studies of the Steam Drive Process*. **Doscher, T.M.** s.l. : DOE/ET/12075-1, First Annual Report, Sept. 1977 - Sept. 1978, Dec. 1980.
102. *A Current Appraisal of Thermal Recovery*. **Prats, M.** 8, s.l. : Journal of Petroleum Technology, August 1978, Vol. 30, pp. 1129-1136.
103. *Scaled Physical Model Studies of the Steam Drive Process*. **Doscher, T.M.** s.l. : DOE/ET/12075-2, Second Annual Report, Sept. 1978 - Sept. 1979, Feb. 1981.
104. **Doscher, T.M.** s.l. : DOE/ET/12075-3, Final Report, Nov. 1982.
105. *Thermal Recovery of Oil and Bitumen*. **Butler, R.M.** Calgary : GravDrain Inc., Oct. 2000, pp. 248-250.
106. *High Pressure Scaled Model Design Techniques for Thermal Recovery Processes*. **Kimber, K.** Edmonton, Alberta, Canada : PhD. Thesis, University of Alberta, 1989.
107. *Scaled model tests of in situ combustion in massive unconsolidated sands*. **Binder, G.G., Elzinga, E.R., Tarmy, B.L., and William, B.T.** Mexico City : s.n., 1967. Proceedings of the 7th World Petroleum Congress. Vol. 3, pp. 477 - 485.
108. *Scaling Criteria For In-Situ Combustion Experiments*. **Islam, M.R. and Farouq Ali, S.M.** Regina, SK : Technical Meeting / Petroleum Conference Of The South Saskatchewan Section, Sep 25-27, 1989. Paper SS-89-01.
109. *The ABCs of In-Situ-Combustion Simulations: From Laboratory Experiments to Field Scale*. **Gutierrez, D., Moore, R.G., Ursenbach, M.G., and Mehta, S.A.** 4, s.l. : Journal of Canadian Petroleum Technology, July 2012, Vol. 51, pp. 256-267.
110. *An Experimental Investigation of the Fireflooding Combustion Zone*. **Kumar, Mridul and Garon, A.M.** 1, s.l. : SPE Reservoir Engineering, Feb 1991, Vol. 6, pp. 55-61.
111. *Volume And Permeability Changes Associated With Steam Stimulation In an Oil Sands Reservoir*. **Scott, J.D., Proskin, S.A., and Adhikary, D.P.** 7, s.l. : Journal of Canadian Petroleum Technology, July 1994, Vol. 33.
112. *Analysis of the Steam Assisted Gravity Drainage (SAGD) Process Using Experimental/Numerical Tools*. **Nasr, T.N., Golbeck, H., and Lorimer, S.** Calgary : SPE International Conference on Horizontal Well Technology, 1996.
113. *Investigation of the VAPEX Process Using CT Scanning and Numerical Simulation*. **Cuthiell, D., McCarthy, C., Frauenfeld, T., Cameron, S., and Kissel, G.** 2, 2003 : Journal of Canadian Petroleum Technology, February, Vol. 42.
114. *Viscous Fingering Effects in Solvent Displacement of Heavy Oil*. **Cuthiell, D., Kissel, G., Jackson, C., Frauenfeld, T., Fisher, D., and Rispler K.** 7, s.l. : Journal of Canadian Petroleum Technology, July 2006, Vol. 45.
115. *Noncondensable Gas Distribution in SAGD Chambers*. **Yuan, J.Y., Chen, J., Pierce, G., Wiwchar, B., Golbeck, H., Wang, X., Beaulieu, G., and Cameron, S.** 3, s.l. : Journal of Canadian Petroleum Technology, March 2011, Vol. 50, pp. 11-20.

116. *Counter-current Aspect of the SAGD Process.* **Nasr, T.N., Law, D., Golbeck, H., and Korpany, G.** Calgary : Annual Technical Meeting, June 8-10, 1998. Paper 98-12.
117. *In Situ Combustion as a Followup Process to CHOPS.* **Chen, J., Coates, R., Oldakowski, K., and Wiwchar, B.** Calgary : SPE Heavy Oil Conference Canada, June 12-14, 2012.
118. *Analysis of the Steam Assisted Gravity Drainage (SAGD) Process Using Experimental/Numerical Tools.* **Nasr, T.N., Golbeck, H. and Lorimer, S.** Calgary : SPE International Conference on Horizontal Well Technology, 1996.
119. *Scaling Accuracy of Laboratory Steam Flooding Models.* **Pujol, L. and Boberg, T.C.** Bakersfield, CA : SPE 4191 presented at the SPE California Regional Meeting, 8-10 Nov. 1972.
120. *Numerical and Experimental Modelling of the Steam Assisted Gravity Drainage (SAGD) Process.* **Sasaki, K., Akibayashi, S., Yazawa, N., Doan, Q., and Farouq Ali, S.M.** 1, January 2001, Journal of Canadian Petroleum Technology, Vol. 40, pp. 44-50.
121. *Experimental and Simulation Studies of SAGD Process in Fractured Reservoirs.* **Bagci, A.S.** Tulsa, Oklahoma : SPE/DOE Symposium on Improved Oil Recovery, April 22-26, 2006. SPE 99920.
122. *Noncondensable gas steam-assisted gravity drainage.* **Canbolat, S., Akin, S. and Kovscek, A.R.** 2004, Vol. 45, pp. 83 - 96.
123. **Butler, R.M.** *Thermal recovery of oil and bitumen.* Englewood : Prentice-Hall, 1991.
124. *Experimental study of co-injection of potential solvents with steam to enhance SAGD process.* **Ardali, M., Mamora, D.D. and Barrufet, M.** Anchorage, Alaska : s.n., May 7-11, 2011. SPE Western North America Regional Meeting. SPE 144598.
125. *Scaling accuracy of laboratory steam flooding models.* **Pujol, L. and Boberg, T.C.** Bakersfield, California : s.n., Nov. 8-10, 1972. SPE/AIME California Regional Meeting. SPE 4191.
126. *Physical modeling of solvent-assisted SAGD.* **Khaledi, R., Beckman, M., Pustanyk, K., Mohan, A., Wattenbarger, C., Dickson, J., and Boone, T.** Calgary, Alberta : s.n., June 12 - 14, 2012. SPE Heavy Oil Conference Canada. SPE 150676.
127. *Experimental investigation of the effect of hexane on SAGD performance at different operating pressures.* **Mohebbati, M.H., Maini, B.B. and Harding, T.G.** Calgary, Alberta : s.n., June 12 - 14, 2012. SPE Heavy Oil Conference Canada. SPE 158498.
128. *Laboratory Experimental Testing and Development of an Efficient Low Pressure ES-SAGD Process.* **O.R. Ayodele, T.N. Nasr, G. Beaulieu, G. Heck.** 9, s.l. : Journal of Canadian Petroleum Technology, 2009, Vol. 48.
129. *Laboratory investigation of the effects of solvent injection on in-situ combustion.* **Cristofari, J., Castanier, L.M. and Kovscek, A.R.** June 2008, SPE Journal, pp. 153 - 163. SPE 99752.
130. *Heavy oil production by in situ combustion - Distinguishing the effects of the steam and fire fronts.* **Freitag, N.P. and Exelby, D.R.** 4, 1998, Journal of Canadian Petroleum Technology, Vol. 37, pp. 25 - 32.
131. *Scaled model experiments of fireflooding in tar sands.* **Garon, A.M., Geisbrecht, R.A. and Lowry Jr., W.E.** 9, September 1982, Journal of Petroleum Technology, Vol. 34, pp. 2158 - 2166. SPE 9449-PA.
132. *Horizontal producer wells in in situ combustion (ISC) processes.* **Greaves, M., Tuwil, A.A. and Bagci, A.S.** 4, 1993, Journal of Canadian Petroleum Technology, Vol. 32, pp. 58 - 67.
133. *THAI - New air injection technology for heavy oil recovery and in situ upgrading.* **Greaves, M., Saghr, A.M., Xia, T.X., Turta, A.T., and Ayasse, C.** 3, 2001, Journal of Canadian Petroleum Technology, Vol. 40, pp. 38 - 47.

134. *3D physical model studies of downhole catalytic upgrading of Wolf Lake heavy oil using THAI.* **Xia, T. and Greaves, M.** Calgary, Alberta : s.n., June 12 - 14, 2001. Petroleum Society's Canadian International Petroleum Conference 2001. pp. 1 -15. Paper 2001-017.
135. *In situ combustion as a followup process to CHOPS.* **Chen, J., Coates, R., Oldakowski, K., and Wiwchar, B.** Calgary : s.n., June 12 - 14, 2012. SPE Heavy Oil Conference Canada. SPE-157847-PP.
136. *Experiments to study to explore the potential of multi-stage combustion assisted gravity drainage (MS-CAGD).* **Lim, G.B. and Chen, J.** Aberdeen : s.n., 2012. World Heavy Oil Congress. WHOC12-152.
137. *Experimental investigation of in situ combustion at low air fluxes.* **Alamatsaz, A., Moore, R.G., Mehta, S.A., and Ursenbach, M.G.** Anchorage, Alaska : s.n., May 7 - 11, 2011. SPE Western North American Regional Meeting. SPE 144517.
138. *Wet Electric Heating for Starting Up SAGD/VAPEX.* **Yuan, J.-Y., Huang, H., Mintz, R., Wang, X., Jossy, C., and Tunney, C.** Calgary, Alberta : s.n., June 8-10, 2004. Petroleum Society's 5th Canadian International Petroleum Conference (55th Annual Technical Meeting). pp. PAPER 2004-130.
139. **Yuan, J.-Y., Isaacs, E.E., Huang, H., and Vandenhoff, D.G.** *Wet electrical heating process.* 6,631,761 B2 US, October 14, 2003.
140. **Bryant, Rebecca S. and Burchfield, Thomas E.** *Applications of MEOR Technology for Petroleum Producers.* s.l. : NIPER, 1988.
141. **Todd, Adrian C.** Core Flooding as Related to Water Injection. [Online] Heriot-Watt University.
http://www.advantekinternational.com/pwrijip2003/pwri/toolbox/monitoring/coreflood/main_core.htm.
142. *Polymer Flood Technology for Heavy Oil Recovery.* **Wassmuth, F.R., Green, K., Hodgins, L., Turta, A.T.** Calgary, Alberta, Canada : Canadian International Petroleum Conference, 2007.
143. *Large-Scale Laboratory Testing of Petroleum Reservoir Processes.* **Yale, David P., Meier, Steven W., Leonardi, Sergio A., Joyce, Gina M., Kushnick, Arnold P., Wang, Jianlin.** Florence, Italy : SPE Annual Technical Conference and Exhibition, 2010.
144. *Extension of Das and Butler Semianalytical Flow Model.* **Knorr, K.D. and Imran, M.** s.l. : Journal of Canadian Petroleum Technology, 2011.
145. *Solvent Chamber Development in 3D Physical Model Experiments of Solvent Vapour Extration Processes (SVX) With Various Permeabilities and Solvent Vapour Qualities.* **Knorr, Kelvin D. and Imran, Muhammed.** Calgary : Canadian Unconventional Resources Conference, 2011.
146. *Upscaling Study of Vapour Extration Process through Numerical Simulation.* **Xu, Suxin, Zeng, Fanhua, Gu, Yongan, and Knorr, Kelly.** Calgary : SPE Heavy Oil Conference, 2012.
147. *New Hybrid Steam-Solvent Processes for the Recovery of Heavy Oil and Bitumen.* **Nasr, T.N., and Ayodele, O.R.** Abu Dhabi, UAE : Abu Dhabi International Petroleum Exhibition and Conference, Nov 5-8, 2006.
148. *Physical Modeling and Mumerical Simulation Of In Situ Recovery Of Bitumen From Oil Sands By Steam Injection.* **Reddy, G.S., Prowse, D.R., and Redford, D.A.** Calgary : Petroleum Society of Canada Annual Technical Meeting, May 25-28, 1980. Paper 80-31-10.
149. *The Use of Solvents And Gases With Steam In Tbe Recovery of Bitumen From Oil Sands.* **Redford, D.A.** 1, s.l. : Journal of Canadian Petroleum Technology, Jan-Feb 1982, Vol. 21.

150. *Hydrocarbon-Steam Processes For Recovery Of Bitumen From Oil Sands*. **Redford, D.A., and McKay, A.S.** Tulsa, Oklahoma : SPE/DOE Enhanced Oil Recovery Symposium, April 20-23, 1980.
151. *Evaluation of the Bottom Water Reservoir VAPEX Process*. **Frauenfeld, T., Jossy, C., Rispler, K., and Kissel, G.** 9, s.l. : Journal of Canadian Petroleum Technology, September 2006, Vol. 45.
152. *Nanotechnology-Based Micromodels and New Image Analysis to Study Transport in Porous Media*. **Javandpour, F., and Fisher, D.** 2, s.l. : Journal of Canadian Petroleum Technology, February 2008, Vol. 47.
153. *Tracking Cold Production Footprints*. **Sawatzky, R.P., Lillico, D.A., London, M.J., Tremblay, B.R., and Coates, R.M.** Calgary : Canadian International Petroleum Conference, June 11-13, 2002. Paper 2002-086.
154. *An Experimental Study of the Pore-Blocking Mechanisms of Aphron Drilling Fluids Using Micromodels*. **Bjorndalen, N., Alvarez, J.M., Jossy, W.E., and Kuru, E.** The Woodlands, Texas : SPE International Symposium on Oilfield Chemistry, April 20-22, 2009. Paper 121417-MS.
155. *CT Imaging of Wormhole Growth Under Solution-Gas Drive*. **Tremblay, B., Sedgwick, G., and Vu, D.** 1, s.l. : SPE Reservoir Evaluation & Engineering, February 1999, Vol. 2, pp. 37-45.
156. *Enhanced Oil Recovery by CO₂ Flooding in Homogeneous and Heterogeneous 2D Micromodels*. **Sayegh, S.G., and Fisher, D.B.** 8, s.l. : Journal of Canadian Petroleum Technology, August 2009, Vol. 48, pp. 30-36.
157. *Design and installation of a high-pressure 3D physical model for evaluation of solvent vapor extraction processes*. **Knorr, K.D., Wilton, R.R., Zeng, F.B., Exelby, D.R., Smith, H.S., Kniaz, D.A., and Mroske, L.G.** Edmonton, Alberta : s.n., March 10 - 12, 2008. World Heavy Oil Congress 2008. Paper 2008-322.
158. *Physical modelling of the electromagnetic heating of oil sand and other earth-type and biological materials*. **Vermeulen, F.E., Chute, F.S. and Cervenak, M.R.** 4, 1979, Canadian Electrical Engineering Journal, Vol. 4.